KAUNAS UNIVERSITY OF TECHNOLOGY

ANDRIUS SOLOŠENKO

CARDIAC ARRHYTHMIA DETECTION IN PHOTOPLETHYSMOGRAM SIGNALS

Doctoral dissertation

Technological Sciences, Electrical and Electronics Engineering (01T)

2018, Kaunas

This doctoral dissertation was prepared at Kaunas University of Technology, Biomedical Engineering Institute during the period of 2013–2017. The research was supported by Research Council of Lithuania.

Scientific Supervisor:

Prof. Dr. Vaidotas MAROZAS (Kaunas University of Technology, Technological Sciences, Electrical and Electronics Engineering – 01T).

Doctoral dissertation has been published in:
http://ktu.edu

Editor:

Dr. Armandas RUMŠAS (Publishing Office "Technologija")

ISBN 978-609-02-1421-3

The bibliographical information of this issue is available at Martynas Mažvydas National Library of Lithuania National Bibliographic Data Bank (NBDB)

KAUNO TECHNOLOGIJOS UNIVERSITETAS

ANDRIUS SOLOŠENKO

ŠIRDIES ARITMIJŲ APTIKIMAS FOTOPLETIZMOGRAMOS SIGNALUOSE

Daktaro disertacija

Technologijos mokslai, elektros ir elektronikos inžinerija (01T)

2018, Kaunas

Disertacija rengta 2013–2017 metais Kauno technologijos universiteto Biomedicininės inžinerijos institute. Mokslinius tyrimus rėmė Lietuvos mokslo taryba.

Mokslinis vadovas:

Prof. dr. Vaidotas MAROZAS (Kauno technologijos universitetas, technologijos mokslai, elektros ir elektronikos inžinerija – 01T).

Interneto svetainės, kurioje skelbiama disertacija, adresas:
http://ktu.edu

Redagavo:

dr. Armandas RUMŠAS (Leidykla „Technologija“)

ISBN 978-609-02-1421-3

Leidinio bibliografinė informacija pateikiama Lietuvos nacionalinės Martyno mažvydo bibliotekos Nacionalinės bibliografijos duomenų banke (NBDB)

Contents

List of terms and abbreviations

Ac	Accuracy
AC	Alternating current
AF	Atrial fibrillation
ANN	Artificial neural network
AV	Atrioventricular node
DC	Direct current
ECG	Electrocardiogram
LED	Light emitting diode
MCC	Matthews correlation coefficient
NLMS	Normalized least mean square algorithm
P	Precision
PB	Premature beats
PD	Photodetector
PP	Peak-to-peak interval
PPG	Photoplethysmogram
PR	Power ratio
PVC	Premature ventricular contraction
QRS	Wave corresponding to ventricular depolarization
ROC	Receiver operating characteristic
RR	Interval between two successive ventricular contractions
$RMSE$	Root mean square error
Se	Sensitivity
Sp	Specificity
SA	Sinoatrial node
SNR	Signal-to-noise ratio
SR	Sinus rhythm

ACKNOWLEDGEMENT

I am willing to express my most profound gratitude to my supervisor, prof. dr. Vaidotas Marozas, for guiding my research. I would like to thank prof. Leif Sörnmo for his participation, guidance and help in writing and improving scientific papers. Also, I would like to thank dr. Andrius Petrėnas for his support, active participation in co-authoring scientific publications, for improving the text of both scientific publications and presentations. My special gratitude goes to my family and medical doctor Agnė Bertašiūtė for the support.

1 INTRODUCTION

Relevance of the Research

Premature ventricular contractions (PVCs) and atrial fibrillation (AF) are the most commonly encountered cardiac disorder in humans, affecting up to 4% and 2% of the general population, respectively (Kostis et al., 1981 [1]; January et al., 2014 [2]).

PVCs are initiated by the secondary pacemakers – the ectopic foci, located in the ventricles, causing them to contract prematurely. It is well known that PVCs may occur even in healthy hearts with no significant impact on the overall well-being. Accordingly, early studies suggested that PVCs could be considered as benign in the absence of structural heart disease (Kennedy et al., 1985 [3]). However, more recent studies have denied the benignity of PVCs by linking them to various health abnormalities. For example, the increased frequency of PVCs has been associated with heart failure and sudden death if a heart disease was suspected (Ng, 2006 [4]; Ephrem et al., 2013 [5]; Ataklte et al., 2013 [6]). PVCs have also been found to be a trigger of other serious heart arrhythmias such as ventricular fibrillation (Santoro et al., 2014 [7]) and atrial fibrillation (Watanabe et al., 2006 [8]; Agarwal et al., 2010 [9]).

Several studies have shown (e.g., (Hirose et al., 2010 [10])) that PVCs have a potential to be used as a predictor of sudden cardiac death in men even without a recognized heart disease. This particularly applies if frequent PVCs occur during physical exercise (Jouven et al., 2000 [11]; Ng, 2006 [4]), and especially during the phase of recovery (Frolkis et al., 2003 [12]; Ng, 2006 [4]). Since PVCs usually cause inefficiency in blood circulation, notably in cases of multiple frequent PVCs, i.e., bigeminy (every 2^{nd} beat is premature) and trigeminy (every 3^{rd} beat is premature), such a condition may lead to dizziness or a temporal loss of consciousness (Zaret et al., 1992 [13]; Reed et al., 2006 [14]; Garcia-Touchard et al., 2007 [15]). In addition, PVCs are common in patients with a chronic kidney disease (Shamseddin et al., 2011 [16]), by being a consequence of electrolyte shifts (e.g., low blood potassium and calcium), resulting in electrolyte imbalance during such procedures as hemodialysis.

AF has emerged as a world-wide cardiovascular epidemic, affecting nearly 3% of adults aged >20 years (Haim et al., 2015 [17]). Considerably greater AF prevalence is found in older individuals and in patients with serious health conditions such as hypertension, heart failure and coronary artery disease. Due to the fast ageing of the society, the prevalence is expected to increase up to 3-fold in the upcoming decades (Colilla et al., 2013 [18]). AF is often asymptomatic; it covers from 55% to 80% of all AF cases (Healey et al., 2012 [19]; Lowres et al., 2013 [20]; Lip et al., 2014 [21]), thus timely diagnosis of subclinical (silent) AF is crucial in

order to prevent severe outcomes such as stroke (Kishore et al., 2014 [22]) and death (Benjamin et al., 1998 [23]).

In most cases, PVCs and AF have a distinctive morphology and thus are relatively easily detectable in an electrocardiogram (ECG). Hence, PVC and AF characterizing properties, such as the frequency and morphology, are usually evaluated by using conventional Holter monitors. Although various technologies have been developed for arrhythmia detection, for many years, only ECG-based Holter monitors and event recorders have routinely been used in the clinical practice to detect PVCs and AF in high-risk patients. Since AF is often asymptomatic (Lowres et al., 2013 [20]; Lip et al., 2014 [21]), patient-friendly screening technologies are highly desirable so that AF can be detected at an early stage. Advancements in the medical technology allow considering alternative strategies. For example, it has been shown that daily intermittent screening by using hand-held ECG recorders results in considerably higher arrhythmia detection rates compared to the standard 24 hour Holter monitoring (Lowres et al., 2016 [24]; Kirchhof, 2017 [25]). Even though such emerging hand-held ECG recorders are particularly easy to use, a 10-s ECG is not enough to detect paroxysmal AF. Moreover, the electrodes used to record ECG are attached to the patient's chest, which results in discomfort, a limited freedom of movement, and also in an increased feeling of unhealthiness, especially after wearing the device for several days (Rosero et al., 2013 [26]). Therefore, it is essential to develop unobtrusive screening technologies capable of monitoring longer periods of time, i.e., days and weeks, resulting in a larger number of identified AF cases (Charitos et al., 2012 [27]).

Currently, implantable devices are the only available technologies providing a convenient way for continuous AF monitoring. However, implantable devices are invasive and costly, therefore, they are not suitable for mass AF screening. Recently, photoplethysmography has been considered as an alternative approach to detect AF (Lee et al., 2013 [28]; McManus et al., 2016 [29]; Chan et al., 2016 [30]; Freedman, 2016 [31]). A smartphone camera-based application allows to acquire photoplehysmogram (PPG) waveform which reflects the blood volume changes in a finger – thus the pulse sequence can be used for detecting AF-caused irregular pulse. While smartphone camera-based AF detector offers a fast way to check for AF, such an approach is inherently not suitable for continuous monitoring.

With an increasing number of commercially available wristwatch or bracelet-type devices capable of acquiring PPG, and thus by default the pulse rate, it opens up the opportunity to screen for PVCs and AF for an unlimited period of time in a cost-effective and unobtrusive way. Although no guidelines currently exist on the clinical interpretation of the PPG signal, and an ECG should inevitably be recorded to confirm the PVC and AF diagnosis, such PPG-based screening is denoted by the potential to be a valuable tool of selecting individuals

from a larger population for prolonged ECG monitoring.

Scientific-Technological Problem

This doctoral thesis covers a scientific-technological problem of clinical relevance whether the most common cardiac arrhythmias, such as the premature ventricular contractions and atrial fibrillation, could be reliably detected by using solely the photoplethysmogram signals? In order to address the problem of unobtrusive and reliable arrhythmia monitoring and detection, the selection of alternative signals, features and noise-related issues, such as the problem of frequent false alarms, has to be solved.

Working Hypothesis

A hypothesis is formulated that not only premature ventricular contractions but also atrial fibrillation could be reliably detected by analyzing the features extracted from signals serving as an alternative to the electrocardiogram, e.g., photoplethysmogram signals, with an addition of automatic signal quality verification. The hypothesis is verified by the comparison of the obtained results with those provided in the scientific literature by using both clinical and simulated datasets.

Research Object

The research is based on the development and investigation of the algorithms for automatic detection of premature ventricular contractions and atrial fibrillation in photoplethysmogram signals.

The Aim of the Research

The aim of this doctoral thesis is to develop and investigate photoplethysmogram signal modeling and processing methods for noninvasive long-term monitoring of cardiac arrhythmia.

The Objectives of the Research

1. To critically analyze the available scholarly literature in the fields of heart arrhythmia and monitoring methods, on the genesis of photoplethysmogram signals and on the availability of biomedical signal databases recorded during arrhythmias.

2. To develop and investigate a photoplethysmogram model capable of simulating various arrhythmias including premature ventricular contractions and atrial fibrillation.

3. To develop and investigate a photoplethysmogram-based method for the detection of premature ventricular contractions.

4. To develop and investigate a photoplethysmogram-based method for the detection of atrial fibrillation.

Scientific Novelty

In this doctoral thesis, a phenomenological photoplethysmogram model, capable of simulating PPG signals during various cardiac events, starting from a normal sinus rhythm and ending with premature contractions and atrial fibrillation is proposed. PPG signals are generated by applying only RR interval series as an input to the model obtained either from ECG signals or by using RR interval simulators. The model also makes use of different PPG pulse types to account for the age and the vascular condition. The described qualities make this model one of a kind and, therefore, suitable for the development and the assessment of PPG-based arrhythmia detection algorithms.

High performance, real-time capable algorithms, one for PVC and the other for AF detection have been developed. Both algorithms rely on the features extracted solely from the PPG signals. Temporal, amplitude and frequency domain features are employed in order to distinguish the arrhythmia of interest from other types of arrhythmias and noises. The algorithms have been developed while having in mind their application in wearable systems. Currently, there are no reliable solutions for long-term PPG-based arrhythmia detection described in the scientific literature. Therefore, ambulatory application of the proposed algorithms would enable an unobtrusive, cost-effective and reliable solution for long-term screening of PVCs and AF.

The PVC detection algorithm relies on three subsequent intervals describing a single beat, the frequency domain features, and the artifact detection. The classification of heart beats into premature and normal is accomplished by the artificial neural network. The extracted features are normalized according to the heart rate of a normal sinus rhythm, and determined by employing a frequency domain-based estimator. Artifact-corrupted PPG segments are detected by the artifact detector and skipped before beat classification, thus reducing false alarms in a low signal to noise ratio environment.

The AF detection algorithm combines the analysis of the time intervals between successive heartbeats and the PPG signal quality assessment. AF detection relies on the improved, modified and PPG-optimized low-complexity algorithm (Petrėnas et al., 2015 [32]). Approaches for minimizing the influence of other types of arrhythmia on the specificity of the algorithm, i.e., ectopic beats, bigeminy and sinus arrhythmia, were employed. Signal quality assessment was performed by comparing the extracted PPG pulses with a predefined template, which adapts to the morphology of a specific PPG signal. The output of the

detector is modified according to the quality of the PPG signal providing a reliable performance in terms of high AF detection accuracy in quality signals and high specificity even at low signal to noise ratios, i.e., during motion-induced artifacts, thus minimizing false alarms.

Practical Significance

1. The developed solutions for ambulatory monitoring of PVCs and AF can be used in the following clinical applications:

   (a) Due to the high resemblance to the real photoplethysmogram signals, the developed photoplethysmogram model could be employed in the development and assessment of the PPG-based arrhythmia detection methods and in signal denoising.

   (b) A photoplethysmogram-based detector of premature ventricular contractions can be used for reliable and unobtrusive ambulatory long-term screening or applied in real-time calculation of premature ventricular beats, e.g., during hemodialysis procedures.

   (c) A method for the detection of atrial fibrillation using photoplethysmogram signals has a potential to be used for reliable, cost-effective ambulatory long-term screening of AF in patients suspected of having brief and rare episodes of AF or in patients after myocardial infarctions or ischemic strokes.

2. The methods provided in this thesis have been developed and used in support of the following projects:

   (a) "Intellectual wearable sensors system for human wellness monitoring – iMON" under the European Social Fund (No. VP1-3.1-SMM-10-V-02-004), 2013-2015.

   (b) "Personalized patient empowerment and shared decision support for cardiorenal disease and comorbidities – CARRE" funded by the European Commission Framework Programme 7 (No. 611140), 2013-2016.

   (c) "Automatic algorithms for atrial fibrillation risk prediction after acute myocardial infarction – AFAMI" supported by the Research Council of Lithuania (No. MIP088/15), 2015-2017.

Approval of the results

The doctoral thesis resulted in two scientific papers published in international scientific journals included in the Thomson Reuters Web of Science database, while, in total, the results have been published in 11 scientific papers. The essential results have been presented in 6 conferences, including

the worldwide-recognized IEEE Biomedical Circuits and Systems Conference (BioCAS) 2014, and the 44th conference of Computing in Cardiology 2017 (CinC2017). The research has been positively assessed both internationally and domestically: the BioCAS 2014 paper has been selected as one of the top 20 contributions to the conference and invited for having the extended version published in the *Special Issue* of the IEEE Transactions on Biomedical Circuits and Systems journal, received the 1st place award for the presentation at the section of "Signals and Modeling" at the conference "Science for Health 2014" (Lithuanian University of Health Sciences) as well as the prize for the most attractive project for business (with coauthors) at the Young Scientists Exhibition *"KTU Technorama 2015"* (Kaunas University of Technology).

The statements presented for defence

1. A photoplethysmogram model for simulating various arrhythmias, including premature contractions and atrial fibrillation, can generate a PPG signal by using the data extracted from ECG signals. The photoplethysmogram model can be used for the development and assessment of the PPG-based arrhythmia detection methods.

2. Premature ventricular contractions can be reliably detected by using rhythm and amplitude-based features, extracted from PPG signals, in combination with artifact detection and artificial neural network-based decision logic.

3. A combination of an ECG-derived and modified rhythm-based atrial fibrillation detector and PPG signal quality assessment provides a reliable approach for the detection of atrial fibrillation by relaying solely on the PPG signal analysis both during screening and long-term monitoring.

Structure of the Doctoral Thesis

The thesis is organized as follows: Chapters 2 and Chapter 3 are designated for the critical analysis of the relevant scientific literature with respect to the clinical significance and the available technologies for the detection of cardiac arrhythmia, namely the premature ventricular contractions and atrial fibrillation. Chapter 4 presents the proposed methods for the modeling of photoplethysmogram, capable of simulating arrhythmia, PPG-based algorithm of the detection of PVCs, as well as PPG-based algorithm of the detection of AF. Chapter 5 describes the data used for the performance evaluation and presents the results obtained for each of the proposed methods. The doctoral thesis is finished with general conclusions in Chapter 6. The thesis consists of 131 pages, 54 figures, and 15 tables. It features a list of references containing 176 positions.

2 CLINICAL SIGNIFICANCE OF PREMATURE VENTRICULAR CONTRACTIONS AND ATRIAL FIBRILLATION

2.1 Medical Background

2.1.1 Introduction to Premature Ventricular Contractions and Atrial Fibrillation

Anatomy and hemodynamics of the heart. The heart is a muscular organ that pumps blood throughout the body via the circulatory system thus supplying the body with oxygen and nutritious materials. Figure 2.1 shows the structure and the main parts of the heart. The heart consists of four chambers, namely, the upper two chambers are the right and left atria, whereas the lower chambers are the right and left ventricles. The blood returning to the heart from the body contain low levels of oxygen and high levels of carbon dioxide. This blood flows into the right atrium and then down into the adjacent right ventricle. After the right ventricle has filled, contraction of the right atrium pumps additional blood into the right ventricle. The right ventricle then contracts and pumps the blood to the lungs where the blood takes up oxygen and gives off carbon dioxide. The blood subsequently flows from the lungs trough the pulmonary veins to the left atrium, and then down into the adjacent left ventricle. The contraction of the left atrium pumps additional blood into the left ventricle. The left ventricle then contracts and pumps the blood to the aorta and then to the rest of the body via the vascular system. The heartbeat (pulse) is caused by the contraction of the ventricles. The most important factor is the heart rate. As the rate increases, more blood is pumped. The heart pumps more blood with each beat when the atria contract and fill the ventricles with additional blood just before the ventricles contract.

The electrical system of the heart. The electrical system of the heart controls the timing of each contraction. This system consists of the sinoatrial (SA) node, the atrioventruclar (AV) node, the bundle of His, Purkinje fibers and special tissues in the atria and the ventricles which conduct the current. The electrical discharge in the heart causes the muscle of the atria and, consequently, the ventricles to contract and pump blood. During normal conditions, this system maintains a steady heart rate (the number of contractions per minute) in a range of 60–100 beats per minute at rest and increases the hear rate to adapt the oxygen delivery during physical activity, stress, or excitement, while lowering the heart rate during low activity and sleep. In a healthy normal heart, the contraction rate of the atria is the same as that of ventricles. The normal synchronized contraction of atria and ventricles is defined as the normal sinus rhythm. However, due to

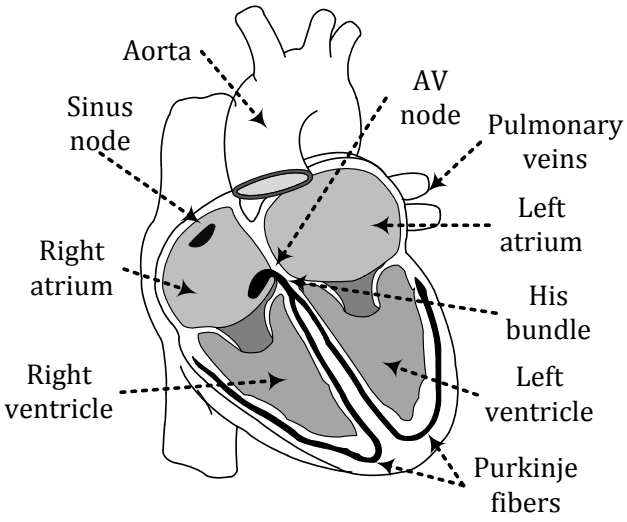

Fig. 2.1. Structure of the heart.

certain conditions or pathologies, either the atria or the ventricles – or both – may contract abnormally in an unsynchronized manner. Specialized heart cells in SA and AV nodes, His, Purkinje, etc., may operate autonomously; therefore, any suppression or enhancement of their activities may lead to abnormal contractions (Mangoni et al., 2008 [33]). Normally, the SA node is the fastest in terms of initiating electrical impulses, while other nodes are slower thus maintaining the normal electrical operation of the heart. The rate at which the normal electrical impulses are initiated depends on the maximal diastolic potential, the action potential threshold, and on the rate of the pacemaker potential. Changes in any of these factors may effect the rate of the electrical impulse initiation (Issa et al., 2012 [34]). Therefore, abnormal contractions are initiated by secondary pacemakers located in the atria and ventricles (defined as *ectopic foci*) which override the activity of the SA node. Such abnormal heart contractions are defined as *arrhythmias* of which the most common are premature ventricular contractions and atrial fibrillation. Figure 2.2 demonstrates the electrical activity of the heart during the normal sinus rhythm, premature contractions and atrial fibrillations.

Normal sinus rhythm. During normal sinus rhythm (SR), the electrical impulse is discharged in a group of special conducting cells at the upper part of the heart which are defined as the SA node. This impulse then propagates down through the heart, triggering the first of two atria, the AV node and then both ventricles through the bundle of His. In a healthy heart, the impulse propagates through the heart rapidly, allowing all the chambers to contract in a smooth, coordinated manner. The sequence of electrical and mechanical events during

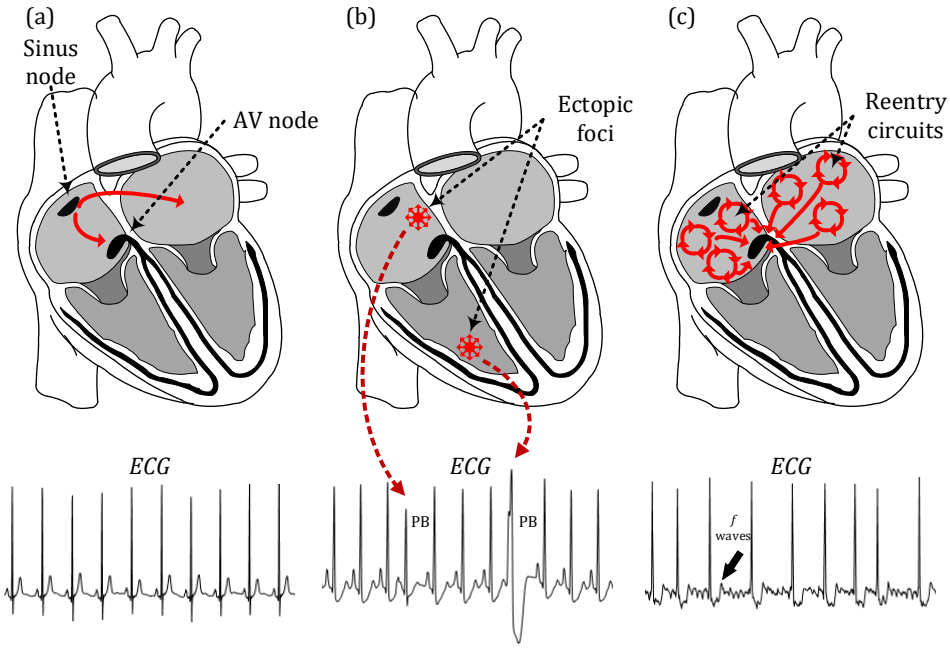

Fig. 2.2. Heart and its electrical activity during: (a) normal sinus rhythm, (b) atrial and ventricular premature beats (PBs), and (c) atrial fibrillation.

the normal cardiac cycle is as follows:

1. The SA node (the primary pacemaker) initiates an electrical impulse.
2. The upper heart chambers (atria) contract.
3. The AV node transmits an impulse into the ventricles.
4. The lower heart chambers (ventricles) contract and pump blood.
5. The SA node transmits another signal to the atria to contract thus starting a new cycle.

Premature ventricular contractions. Premature ventricular contractions (PVCs) are early contractions of the hearts' ventricles, which may occur due to various conditions both in structurally normal and abnormal hearts. In contrast to the normal sinus rhythm, during the PVCs, the electrical impulse is initiated by the secondary pacemakers located in the ventricles and are defined as the ectopic foci. PVCs occur before the impulses are initiated in the SA thus overriding its operation and normal sinus rhythm contraction. Since an electrical impulse occurs in ventricles, the resulting QRS complex is of high voltage and of abnormal

morphology. The sequence of electrical and mechanical events during the PVC is as follows:

1. The ectopic focus (the secondary pacemaker) initiates an electrical impulse in the ventricles.
2. The lower heart chambers (ventricles) contract earlier than normal, while lower chambers (atria) do not, which causes a lower amount of blood to be pumped.
3. A pause is followed after the PVC, allowing ventricles to fill with more blood.
4. The following cycle might be initiated by the SA node.

PVCs maybe classified according to the frequency of occurrence and their relationship to normal beats. Frequent PVCs are considered if the occurrence is $\geqslant$10 PVCs per hour or $\geqslant$6 PVCs per minute. In relation to normal beats, PVCs may be classified to:

1. Bigeminy: every second beat is PVC.
2. Trigeminy: every third beat is PVC.
3. Quadrigeminy: PVC occur at every fourth beat.
4. Couplet: two consecutive PVCs.
5. Non-sustained ventricular tachycardia: $\geqslant$3 PVCs in a row take place.

Atrial fibrillation. Atrial fibrillation (AF) is an abnormal rhythm during which the electrical impulses are generated chaotically throughout the upper atria of the heart, characterized by rapid and irregular contractions. It is a most common type of supraventricular tachycardia. During AF, the electrical impulses are not generated solely by the SA node; however, they are initiated in other parts of the atria. These abnormal impulses occur more rapidly and irregularly and may exceed 350 bmp. Instead of producing an atrial beat, the muscles just fibrillate ineffectively and resulting in no P waves. The rapid and irregular impulses cause inefficient contractions of the atria thus reducing the ability of the atria to pump blood into the ventricles. The ventricles are excited by the fast, irregularly spaced atrial impulses; however, ventricles are partially protected by the AV node when they pass through it. The AV node dampens a number of those rapidly initiated atrial impulses before conducting some of the impulses to the ventricles. Still, the ventricular rate is usually much faster than normal, and it is also irregular. The contractions of the ventricles may average 150 bpm, which is much slower

than the rate in the atria since the ventricles are unable to contract at 350 bpm. Even at an average rate of 150 bpm, the ventricles may not have enough time to completely fill with blood before the following contraction, particularly without the normal contraction of the atria. Thus AF decreases the amount of blood pumped by the ventricles because of their rapid rate of contraction and the absence of normal atrial contractions. The sequence of electrical and mechanical events during the AF is as follows:

1. Chaotic impulses occur in the atrial tissue fibrillated atria.
2. Irregular pulses pass the AV node and ventricles in an irregular fashion, which results in inefficient pumping of blood.
3. The following cycle might be irregular if the AF episode is not over or if AF is permanent – otherwise it returns to the normal SR.

AF often starts as brief periods of irregular rhythm which become longer and possibly constant over time; thus AF is classified into three major types (Zoni-Berisso et al., 2014 [35]):

1. The paroxysmal type is observed when episodes of AF occur spontaneously and may stop on their own, without any treatment being involved. The rhythm may return to SR within a week, usually in <24 hours. In some cases, the duration of AF episodes may be ⩽30 s.
2. The persistent type occurs when the rhythm of AF continues for more than a week. It may stop on its own, or it may still be restored to SR with some treatment involved.
3. The permanent type of AF takes place when the normal heart rhythm cannot be restored with treatment.

2.1.2 Epidemiology and comorbidities

Premature ventricular contractions. PVCs are one of the most common heart rhythm abnormalities which are commonly referred to as being benign (Kennedy et al., 1985 [3]; Gaita et al., 2001 [36]). It is estimated that PVCs are encountered in 1–4 % of the general population (Kennedy et al., 1985 [3]). The frequency of the PVC occurrence in the adult population varies and depends on various factors such as the medical condition, the physical activity, etc. More than a half (69 %) of the population had at least 1 PVC event during the 24-hour monitoring period Rotz et al., 2016 [37]. In a population of normal and healthy subjects, PVCs have been detected in 1 % of the subjects when using standard 12-lead electrocardiography and in 40–75 % of subjects when performing 24–48-hour Holter monitoring (Ng, 2006 [4]). The prevalence of PVCs is mostly

age-dependent (Messineo, 1989 [38]), ranging from <1 % in children under 11 years old (Southall et al., 1981 [39]), ⩽69 % in healthy adults aged 25–41 (Rotz et al., 2017 [40]), and ⩾69 % in subjects aged >75 (Camm et al., 1980 [41]). During physical exercise testing, PVCs were detected in 27 % of subjects with a known cardiac disease and had a small, however statistically significant increased mortality hazards ratio of 1.71–1.86 (Morshedi-Meibodi, 2004 [42]). However, subjects suffering from a heart disease are denoted by a higher incidence of complex or frequent PVCs (Bikkina et al., 1992 [43]). Overall, PVCs appear to be a frequent finding with a small but statistically significant increase in risk of sudden cardiac death and mortality (Abdalla et al., 1987 [44]). Since, PVCs are common on routine screening ECGs, a total of 1415 (5.8 %) participants had at least 1 PVC at baseline, and 591 developed an incident ischemic stroke during an average (SD) follow-up of 6.0 (2.0) years, resulting in a 38 % increased risk of ischemic stroke (Agarwal et al., 2015 [45]).

PVCs are thought to induce cardiomyopathy Duffee et al., 1998 [46], since pharmacological suppression of PVCs in patients with presumed idiopathic dilated cardiomyopathy subsequently improved the left ventricular (LV) systolic dysfunction. Many of these patients often have no underlying structural heart disease and subsequently develop LV dysfunction and dilated cardiomyopathy; in cases of those with an already impaired LV function from the underlying structural heart disease, the worsening of the LV function may occur (Sarrazin et al., 2009 [47]; Singh, 1997 [48]). The exact prevalence of PVC-induced cardiomyopathy is not known; it is an underappreciated cause of LV dysfunction, and it is primarily observed in older patients (Gaita et al., 2001 [36]). This observation could be due to the fact that the prevalence of PVCs increases with age or with the possibility that PVC-induced cardiomyopathy develops in a time-dependent fashion (Yarlagadda et al., 2005 [49]). In fact, Niwano et al., 2009 [50] demonstrated progressive worsening of the LV function in patients with frequent PVCs (>1000 beats/day) as measured by the LV ejection fraction (LVEF) and LV end-diastolic dimension over a follow-up period of 4 to 8 years. On the other hand, PVCs in apparently healthy people were associated with a twofold increase in the risk of all-cause mortality, myocardial infarction and cardiac death (Ng, 2006 [4]).

In meta-analysis of 11 studies, subjects with frequent PVC (⩾1 time during a standard ECG recording or ⩾30 times over a one-hour recording) were facing two-times higher risk of cardiac death than the subjects without frequent PVC. Although most studies made attempts to exclude high-risk subjects, such as those with histories of a cardiovascular disease, they did not test the participants for any underlying structural heart disease (Ataklte et al., 2013 [6]).

In a study of 239 subjects having frequent PVCs (>1000 beats/day) without structural heart disease (i.e., in the presence of the normal heart function), there were no serious cardiac events during 5.6 years on average, but there was

a negative correlation between the PVC prevalence and a decrease of the left ventricular ejection fraction and positive correlation between the PVC prevalence and the increase of left ventricular diastolic dimension. In this study, the absence of a heart disease was excluded by echocardiography, cardiac magnetic resonance imaging in 63 subjects and Holter monitoring (Niwano et al., 2009 [50]).

In the ARIC study of 14.783 subjects followed for 15 to 17 years, those with the detected PVC during a 2-minute ECG, and without hypertension or diabetes at the beginning, were facing a risk of stroke increased by 109 % (Worthington et al., 2010 [51]). Hypertension or diabetes, both being risk factors for stroke, did not change significantly the risk of stroke for the subjects with PVCs (Worthington et al., 2010 [51]). It is possible that PVCs identified those at risk of stroke with blood pressure and impaired glucose tolerance on a continuum of risk below the conventional diagnostic thresholds for hypertension and diabetes (Worthington et al., 2010 [51]). Subjects in the ARIC study with any PVC were running a risk of heart failure increased by 63 % (Agarwal et al., 2012 [52]) and were >2 times as likely to die due to coronary heart disease. Furthermore, the risk was also higher for subjects with or without baseline coronary heart disease (Massing et al., 2006 [53]).

In the Niigata study of 63.386 subjects with a 10-year follow-up period those with PVC during a 10-second recording were facing a risk of AF increased nearly 3 times independently from such risk factors as age, male gender, body mass index, hypertension, systolic and diastolic blood pressure, and diabetes (Watanabe et al., 2006 [8]).

Ventricular ectopy is more prevalent in men than in women of the same age. The male gender alone runs the increased risk of identifying PVCs on routine screening, with an odds ratio for the male gender equalling to 1.39 compared with women. Furthermore, the frequency and probability of PVC occurrence increases with age (see Fig. 2.3), reflecting the increased prevalence of hypertension and cardiac disease in ageing populations (Kostis et al., 1981 [1]).

PVCs have been examined as predictors of cardiovascular morbidity and mortality, especially with a pre-existing heart disease (Massing et al., 2006 [53]). Structural anomalies in the myocardium and/or pericardium were present in 85% of patients with exercise-induced PVCs. The majority of subjects with exercise-induced PVCs show evidence of myocardial disease consistent with acute or previous myocarditis or myopericarditis (Jeserich et al., 2015 [54]).

PVCs in subjects with heart diseases, i.e., myocardial infarction, may be associated with a variety of underlying cardiac conditions such as cardiomyopathy and increased risks of developing ventricular tachycardia, or a sustained run of rapid ventricular contractions (Koplan et al., 2009 [55]). Prolonged ventricular tachycardia may result in a low cardiac output, low blood pressure, and fainting (syncope). Ventricular tachycardia is life-threatening; it may occur suddenly

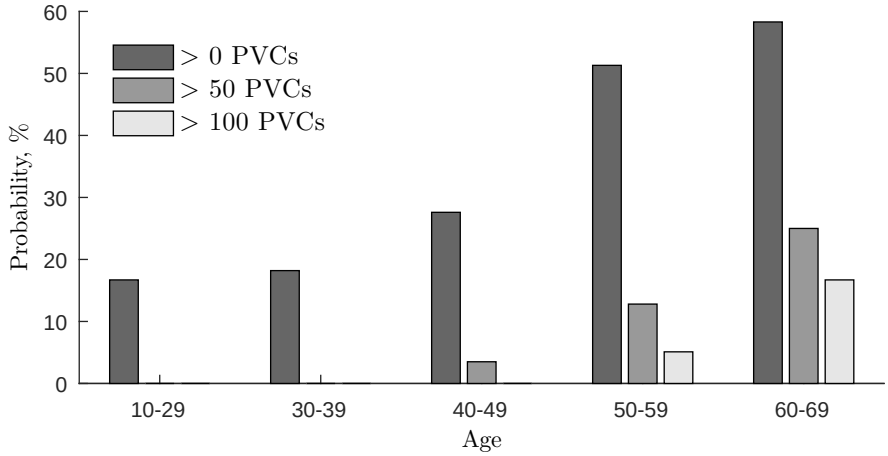

Fig. 2.3. Probability (%) of PVC occurrence during 24 hours in healthy subjects as a function of age (Kostis et al., 1981 [1]).

with no prior warning, and frequently develops into ventricular fibrillation. It is a chaotic rhythm when the ventricles fibrillate rapidly and randomly. When ventricular fibrillation occurs, the heart is unable to pump blood into the brain and the rest of the body effectively, thus, if untreated, it can be fatal within minutes, killing 250,000 Americans annually due to the incidence of sudden cardiac death (Chugh et al., 2008 [56]).

Recent studies have shown that those subjects with frequent occurrence of PVCs, i.e., several thousand a day, are associated with the left atrial enlargement in patients with the normal left ventricular ejection fraction – thus they can develop cardiomyopathy (Park et al., 2014 [57]). In such cases, if the PVCs are reduced or removed, e.g., via ablation therapy, cardiomyopathy usually regresses (Shiraishi et al., 2002 [58]; Belhassen, 2005 [59]).

Atrial fibrillation. Atrial fibrillation is the most common and ubiquitous type of cardiac arrhythmia (Ball et al., 2013 [60]; Munger et al., 2014 [61]).

Epidemiological evidence collected over the past few decades suggests a rapidly increasing prevalence of AF, e.g., the analysis of the current global epidemiological data has shown that the number of new AF cases increased by about 5 million from 1990 to 2010 (Chugh et al., 2013 [62]). AF resulted in 112,000 deaths in 2013, up from 29,000 in 1990 (Naghavi et al., 2015 [63]).

Recent estimates also suggest that 12.1 to 15.9 million patients will have AF in the United States by 2050 (Miyasaka et al., 2006 [64]) and 17.9 million people in Europe by 2060 (Chugh et al., 2013 [62]; Krijthe et al., 2013 [65]).

The estimated AF prevalence in the United States in 2010 was 2.7 to 6.1 million, and is expected to rise to the level of between 5.6 and 12 million in 2050 (Roger et al., 2011 [66]; Menezes et al., 2013 [67]). In Europe and North

America, as of 2014, it affects about 2 % to 3 % of the population (Zoni-Berisso et al., 2014 [35]). This is an increase from 0.4 to 1 % of the population around 2005 (Fuster et al., 2007 [68]). According to the latest trends, the prevalence of AF will increase dramatically in the near future. Various studies expect a 2-to-3 fold increase in the prevalence of AF by the year of 2050 (Go et al., 2001 [69]; Miyasaka et al., 2006 [64])

The estimated numbers of individuals to be affected by AF in the upcoming decades varies quite substantially among different surveys, falling between 5.6 million (Go et al., 2001 [69]) to 15.9 million (Miyasaka et al., 2006 [64]) in the United States alone. Similarly, the most recent data suggest the AF prevalence in the US will rise from 5.2 million in 2010 to 12.1 million by 2030 (Colilla et al., 2013 [18]). A discrepancy among the different studies is mainly caused by the incorrectly estimated baseline numbers of the population suffering from AF.

It has been estimated that 33 million people around the world are suffering from AF (Chugh et al., 2013 [62]). Nevertheless, given that AF is usually asymptomatic and consequently undiagnosed for many patients, these numbers most likely represent an underestimate. Therefore, reasonably larger numbers of the actual prevalence are expected, reaching up to 2 % of the general population (Camm et al., 2010 [70]).

The prevalence of AF increases substantially with age (see Fig. 2.4) as 0.14 % of the individuals under 50, 4 % between 60 and 70 years old, and 14 % over 80 years old are affected (Marini et al., 2005 [71]; Barrios et al., 2012 [72]; Zoni-Berisso et al., 2014 [35]). It is also higher in men than women with the odds of developing AF being twice as high for each advancing decade of age (Benjamin et al., 1994 [73]; Marini et al., 2005 [71]; Heeringa et al., 2006 [74]; Lloyd-Jones, 2004 [75]). Consequently, more than 12 % of adults aged >75 years have a diagnosis of AF (Heeringa et al., 2006 [74]).

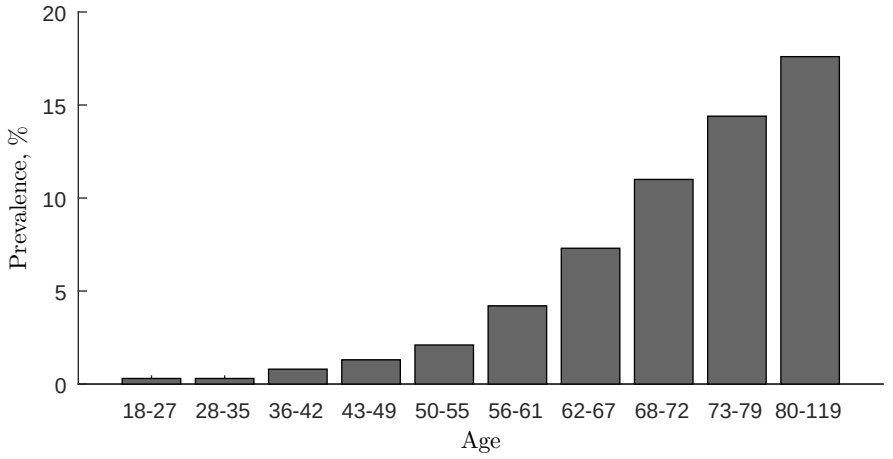

Fig. 2.4. Prevalence (%) of AF as a function of age (Barrios et al., 2012 [72]).

AF is a most common secondary occurence to cardiovascular pathologies as well as to systemic disorders; this relationship was first demonstrated in (Benjamin et al., 1994 [73]; Menezes et al., 2013 [67]). It has a significant impact on morbidity and mortality: it is estimated that AF increases the risk of stroke fivefold, and about 15 % of all the patients experiencing stroke have AF as well (Roger et al., 2011 [66]; Menezes et al., 2013 [67]). The percentage of strokes attributable to AF increases from 1.5 % at 50–59 years of age to 23.5 % at 80–89 years of age (Roger et al., 2011 [66]).

AF is associated with an increased risk of heart failure, dementia, and stroke (Justin et al., 2013 [76]). The presence of AF at the stroke onset as well as during the acute phase was confirmed by a standard electrocardiogram in 869 (24.6 %) of 3530 patients with ischemic stroke. With respect to patients without arrhythmia, those with AF in more cases were women, aged 80 years and older, suffering from coronary heart disease and peripheral arterial disease. High prevalence of AF was found in patients with a first-ever ischemic stroke, especially among elderly women (Marini et al., 2005 [71]).

AF, together with related complications (i.e., heart failure, stroke, dementia) (Gross et al., 2013 [77]), imposes a huge economic burden on many countries reaching 1–2 % of the total health care expenditure (Wolowacz et al., 2011 [78]). For instance, in the US, the annual AF-related cost was estimated to be in the range from 6.0 (exclusively AF-related costs) to 26.0 billion dollars (including indirect costs; Kim et al., 2011 [79]). A wide range of the estimated costs was suggested in order not to underestimate the lower boundary, since it is not completely clear to what extent AF contributes to detrimental comorbidities requiring special medical care. Comparable numbers of AF-related costs have been estimated in the countries of the European Union.

The Euro Heart Survey on AF (Ringborg et al., 2008 [80]) counted the combined annual cost of 6.2 billion euros in just five European countries (Greece, Italy, the Netherlands, Poland, and Spain). Approximately one-third of AF costs are due to hospitalizations, whereas outpatient medical and pharmacy expenditure accounts for the remaining two-thirds (Kim et al., 2011 [79]). In addition, individuals with AF are hospitalized twice as many times as those without AF, while multiple cardiovascular hospitalizations are even 8 times more common. As a result, the total direct medical costs are considerably higher (around 70 %) for patients with AF than for those without AF (Kim et al., 2011 [79]). It has been speculated that at least 2-fold reduction in AF prevalence could be achieved if other cardiovascular risk factors were maintained under the safe levels (Huxley et al., 2011 [81]).

Several important factors are considered to be among the most influential points concerning the growing AF epidemic: the ageing of population, the globally increasing numbers of people affected by hypertension and obesity, and the considerably improved survival from other cardiovascular diseases, such as heart

failure and myocardial infarction. These conditions cause structural changes in myocardium, and therefore increase the risk for developing AF (Chugh et al., 2013 [62]). On the other hand, the emerging novel technologies for arrhythmia detection, i.e., implantable cardiac monitors, internal and external loop recorders, together with new strategies, contribute to the increased numbers of newly diagnosed AF cases. As a result, the increased AF awareness and the initiatives to improve the detection of AF (Fitzmaurice et al., 2007 [82]; Lowres et al., 2013 [20]; Lowres et al., 2014 [83]) have contributed to the greater incidence and reported prevalence of AF in addition to the ageing population and the improved survival from other cardiovascular diseases.

2.1.3 Mechanism and Pathophysiology

Premature ventricular contractions. The underlying mechanism of the PVC origin may vary depending on the clinical circumstances. The occurrence of PVCs is explained by three known physiological mechanisms, namely, the automaticity (e.g., enhanced normal and abnormal), the reentry (e.g., anatomic and functional), and the triggered activity (e.g., delayed and early afterdepolarization) (Gaztañaga et al., 2012 [84]).

The enhanced cardiac automaticity refers to the accelerated initiation of an action potential by either a normal pacemaker tissue (i.e., enhanced normal automaticity) or by abnormal ventricular tissue within the myocardium (i.e., abnormal automaticity). Enhanced automaticity suggests an ectopic focus of pacemaker cells in the ventricle that has a subthreshold potential for firing. The basic rhythm of the heart raises these cells to the threshold which precipitates an ectopic beat. This process is the underlying mechanism for arrhythmias due to excess certain organic compounds and some electrolyte deficiencies, particularly low blood potassium (also known as hypokalemia). This ectopy of the ventricles when associated with a structurally normal heart most commonly occurs from the right ventricular outflow tract, and the mechanism behind this is thought to be 'enhanced automaticity' versus 'triggered activity'. PVCs can be triggered when inhibitors, such as caffeine, lead to the increased intracellular concentration of calcium ions (Huizar et al., 2011 [85]). The discharge rate of normal or abnormal pacemakers may be accelerated by drugs, various forms of cardiac disease, reduction in extracellular potassium, or alterations of the autonomic nervous system tone. Enhanced normal automaticity accounts for the occurrence of sinus tachycardia, while abnormal automaticity may result in various atrial or ventricular arrhythmias. Potassium ion concentrations are a major determinant in the magnitude of the electrochemical potential of the cells, and hypokalemia makes it more likely that cells will depolarize spontaneously. Hypercalcemia has a similar effect, although clinically it is of less concern. Magnesium ions affect the flow of calcium ions, and they also affect the function necessary for maintaining the potassium levels; therefore, low blood magnesium may also result in

spontaneous depolarization.

Reentry usually occurs when a slowly conducting tissue, e.g., in case of post-infarction myocardium, develops adjacent to the normal tissue. Post-infarction PVCs, on the other hand, tend to occur in regions of scar and/or damaged myocardium and may be due to enhanced automaticity, triggered activity, or possibly reentry. It has been postulated that reentry may play a role in such cases, because post-infarction PVCs often exhibit characteristics similar to post-infarction ventricular tachycardia (Hachiya et al., 2002 [86]). This condition is frequently observed in patients with underlying heart disease creating areas of differential conduction and recovery due to myocardial scarring or ischemia. During ventricular activation, one bundle tract's area of slow conduction activates the other tract's bundle fibers post block after the rest of the ventricle has recovered, resulting in an extra beat. Reentry can produce single ectopic beats, or it can trigger paroxysmal tachycardia. Triggered beats are considered to be caused by after-depolarizations triggered by the preceding action potential. These are often seen in patients with ventricular arrhythmias due to digoxin toxicity and reperfusion therapy after myocardial infarction. The already existing damage to the myocardium can also provoke PVCs. The myocardial scarring that occurs in myocardial infarction and also due to the surgical repair of congenital heart disease can disrupt the conduction system of the heart and may also irritate the surrounding viable ventricular myocytes thus making them more likely to depolarize spontaneously.

The triggered activity occurs due to the after-depolarizations, i.e., the oscillations of the membrane potential before or after the completion of repolarization, which are triggered by the preceding action potential (Zipes, 2003 [87]). When oscillations depolarize the cell to the level of the threshold potential, they induce spontaneous action potentials (triggered activity) which are responsible for premature beats and tachycardias. After-depolarizations occur, only in the presence of a previous action potential (the trigger), and when they reach the threshold potential, a new action potential is generated. This may be the source of a new triggered response, leading to self-sustaining triggered activity. Afterdepolarization can occur either during (early) or after (delayed) completion of repolarization. Early afterdepolarizations are usually responsible for bradycardia-associated PVCs as well as for ischemia and electrolyte disturbance.

Atrial fibrillation. The pathophysiology and the underlying mechanisms of AF are not yet fully understood. Nevertheless a number of theories and hypotheses tempting to explain the mechanism of atrial fibrillation have emerged (see Fig. 2.5). Theories and hypotheses of mechanisms can be divided into two major groups, namely, single-focus (Fig. 2.5 (a)–(d)) and multiple-source (Fig. 2.5 (e)–(h)).

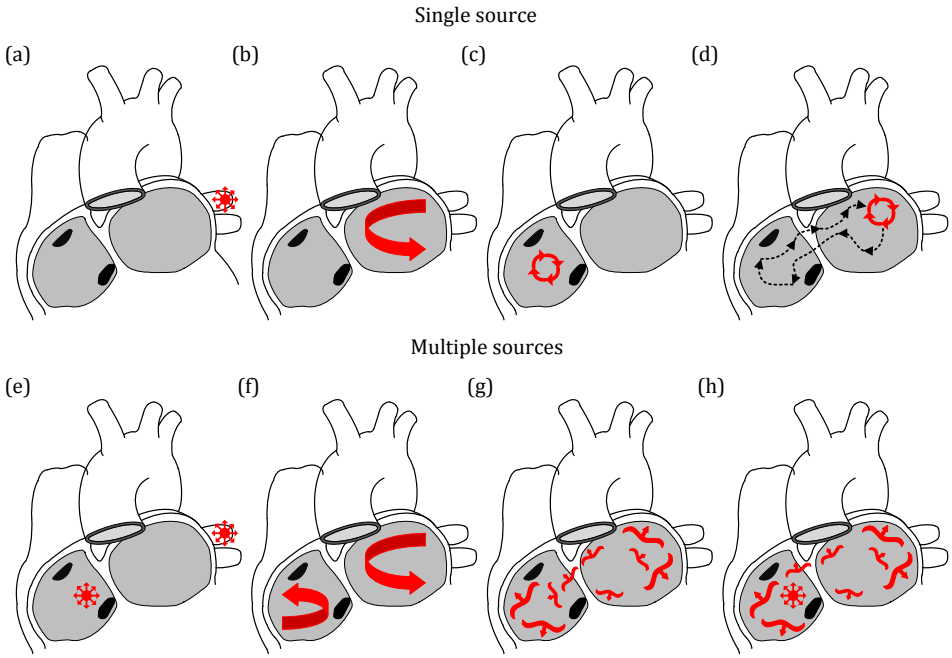

Fig. 2.5. AF mechanisms: (*a*) single automatic focus, (*b*) mother wave, (*c*) fixed rotor, (*d*) moving rotor, (*e*) multiple foci, (f) unstable re-entry circuits, (*g*) multiple wavelets, (*h*) single focus together with multiple wavelets (partially based on Camm et al., 2009 [88]).

Single-focus hypotheses state that AF occur due to the increased automaticity or a single rapid macro re-entry circuit in the area of focal activity, with wavefronts emerging from the primary driver circuit (i.e., the rotor) breaking against regions in the atria of the variable refractoriness thus causing arrhythmia (Camm et al., 2005 [89]). The excitation impulses arising from different areas of focal activity may result in the ectopic beats which, if rapid enough, may produce fibrillatory conduction and triggering of AF.

According to the multiple sources hypothesis, electrical activation in AF proceeds as multiple re-entrant wavelets separated by lines of functional conduction block generating irregular re-entrant activity which occurs in an asynchronous fashion in different regions of the atrial (i.e., it is a multiple circuit re-entry). These wavelets continuously initiate themselves (i.e., a leading circle re-entry) or each other (i.e., a random re-entry). The modelling of multiple wavelet hypothesis by Moe et al., 1964 [90] showed that fibrillatory conduction during episodes of AF may be initiated and sustained by the propagation of random wavelets in the heterogeneous arterial tissue. It was concluded that wavelets and the subsequent 'daughter wavelets' may stem from any triggering mechanisms. AF is sustained as long as an adequate number of wavelets propagates simultaneously, in turn depending on the minimally sufficient atrial

mass. Therefore, this hypothesis defines AF as a self-sustaining process independent either from a single source initiator, i.e., an ectopic focus, or the atrial structure needed to sustain a circular propagation. A couple of decades later, the hypothesis was supported with the experiments by Allessie et al., 1985 [91], demonstrating that a minimum of 4–6 wavelets may be and adequate number to sustain AF.

The evolution of AF from paroxysmal to persistent and then to permanent is influenced by the atrial re-modeling caused by arrhythmia per se and/or by the progression of the underlying heart disease (Nattel et al., 2008 [92]). Allessie et al., 1985 [91] suspected that AF produces both electrophysiological and structural abnormalities which may result in a permanent AF. It was revealed that the sources of focal triggering located on the surface of pulmonary veins are responsible for the initiation of AF Haïssaguerre et al., 1998 [93]. In case of paroxysmal AF, the electrophysiological remodeling and development of functional re-entry substrates stemming from the altered expression and/or function of the cardiac ion channels can reverse-remodel when AF has been terminated (Allessie et al., 2002 [94]; Nattel et al., 2008 [92]). Ultimately, if AF frequently reoccurs and is sustained for longer periods of time, a hazardous condition of atrial remodelling may start, which further leads to an extremely undesired and difficult to manage phenomenon when 'AF begets AF' (Wijffels et al., 1995 [95]). In other words, atrial cells start to remodel electrophysiologically during prolonged episodes of AF, therefore, a more abnormal atrial substrate is created, which promotes the sustenance of AF even longer. As atrial disease progresses to irreversible structural changes, AF becomes permanent (Nattel et al., 2008 [92]). The propagation may be restricted, but AF will not terminate during catheter ablation due to lack of a localized source. However, owing to the complex temporal interplay between the AF driver and the atrial substrate, electrical and structural re-modeling may allow AF to persist even after the driver has been removed. As a result, depending on the amount of substrate in the atrial tissue, re-entry can originate in multiple circuits. During even more advanced stages of AF, i.e., chronic AF, multiple re-entry circuits may become highly unstable, engaging a rotor re-entry. Therefore, if AF is treated early, especially when AF episodes are rare and short, its progression can be halted.

2.1.4 Symptoms, Risk Factors, Treatment and Management

Symptoms and risk factors. Mostly, both PVC and episodes of AF are asymptomatic (Bhandari et al., 1992 [96]); however, the symptoms listed in Table 2.1 may be experienced during these arrhythmic events:

Many risk factors may be responsible for causing PVC and AF; therefore, a number of risk factors and possible complication are presented in Table 2.2.

Table 2.1. List of symptoms experienced during arrhythmic events

No.	Symptom	PVC	AF
1	Heart palpitations	Y	Y
2	Dizziness	Y	Y
3	Fainting (syncope)	Y	Y
4	Lightheadedness	Y	Y
5	Weakness (rest, exercise / activity)	Y	Y
6	Fatigue	Y	Y
7	Shortness of breath	Y	Y
8	Chest pain	Y	Y

* Y stands for YES

Table 2.2. List of arrhythmia-causing risk factors and complications

No.	Risk factor and complications	PVC	AF
1	Myocardial infarction	Y	Y
2	Heart failure	Y	Y
3	Stroke	Y	Y
4	Coronary artery disease	Y	Y
5	Blood pressure (hypertension)	Y	Y
6	Cardiomyopathy	Y	Y
7	Congestive heart failure	Y	Y
8	Congenital heart disease	Y	Y
9	Disease of heart valves (prolapse)	Y	Y
10	Rheumatic fever and heart disease	Y	Y
11	Other heart rhythm problems	Y	Y
12	Chronic obstructive pulmonary disease	Y	Y
13	Hypoxia (lung diseases)	Y	Y
14	Hyperthyroidism (thyroid dysfunction)	Y	Y
15	Myocarditis (muscle inflammation)	Y	Y
16	Cardiac contusion (heart muscle injury)	Y	Y
17	Anemia	Y	Y
18	Electrolite imbalance (hypokalemia, hypomagnesemia)	Y	Y
19	Stress, anxiety	Y	Y
20	Infections	Y	Y
21	Raised hormone level (adrenaline, thyroid)	Y	Y
22	Excessive caffeine or alcohol intake	Y	Y
23	Stimulant drugs and antidepressant medications	Y	Y
24	Smoking	Y	Y
25	Diabetes mellitus	Y	Y
26	Obesity	Y	Y
27	Sleep apnea	Y	Y
28	Chronic kidney disease	Y	Y

* Y stands for YES

Treatment and Management of Premature Ventricular Contractions. Premature ventricular contractions (PVCs) are the most common type of irregular heartbeats. The reason for treating PVCs is to relieve the symptoms of palpitation or to treat the conditions which cause PVCs since such conditions are potentially life-threatening. Figure 2.6 shows the options used for the treatment and management of PVCs. In most cases, PVCs can be controlled with lifestyle changes, such as reducing or eliminating caffeine, tobacco and alcohol intake or reducing stress and anxiety. A beta blocker medication may also be prescribed for patients with PVCs. Anti-arrhythmics and ablation is another treatment option for some patients with frequent or prolonged PVCs.

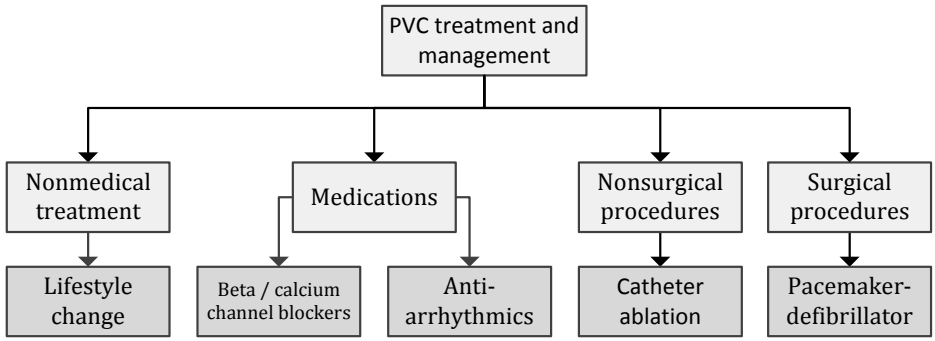

Fig. 2.6. General approaches to treat and manage PVCs.

In the absence of heart disease and if PVCs are infrequent or if PVCs reduce in frequency when performing the exercise tolerance test, and there is no documented ventricular tachycardia, no further investigation and treatment is required, particularly if PVCs are relatively asymptomatic. Subjects with significant symptoms should have their blood pressure checked and investigated, and treated if the pressure is high. For the relief of palpitations, some preventative measures to eliminate the triggers might be considered, such as stopping alcohol and caffeine intakes, quitting the use of medications containing adrenaline, stopping drug abuse, and giving up smoking. In healthy individuals, PVCs can often be resolved by restoring the balance of magnesium, calcium and potassium within the body.

Beta-blockers may be used to control symptoms in patients where PVCs arise from multiple sites. It should also be considered in patients with the impaired ventricular systolic function and/or heart failure. There is no evidence to support the use of other anti-arrhythmic agents simply for the sake of suppressing PVCs, especially considering their pro-arrhythmic and other side effects (Ng, 2006 [4]). A therapeutic medical trial or catheter ablation may be considered in patients with left ventricular dysfunction and frequent PVCs (a generally accepted range is referred to as >10,000–20,000 or >10 % of the total beats per 24 hours) if the clinical suspicion for PVC-induced cardiomyopathy is high (Kanei

et al., 2008 [97]; Niwano et al., 2009 [50]).

Anti-arrhythmia medications are used to control PVCs in order to prevent ventricular tachycardias, ventricular fibrillations, and sudden death. Unfortunately, there is little scientific evidence that suppressing PVCs with anti-arrhythmic medications will prevent ventricular tachycardias, ventricular fibrillations, and sudden death. Some anti-arrhythmia medications can actually cause abnormal heart rhythms. Thus anti-arrhythmic medications are only prescribed cautiously for patients at high risk of developing ventricular tachycardia and ventricular fibrillation, and, usually, initially such prescriptions are made in the hospital setting. Although anti-arrhythmic medications could suppress PVCs, they increase the risk of death (Ng, 2006 [4]). This does not apply to beta-blockers which are prescribed to many heart patients for many reasons, and which not only do not accelerate arrhythmias, but usually decrease premature ventricular contractions. In many patients with PVCs and a significant underlying cardiac disease, or with severe symptoms, electrophysiology testing may be recommended. This is a test performed with catheters to see if a patient is at risk of life-threatening ventricular arrhythmias, which are treated with either medications or, sometimes, with implantable defibrillators.

Catheter ablation treatment is advised for subjects with ventricular dysfunction and frequent arrhythmias or very frequent PVC ($>$20 % in 24 h) and normal ventricular function (Niwano et al., 2009 [50]). This procedure destroys the area of the heart tissue that is causing the irregular contractions characteristic of PVCs by using the radio frequency energy. Reducing frequent PVCs (i.e., $>$20 %) by antiarrhythmic drugs or by catheter ablation significantly improves the heart performance (Belhassen, 2005 [59]; Ng, 2006 [4]).

Heart attacks can increase the likelihood of having PVCs. In severe cases, an implantable defibrillator may be used for patients with nonsustained ventricular tachycardia due to prior myocardial infarction, left ventricular ejection fraction less than or equal to 40 %, and inducible ventricular fibrillation or sustained ventricular tachycardia at electrophysiological testing (Ng, 2006 [4]; Ahn, 2013 [98]).

Treatment and management of atrial fibrillation. The strategy for atrial fibrillation treatment and management depends on the type of AF and its progression (i.e., paroxysmal, sustained or permanent), the severity of symptoms, the underlying cause of AF (e.g., thyroid disorder) and other problems with the heart. Generally, the main goals of the AF treatment are to reset the rhythm or to control the rate and to prevent blood clots. Figure 2.7 shows the available options for the treatment and management of AF.

Many people experience episodes of AF and yet are not aware of them. Therefore lifelong anticoagulants, such as aspirin, or anti-clotting medications, such as warfarin, or a novel oral anticoagulant may be recommended to minimize

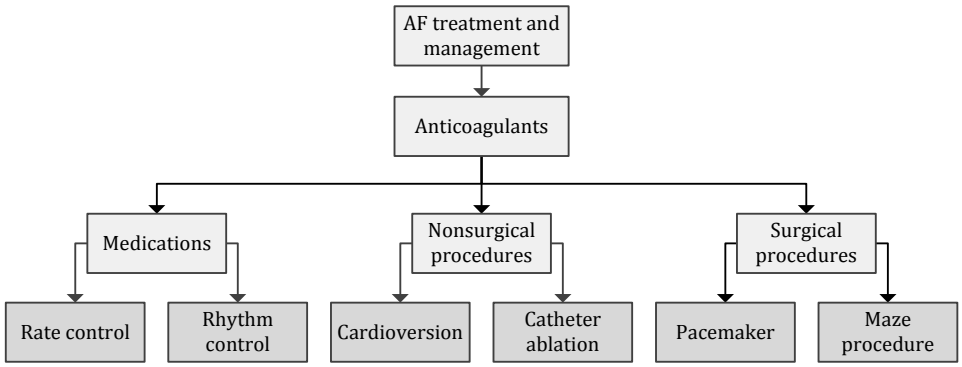

Fig. 2.7. General approaches towards the treatment and management of AF.

the risk of stroke even after the rhythm has been restored to normal. (Munger et al., 2014 [61]).

If there is a possibility and no contraindications, AF is often treated with medications to slow the heart rate to a near normal range (known as the rate control) or to convert the rhythm to the normal sinus rhythm (known as the rhythm control) (Anumonwo et al., 2016 [99]). However, in some cases, a more invasive treatment, such as surgery or medical procedures using catheters, may be required.

When the symptoms of AF are bothersome and AF is not permanent, the rhythm may be reset to the normal sinus rhythm by applying cardioversion. Cardioversion can be conducted in two ways, by using electrical cardioversion or cardioversion with drugs.

Electrical cardioversion is used to convert AF to a normal sinus rhythm and is often used emergently, when the subject is unstable (Oishi et al., 2013 [100]). During electrical cardioversion, an electrical impulse is delivered to the heart through the electrodes on the chest which temporary pauses the electrical activity of the heart. When the electrical activity of the heart restarts, the heart may resume its normal rhythm. The procedure is performed during sedation, so there is no sensation of the electric impulse. As a preventative measure for future AF episodes, anti-arrhythmic medications may be prescribed after the procedure.

Cardioversion with drugs uses medications called anti-arrhythmics in order to restore the normal sinus rhythm. Depending on the heart condition, intravenous or oral medications may be recommended. The treatment is often conducted during continuous monitoring of the heart rate. If the heart rhythm returns to normal, the same or similar anti-arrhythmic medication may be prescribed so that to prevent recurrence of AF. Prior to cardioversion or in case of permanent AF, an anticoagulant medication, e.g., warfarin, may be given to reduce the risk of blood clots formation and stroke. Anticoagulant medication

may also be taken to prevent blood clots from forming even after the rhythm of heart has been restored to normal. Although medications may help to maintain the normal heart rhythm, they can cause various adverse effects such as life-threatening ventricular arrhythmias, e.g., ventricular tachycardia and ventricular fibrillation, worsening of heart failure and low blood pressure, or major bleeding (Jun et al., 2015 [101]; Heidbuchel et al., 2015 [102]). However, sometimes even medications or cardioversion may not provide a significant effect, and there is always a possibility that AF will recur.

In such cases, the catheter ablation procedure may be used to eliminate the area of heart tissue that is causing the erratic electrical signals in order to restore the normal heart rhythm. In case of catheter ablation, catheters are inserted and guided through blood vessels to the heart. Electrodes at the catheter tips apply radiofrequency energy, extreme cold (e.g., cryotherapy) or heat to destroy and scar tissues causing erratic impulses. Since the scar tissue does not carry electricity, the rhythm can thus be normalized. Catheter ablation may correct AF without the need for medications or implantable devices and may also prevent recurrence in some people (Amerena et al., 2013 [103]). A surgical procedure to implant a pacemaker might be required to keep the ventricles beating properly.

Surgical procedures, such as the maze procedure, are generally reserved for subjects not responding to other treatments or when they may be performed during other necessary heart surgery, such as the coronary artery bypass surgery or heart valve repair. The surgical maze procedure is conducted while performing an open-heart surgery where precise incisions in the upper chambers of the heart are made to create a pattern of the scar tissue.

2.2 Diagnosis of Premature Ventricular Contractions and Atrial Fibrillation

2.2.1 Diagnosis of the Arrhythmia

The diagnosis is made by sensing the pulse and is confirmed by using an electrocardiogram (ECG) (Ferguson et al., 2014 [104]), i.e., a typical ECG during PVCs shows a wide and abnormal QRS complex with a shorter preceding and longer succeeding intervals, while the ECG during AF shows no P waves and produces irregular ventricular contractions (Ferguson et al., 2014 [104]). The evolving technologies provided a wide array of monitoring options for patients suspected of having cardiac arrhythmias, with each modality differing in terms of the duration of monitoring, quality of recording, convenience, and invasiveness.

There are three forms of ECG testing which are used to assess the electrical activity of the heart under different circumstances: resting ECG, ECG stress test, and ambulatory ECG. Physicians also use electrophysiologic testing to diagnose arrhythmias. Electrophysiologic monitoring examines the electrical function of the heart within the heart itself by inserting catheters – usually thin,

flexible tubes – into the coronary arteries. Resting ECG, ECG stress tests, and electrophysiologic testing are typically used for detecting frequently occurring arrhythmias, while ambulatory ECG is used for infrequent arrhythmias.

For frequent or constant arrhythmias, physicians perform a resting ECG or an ECG stress test at a physician's office or at a hospital as 10–15 electrodes are placed on the subject's chest, arms, and legs. For the resting ECG, the patient lies down during the test. For the ECG stress test, patients walk on a treadmill for 5–15 minutes. For subjects who are unable to exercise, the effects of the exercise test on the heart can be simulated with drugs.

To monitor infrequent arrhythmias, the physician uses ambulatory ECG, or event recording. The patient wears portable ECG devices recording arrhythmic events while the patient is away from the physician's office. Ambulatory monitoring devices include: Holter monitors and intermittent recorders.

2.2.2 Ambulatory Arrhythmia Monitoring and Screening

Many heart problems are noticeable only during certain activities, including exercise, eating, sex, stress, bowel movements, and even sleeping; therefore, an ambulatory ECG is more likely to detect abnormal heartbeats occurring during these activities. Many people experience irregular heartbeats (i.e., arrhythmias) from time to time. What this means depends on the type of pattern they produce, how often they occur, how long they last, and whether they occur at the same time the symptoms are felt. As arrhythmias can come and go, it may be hard to record one while the subject is visiting a physician. There are several different types of ambulatory monitors. The physician decides upon the type that should work best for the subject and is the most likely to help diagnoze the heart problem (Hoefman et al., 2010 [105]; Subbiah et al., 2013 [106]). An ambulatory ECG monitor records the electrical activity of the heart while the subject is performing the usual daily activities. The ambulatory test means that the subject walks during the test. This type of monitoring may also be called ambulatory ECG, Holter monitoring, 24-hour ECG, or cardiac event monitoring. A continuous recorder gives a 24–72 hour record of the electrical signals from the heart. A standard ECG monitor records only 40–50 heartbeats during the brief time when the subject is attached to the machine, whereas a continuous recorder monitors 100,000 heartbeats in 24 hours. Therefore, it is more likely to capture any heart problems happening in the course of activity.

Holter monitors. A Holter monitor is used to record ECG continuously during a period of at least 24–72 hours while the subject is performing his/her regular daily tasks. A Holter monitor is usually applied if a subject is suspected of having cardiac arrhythmia less frequently and this arrhythmia fails to be detected with a conventional ECG recorder. This kind of monitoring is usually performed so that to verify whether there are any dangerous cardiac arrhythmias that might require

treatment. A relatively compact recorder (see Fig. 2.8) is worn and attached to the body with straps for fastening the device itself and sticker electrodes similar to those applied during the conventional ECG recordings.

Fig. 2.8. Holter monitor *Medilog*® FD12 plus by *Schiller AG*.

Wires from the electrodes lead to a small battery-powered device that can be clipped onto a waistband or a belt, or placed in a small carrying case and slung over a person's shoulder. The electrode pads are then attached to the skin of the chest. Thin wires are connected to the electrodes and the monitor. To verify whether the electrodes are attached correctly, the subject may be briefly hooked up to a standard ECG recorder. A conventional ECG recorder employs 12 leads which are useful when diagnosing, e.g., heart attack; however, usually, not all the leads are of interest. Additionally, it is highly inconvenient for the subject to wear 10 electrodes for a longer period of time. Therefore, the majority of portable Holter monitors are designed with 3–7 electrodes capable of recording 1, 2, 3, or 5 channels.

Holter recording is noninvasive and painless; however, sometimes, the sticker electrodes might irritate the skin during the recording time. Subjects are asked to keep a diary of events during the 24–72 hour period, which is helpful for knowing when the subject was active, sleeping or having any symptoms that might be caused by cardiac arrhythmia. Subjects keep a diary of their activities, such as sleeping or eating, so that physicians could associate any arrhythmia with a specific activity. Once the recording has been completed, the recorder and sticker electrodes are disconnected, and the recorder is taken back to the physician for the ECG analysis and interpretation. A technician will process the information from the recorder for the cardiologist to review. Since a Holter recorder is usually only worn for 24–72 hours, it is particularly helpful when any symptoms occur at least once a day. If the symptoms happen less frequently, an intermittent event recorder may be recommended instead. During Holter monitor testing,

patients should avoid taking showers or baths; they should also limit the use of small electrical devices, such as electric toothbrushes or razors. Furthermore, the electrodes used to record ECG are attached to the patient's chest, which results in discomfort, limited freedom of movement, and an increased feeling of unhealthiness, especially after wearing the device for several days (Rosero et al., 2013 [26]). A study conducted by Asmundis et al., 2014 [107] showed that intermittent monitoring is more effective in detecting arrhythmic events than the use of Holter monitors.

Intermittent recorders. An intermittent recorder is employed when the symptoms of an irregular heart rhythm are rare. Compared to the Holter monitors, the intermittent recorder can be used for a longer period of time. The information collected by an intermittent recorder can often be sent over the phone to a physician for the analysis, interpretation, and further actions. The approach by which the intermittent recording is performed depends on the type of monitor in use.

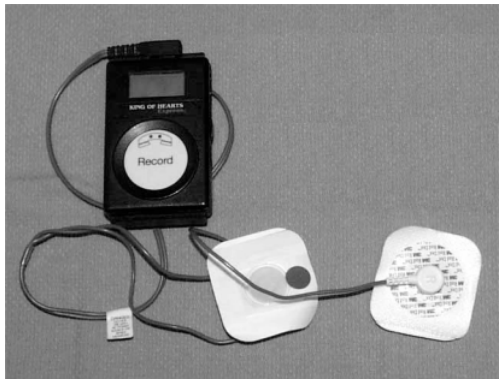

Fig. 2.9. External loop recorder *King of Hearts*® by *CardioComm Solutions*, Inc.

Loop recorder. A loop recorder is used to perform a continuous recording of the ECG signal (see Fig. 2.9). It records ECGs when some symptoms are present. Loop recorders also save a small amount of information about how the heart was beating when the subject pressed the recording button. A continuous loop recorder captures only a few minutes worth of the ECG at a time on its memory. It continuously records new information and discards the oldest information, so that at any time it contains only the last few minutes of ECG in the memory. Since the loop recorder is continuously refreshing its memory, the loop recorder can be carried for long periods of time. This is called *pre-symptom recording*. This feature is especially useful for patients who faint when their heart problems occur and can press the button only after they wake up. Electrodes are attached to the chest in the same way as a Holter monitor is. When symptoms are being

experienced, the subject presses a button on the monitor to start recording the heart rhythm. The recorder may start recording on its own when an irregular rhythm is detected. Instead, an additional hand-held device might also be used to start the monitor when symptoms occur. The recorder can be worn for several weeks. This may be a good choice for subjects experiencing rarely occurring symptoms, such as once every 6 months. Furthermore, loop recorders are optimal for capturing brief arrhythmia episodes when it takes too long to apply an event recorder or for capturing ECG recordings of episodes that are associated with incapacitating symptoms such as syncope. Subjects experiencing symptoms only a few times a year may be recommended to wear an implantable device which is inserted in the chest for up to 18 months.

Fig. 2.10. Implantable loop recorder *Reveal LINQ*™ by *Medtronic*, PLC.r (left) and an AAA battery (right) for size comparison.

Implantable loop recorders. The implantable loop recorder (see Fig.2.10) is a miniature, usually single-lead, subcutaneous loop recorder which is implanted between the chest skin and the rib cage, above the heart, by means of surgery, sometimes using only local anaesthesia. Same as the standard loop recorder, the implantable one can be programmed for automatic recording whenever irregular rhythm is detected. Furthermore, the implantable loop recorder may be triggered externally from the remote control, e.g., attached to the wrist. Implantable loop recorders are particularly useful either when symptoms are infrequent and are not amenable to diagnosis when using short-term external ECG recording techniques or when it is required to aggregate long-term data, e.g., a burden of PVCs or AF. This kind of implantable devices may operate for up to 6 years and may even be recharged by using wireless charging. The stored data is retrieved through the skin by using wireless communication. There is no need to unplug the device, e.g., when taking a shower, and there is no discomfort in wearing it; also, there is no difficulty related with attaching and reattaching electrodes since no external electrodes or power sources are required. Such characteristics are suitable for long-term continuous monitoring in high-risk subjects with recurrent episodes of palpitations or syncope and documented premature beats or AF, and for risk stratification in subjects who have sustained myocardial infarc-

tion and for those who have certain genetic disorders (Krahn et al., 2004 [108]). However, the presence of an active infection or bleeding diathesis may preclude implantation. Other adverse factors include the need for a minor surgical procedure, the difficulty of always being able to differentiate supraventricular from ventricular arrhythmias, the presence of under- or over-sensing that may exhaust the memory of the implantable loop recorder, and the cost of the device. The implantable loop recorder has a high initial cost; however, it may actually be more cost-effective than a strategy incorporating multiple nondiagnostic investigations (Davis et al., 2012 [109]).

Event monitor. Event monitors are used when symptoms are presumed to be due to the rhythm disturbances when they occur less frequently than once during a 24–48 hour period. Like loop recorders, event monitors tend to be smaller than Holter monitors due to the lesser information storage capacity since the recording is only enabled when an incidence occurs (as opposed to continual recording). Event monitors are capable of recording short episodes of an ECG and need not be worn continuously. Although an event monitor could be detached from the body for hygiene procedures, it should still be reattached afterwards and worn for at least 24 hours. There is a number of different types of event monitors, some of which require attaching electrode patches with wires to the chest area and linking the wires to a recording device. Others require no patches, however such devices are worn as a bracelet or a wrist watch or used as thumb ECG devices (see Fig. 2.11). In these cases, the ECG is recorded by contacting a second electrode with the opposite hand or by touching both electrodes with thumbs. When symptoms are present, the monitor could be temporarily attached to the body. Depending on the design, the back of the device might have small metal electrodes – or if the device is of the bracelet type, it usually has one electrode on the back and the second electrode on the top of the bracelet. The recording is usually activated by pressing the record button on the monitor attached to the chest or by touching the bracelet. The recording might last for up to a minute or slightly more. The recorded ECG might then be transmitted, for example, over the smartphone via the internet connection to the physician for further analysis and interpretation. An event monitor might be issued for at least one month to allow capturing suspicious cardiac events.

Alternative screening approaches. New, more convenient and cost-effective solutions, strategies and technological approaches for the monitoring of arrhythmia have been emerging, for instance, the use of a smartphone camera and a dedicated App (Freedman, 2016 [31]; Garabelli et al., 2017 [110]). Such approaches allow for the initial arrhythmia monitoring without attaching multiple electrocardiogram electrodes to the body. However, camera-based approaches are not intended for long-term continuous arrhythmia screening. Long-term

Fig. 2.11. Event monitor *Zenicor thumb-ECG* by *Zenicor Medical Systems* AB.

photoplethysmogram-based screening requires continuous recording and analysis of the photoplethysmogram signals, which is associated with motion-induced artifacts and may dramatically increase the rate of false alarms. Therefore, approaches capable of distinguishing between the normal and abnormal rhythm from the artifacts are required. This would allow for reliable, long-term continuous arrhythmia screening by employing unobtrusive, e.g., wrist-band type, devices without using electrocardiogram signals.

2.3 Conclusions of the Chapter

1. The prevalence and frequency of premature ventricular contractions as well as atrial fibrillation has been increasing because of the ageing population.

2. Premature contractions may be both the symptom of the disease, e.g., myocardial infarction, or its cause, e.g., cardiomyopathy. Frequent premature ventricular contractions, especially in subjects suffering from heart disease and severe symptoms, must be investigated, and treatment should be considered.

3. Atrial fibrillation tends to progress without noticeable symptoms and may become incurable with serious comorbidities, e.g., stroke and myocardial infarction; therefore means for early detection and management are of major interest.

4. Cardiac arrhythmias are usually detected and evaluated by using electrocardiogram recordings; however, more convenient and cost-effective approaches are needed.

3 OVERVIEW OF PPG-BASED METHODS FOR ARRHYTHMIA DETECTION

3.1 Introduction to Photoplethysmography

3.1.1 Principles of Photoplethysmography

Photoplethysmography is a relatively simple, optical, non-invasive technique, primarily used for the monitoring of local hemodynamical changes in the vascular system by illuminating tissues with the light of a certain wavelength. The principle of photoplethysmography utilizes the property of blood to absorb light more strongly compared to the surrounding tissues. The photoplethysmography sensor is composed of a light-emitting diode (LED) light source and a photodetector (PD), usually a photodiode, serving the objective to receive the unabsorbed light. The intensity of the light received by PD, changes the output voltage signal which is proportional to the volume of blood in the blood vessels pumped during each cardiac cycle. This output voltage provides only a relative change in blood volume and, therefore, the exact amount of blood is not quantified.

Two main configurations of photoplethysmography sensors are employed for PPG acquisition, namely, the reflection and transmission modes. A detailed illustration of these two configurations is demonstrated in Fig. 3.1.:

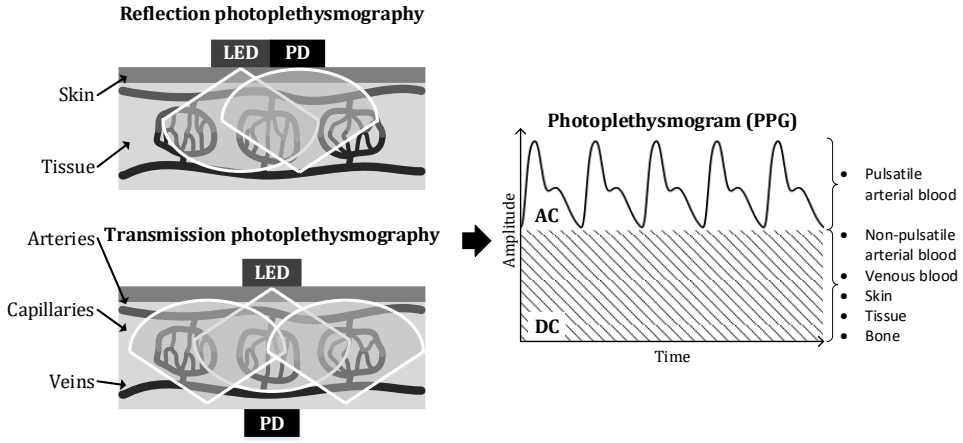

Fig. 3.1. Principle of reflection and transmission photoplethysmography as well as the composition of the resulting PPG signal.

In the reflection sensor configuration, the light source and PD are posi-

tioned next to each other. In this configuration, PD receives the light which is back-scattered or reflected from blood vessels, tissue, bone, etc. The reflection configuration poses virtually no restrictions or problems associated with the placement of the sensors; a variety of measurement sites can be used.

In the transmission configuration, the light source and PD are positioned on the opposite sides of the tissue, e.g., an earlobe is located between the light source and the PD. In this configuration, the light transmitted through the medium is received by a PD which is spatially opposite the LED source. Clearly, in contrast to the sensors with the reflection configuration, the application of a transmission sensor is limited by the measurement site. The earlobe and the finger are the most common monitoring positions used with a transmission type sensor.

As seen in Fig. 3.1, a PPG signal is composed of several components, one being alternating (AC) and the other being constant (DC) offset. When light propagates through biological tissues, it is absorbed by pulsatile arterial blood, venous blood, bones, skin pigments and other surrounding tissues. Therefore, the AC component corresponds to variations in the blood volume in synchronization with the heart-beat. The DC component arises from the optical signals reflected or transmitted by the tissues and is determined by the tissue structure as well as venous and arterial blood volumes. The DC component shows minor changes with respiration. The basic frequency of the AC component varies with the heart rate and is superimposed on the DC baseline. The PPG signal consists mainly of the following components:

1. Arterial blood volumetric changes reflecting the cardiac activity. Absorption due to pulsatile arterial blood (AC).

2. Venous blood volume changes resulting in a slow changing signal having a modulatory effect on the PPG signal. Absorption due to nonpulsatile arterial blood and venous blood (DC).

3. A DC component due to the optical property of the biological tissue. Absorption due to skin, bone and tissue.

Originally, photoplethysmography employs two LEDs emitting light at different wavelengths, one being red (660 nm), the other being infrared (900–940 nm). These wavelengths are the most suitable for the use in the cases of oxygen saturation (SpO_2), since oxygenated hemoglobin absorbs more infrared light and allows more red light to pass through. However, this works in the opposite direction for deoxyhemoglobin. Deoxyhemoglobin absorbs more red light and allows infrared light to pass through. As a result, the pulse oximeter needs to have both red and infrared light emitters so that to estimate the SpO_2. However, red and, especially, infrared light penetrates deep into the tissue and, for certain applications, such as the heart rate measurement, this may result in additional sources of unwanted noise, since the deeper the light goes, the more

tissue reflects and scatters it. Various studies showed that green light penetrates deep enough to sense pulsatile blood variations; however, it is not deep enough for the light to be affected by deeper tissues (Lee et al., 2013 [28]; Matsumura et al., 2014 [111]). Figure 3.2 shows skin penetration depth by light at different wavelengths (Bashkatov et al., 2005 [112]).

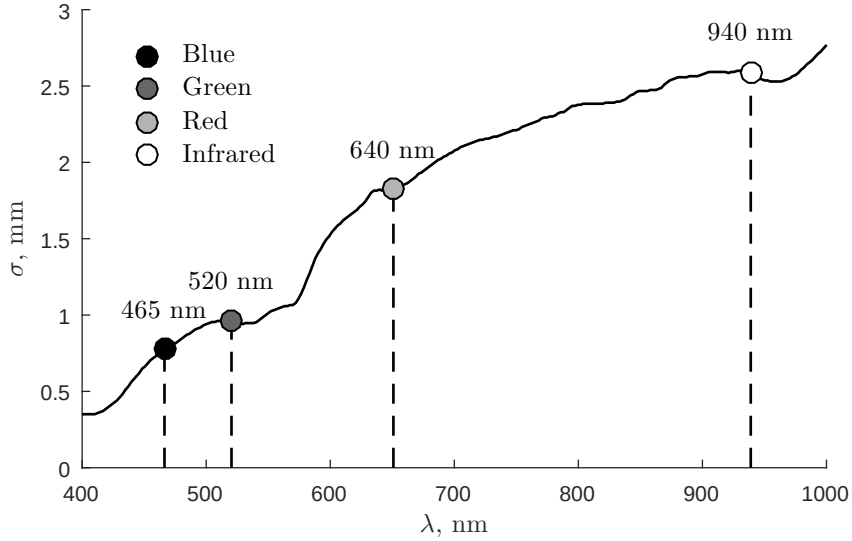

Fig. 3.2. Optical penetration depth of skin σ as a function of wavelength λ ranging from 400 nm to 1000 nm (Bashkatov et al., 2005 [112]).

In order to be effective, the photoplethysmography sensor must be located on the body at a site where the transmitted light can be readily detected. Table 3.1 shows PPG measurement sites:

3.1.2 Waveform of PPG

The morphology of the PPG waveform differs from subject to subject and depends on various factors starting from the location where and how the PPG sensor is attached and ending with the physiological peculiarities, such as vascular compliance. The pulsatile (AC) component of the PPG signal is comprised of individual pulses, associated with a single cardiac cycle. The formation of typical PPG pulse morphology is divided into two major phases: the anacrotic phase, associated with the systole and the rising edge of the pulse and the catacrotic phase associated with the diastole and the falling edge of the pulse. The principle of PPG pulse formation is illustrated in Fig. 3.3. During the anacrotic phase, the direct pulse wave (W_D) propagates from the ventricle along the aorta to the periphery, whereas, during the catacrotic phase, the pulse wave upon being reflected from the periphery (W_R), mainly in the lower body, returns back. The sum of W_D and W_R waves results in the PPG pulse with the gap between

Table 3.1. List of sites suitable for the measurement of photoplethysmogram for reflection and transmission sensor configurations

No.	Measurement site	Reflection configuration	Transmission configuration
1	Wrist	Y	N
2	Finger	Y	Y
3	Upper arm	Y	N
4	Toe	Y	Y
5	Earlobe	Y	Y
6	Ear canal	Y	N
7	Cheek	Y	Y
8	Tongue	Y	Y
9	Neck	Y	N
10	Forehead	Y	N
11	Upper eyebrow	Y	N
12	Temple	Y	N
13	Nasal septum	Y	Y
14	Vagina	Y	N

* Y/N stands for YES/NO

the two waves called the dicrotic notch. A dicrotic notch, as shown in Fig. 3.3, is usually seen in young subjects with healthy arteries and is related to the compliance of the arteries.

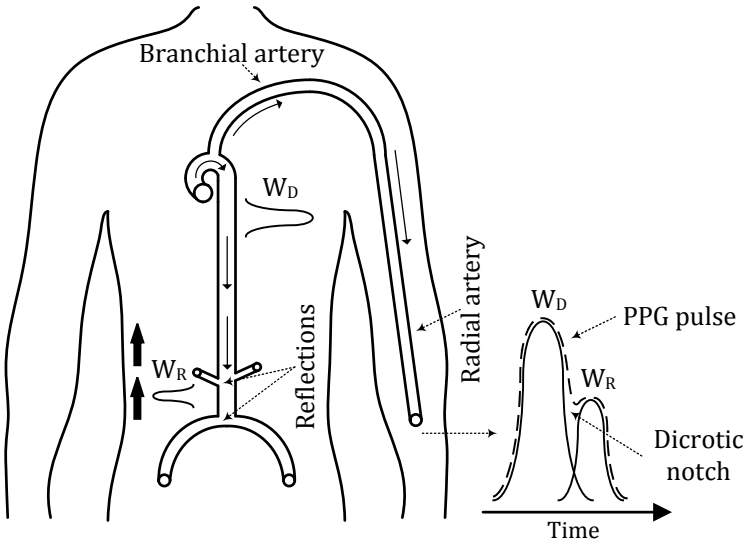

Fig. 3.3. Formation of PPG pulse waveform (partially based on Baruch et al., 2011 [113]).

Due to the advancing age and/or increasing arterial stiffness, the elastic-

ity and damping function gradually degrades. Therefore, both the direct and the reflected wave, W_D and W_R, respectively, propagate faster and tend to get closer. The decreasing delay of the returning wave results in an increasing overlap and reduce the gap between the two waves, finally declining the dicrotic notch. Figure 3.4 demonstrates the formation of the PPG pulse depending on the age and/or arterial stiffness.

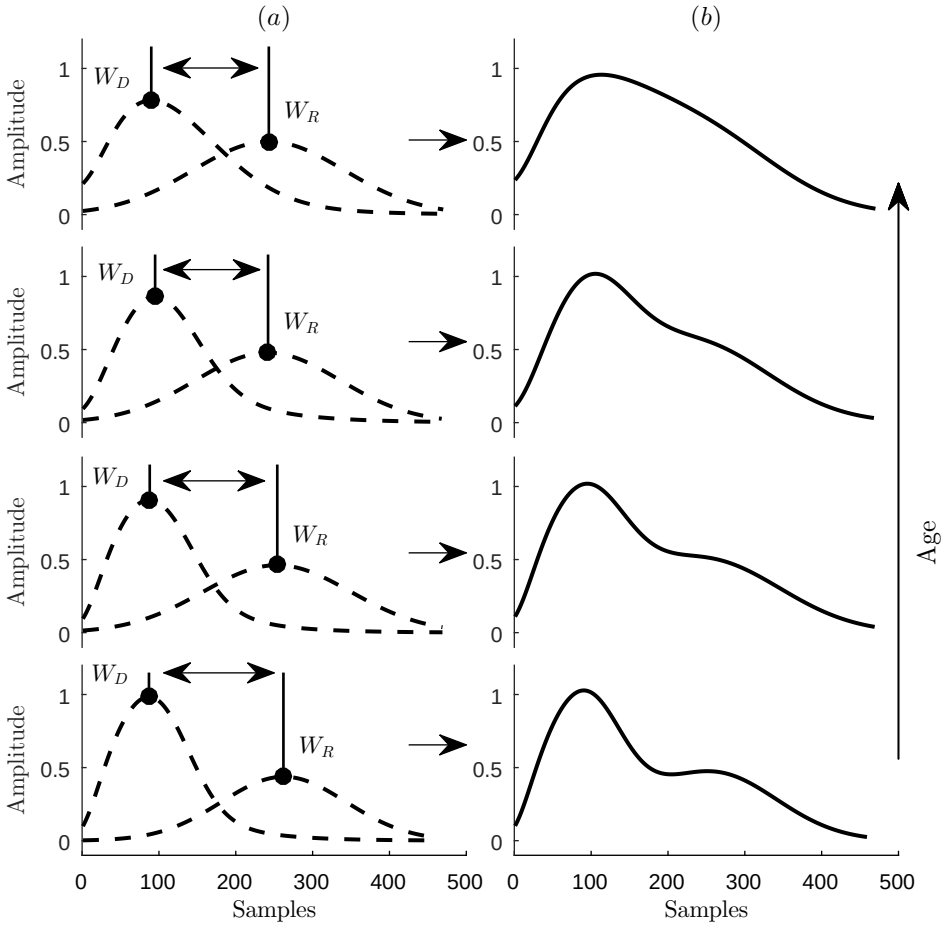

Fig. 3.4. Formation of the PPG pulse depending on the age and arterial stiffness: (a) direct and reflected waves, (b) resulting pulse.

Since the PPG waveform reflects the hemodynamics in the vascular system, various heart rhythm irregularities also change the morphology of the PPG signal. Figure 3.5 demonstrates the morphology of the PPG waveform during the normal sinus rhythm and various arrhythmias, namely, premature beats and atrial fibrillation, together with the synchronously recorded ECG signals as the reference.

During the normal sinus rhythm, the ventricular filling time remains rela-

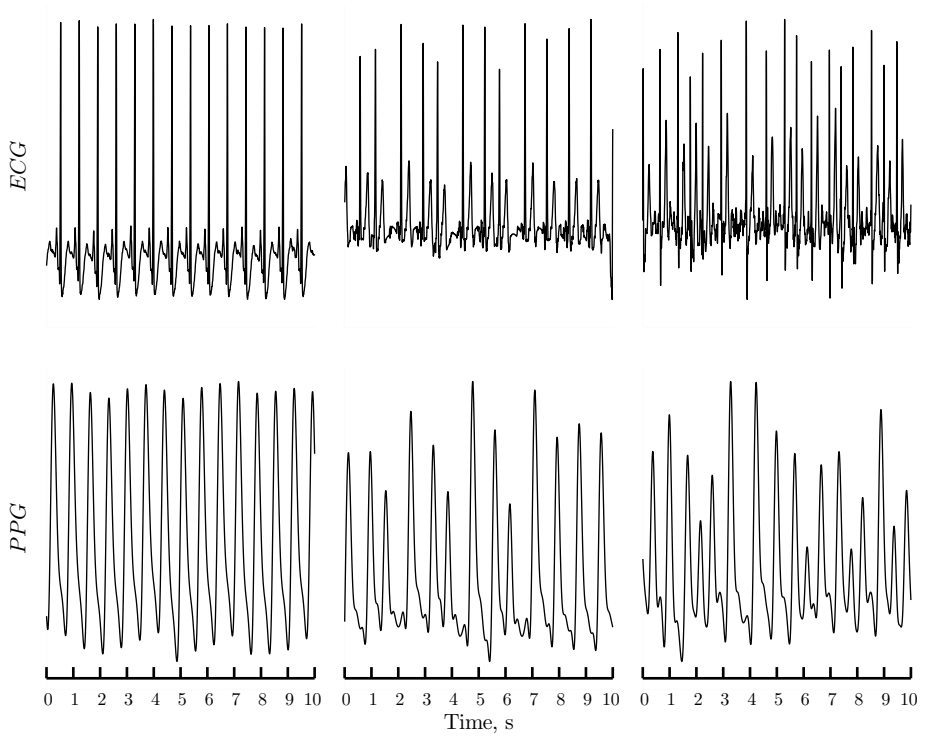

Fig. 3.5. Segments of synchronously recorded ECG and PPG signals during sinus rhythm, premature beats and atrial fibrillation.

tively constant as is the cardiac output. However, during arrhythmia (premature beats or atrial fibrillation), beat-to-beat intervals are irregular, resulting in the varying ventricular filling time. Early heart contraction causes the ventricle to fill less, thus decreasing the cardiac output and resulting in a decrease of the PPG amplitude. On the contrary, during a prolonged interval between two cardiac cycles, e.g., in the case of a compensatory pause, the ventricles are allowed to fill with more blood, thus producing an increase in the PPG amplitude.

3.1.3 Artifacts in PPG

It is widely acknowledged that the acquisition of PPG is sensitive and susceptible to various noise sources which introduce signal corruptions, referred to as *artifacts*. Artifacts limit the accuracy of the parameter extraction from the PPG signal or even make the extraction impossible thus leading to misinterpretations or false alarms, e.g., due to the erroneously calculated heart rate. Figure 3.6 shows segments of the synchronously recorded ECG and partially corrupted PPG signals. Generally, artifacts are induced by the motion of the sensor relative to the skin thus altering and affecting the paths of the propagating light due to the following reasons:

1. Deformation and movement of both external and inner tissue.
2. Blood movement, unrelated to the cardiac cycle.
3. Alternating distance between the skin and the sensor.
4. Varying contact pressure between the skin and the sensor.
5. Ambient light interference.

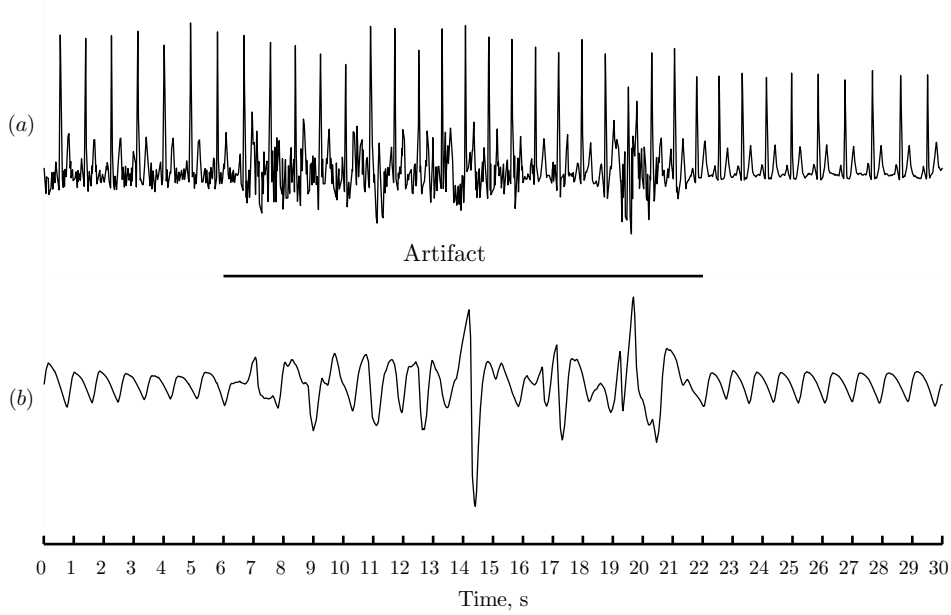

Fig. 3.6. Synchronously recorded segments of: (a) ECG (b) PPG with artifacts.

Other types of artifacts may be induced by the sources other than the sensor movement, of which the most common ones are:

1. Respiratory artifacts, occurring due to the changes in the thoracic volume during breathing.
2. Power line interference, i.e., 50/60 Hz depending on the country (Elgendi, 2012 [114]).
3. Decrease or absence of PPG amplitude due to dirty or scratched sensor, sensor positioning, irregular heart contractions (ventricular fibrillation), low blood perfusion (caused by low ambient temperatures, hypotension, vascular occlusion, or other pathologies).

The effect of artifacts on the PPG is devastating, since artifacts overlap with the frequency band of the PPG signal. The baseline wandering, e.g., due

to respiration is in the frequency range of 0.04–2 Hz, while the motion-induced artifacts may occur in the frequency range of 0.1–10 Hz. Therefore, simple filtering techniques such as band-pass filtering can not significantly improve the quality of the corrupted PPG, since these techniques are only suitable for the removal of non-overlapping noises, e.g., baseline wandering (partially) and power line interferences.

The influence of artifacts can be reduced by suitably attaching the sensor to the skin in order to restrict the excessive movement as well as by positioning it perpendicularly to the skin. The PPG probe should be held securely in place to minimize the probe-tissue movement artifacts. Other techniques used to improve the quality of PPG signals rely on digital signal processing. The application of adaptive filtering techniques showed promising results in the removal of the overlapping noises by using the accelerometer signal as a motion reference (Warren et al., 2016 [115]; Wijshoff et al., 2017 [116]). However, neither of the previously outlined artifact reduction means manages to ensure the acquisition of a good quality PPG signal. Therefore, the automatic signal quality assessment and detection of motion artifacts, especially their separation from the good quality recordings, is highly desirable.

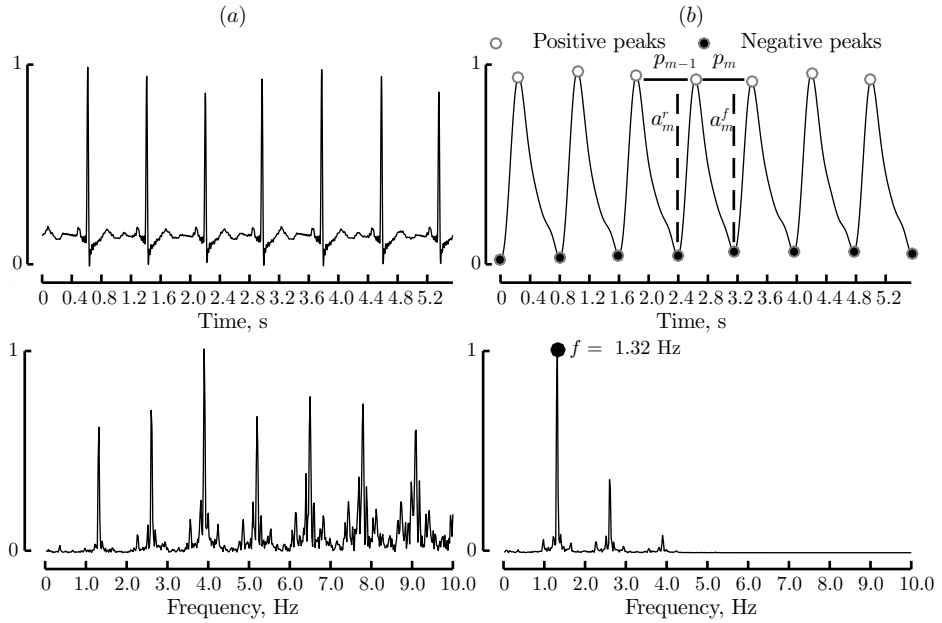

Fig. 3.7. (a) Reference ECG signal together with its spectrum bellow, (b) PPG signal with marked temporal features (preceding and current intervals p_{m-1} and p_m, respectively) and amplitude features (rising and falling edges a_m^r and a_m^f, respectively) and spectral features bellow (here the largest peak correspond to the average heart rate in the PPG segment).

3.1.4 Parameterization of PPG

Despite different origins of ECG and PPG signals, one being electrical, and the other being mechanical, similar parameters could still be derived and calculated solely from the PPG signal, e.g., the intervals between successive heart cycles, referred to as *peak-to-peak* (PP) intervals. PP intervals are equivalent to the ECG RR intervals, since R wave corresponds to the contraction of ventricles, whereas PPG pulse maxima corresponds to the systole. Figure 3.7 shows a number of parameters which could be obtained from the PPG signal. We should note that the PPG signal lags behind the ECG signal due to the time required for the pulse wave to propagate after the electrical activation of ventricles. Furthermore, the morphology of the PPG signal is less complex compared to that of ECG signals, which is clearly visible by comparing the spectra of ECG and PPG signals. The advantage of less complex signal morphology is that it allows the sampling of the signal while using lower sampling frequencies, thus reducing the amount of data and time for preprocessing and processing.

3.1.5 Devices and Applications of Photoplethysmography

Due to its wearablity, non-invasiveness, low-cost and versatility, photoplethysmography has been applied in many different clinical and non-clinical settings. Some possible applications of photoplethysmography are listed in Table 3.2:

Table 3.2. Applications of photoplethysmography in clinical and non-clinical practice

No.	Application
	Clinical physiological monitoring:
1	Blood oxygen saturation (SpO_2) measurement
2	Heart rate measurement
3	Blood pressure measurement
4	Cardiac output measurement
5	Respiration monitoring
6	Arrhythmia monitoring
7	Non-invasive haemoglobin concentration monitoring
8	Sleep apnea monitoring
9	Remote vital sign monitoring (via camera)
	Vascular system assessment:
10	Arterial compliance and ageing assessment
11	Venous assessment
12	Endothelial function assessment
13	Microvascular blood-flow monitoring
14	Tissue viability assessment
15	Would healing monitoring
16	Vasospastic condition assessment
	Autonomic nervous system function assessment:
17	Vasomotor function and thermoregulation assessment
18	Heart rate variability assessment
19	Blood pressure variability assessment
20	Orthostasis intolerance assessment
21	Neurology and other cardiovascular variability assessment

3.2 Available PPG-based Approaches and Strategies for Detection of Premature Ventricular Contractions and Atrial Fibrillation

3.2.1 Background of Arrhythmia Detection using Photoplethysmography

Photoplethysmography has been suggested for arrhythmia detection by Shelley, 2007 [117]. On the contrary to Holter monitors, photoplethysmography–based devices offer a cheaper and a more convenient way for daily life screening, since no electrodes are needed (Allen, 2007 [118]). In contrast to ECG electrodes, photoplethysmographic sensors are more patient–friendly since the sensor can be attached to a finger (Suzuki et al., 2009 [119]), to be integrated into earphones (Wang et al., 2007 [120]; Tamura et al., 2014 [121]), implemented in a forehead band (Tamura et al., 2014 [121]; Li et al., 2012 [122]) or used as a wrist sensor (Li et al., 2012 [122]; Haahr et al., 2012 [123]; Tamura et al., 2014 [121]). Therefore, so far, photoplethysmography has been considered for the detection of premature beats (Suzuki et al., 2009 [119]; Gil et al., 2013 [124]; Drijkoningen et al., 2014 [125]; Polania et al., 2015 [126]) and for the detection of AF by using

a smartphone camera (Lewis et al., 2011 [127]; McManus et al., 2013 [128]; Lee et al., 2013 [28]; Chan et al., 2016 [30]; Freedman, 2016 [31]).

3.2.2 Available Databases of Biomedical Signals for Testing and Validation of Arrhythmia Detectors

We may wonder why we should simulate PPG signals when they can be easily recorded? An important advantage of the simulated signals is that they can be annotated by design, thus avoiding the time-consuming manual process which is very costly when annotating day-long signals. In fact, simulated PPG signals can, at least to some extent, compensate for the current lack of annotated, public PPG databases. Such databases are urgently needed to facilitate the ongoing development and testing of PPG-specific AF detectors (due to the lack of guidelines for PPG-based arrhythmia diagnosis, the annotation of arrhythmias in the PPG today has to be based on a simultaneously acquired ECG). Another advantage is that simulated signals allow control of the signal-to-noise ratio, which acquired signals do not offer – this is an aspect which is critical to investigate in *mHealth* applications (Steinhubl et al., 2016 [129]). To the best of our knowledge, only the Physionet MIMIC, MIMIC II and the University of Queensland Vital Signs Dataset (UQVSD) databases feature synchronously recorded, but unannotated, PPG and ECG signals (Moody et al., 1996 [130]; Goldberger et al., 2000 [131]; Saeed et al., 2011 [132]; Liu et al., 2012 [133]). Given that Physionet provides many ECG databases with annotated arrhythmias (i.e., MIT–BIH Arrhythmia, MIT–BIH Atrial Fibrillation, MIT–BIH Supraventricular Arrhythmia), these public databases may be employed to produce simulated PPG signals.

Several approaches have been proposed for modeling a single PPG pulse, most of them being based on fitting multiple Gaussian waveforms (Wang et al., 2013 [134]; Liu et al., 2014 [135]). Gaussian waveforms have also been combined with the gamma waveform to account for the skewed shape of PPG pulses (Huang et al., 2013 [136]). Yet another approach relies entirely on the log-normal waveform (Huotari et al., 2011 [137]).

While there have been attempts to concatenate individual PPG pulses into a sequence, none of them is intended for modeling arrhythmia. Clifford et al. (Clifford et al., 2004 [138]) proposed a realistic model of blood pressure signals, intended for assessing noise performance of biomedical signal processing techniques. The model developed by Nabar et al., 2011 [139] is intended for a resource-efficient wireless PPG monitoring system where the received PPG signal is modeled according to the received PPG parameters. The model by Martin-Martinez et al., 2013 [140] was developed for the tracking of physical activity so that to obtain statistics of clinical parameters, and to recover corrupted or missing signal epochs. The modeling of hemodynamics by Scarsoglio et al., 2014 [141] is aimed at investigating the impact of AF on the cardiovascular system.

3.2.3 Automatic Detection of Premature Ventricular Contractions by using Photoplethysmography

The study by Suzuki et al., 2009 [119] is among the first attempts that have been published on the topic of automatic PPG-based premature beat detection. The algorithm makes use of the peak-to-peak (PP) intervals and the pulse amplitude obtained from the PPG signal thus seeking to distinguish between irregular rhythm stemming from arrhythmia and that caused by the artifact. The goal of this study was to detect the arrhythmic pulses possessing comparable detection accuracy to that of ECG signals recorded by using the Holter monitor. Wearable wristband type reflection photplethysmography sensor with sensor head worn on the finger was employed to record the PPG signal. The integrated 3-axis accelerometer was used to record the movement. Since the ECG signal was used as a reference, the 2-lead ECG and the wearable photplethysmography sensor were synchronously measured during the night.

The authors of the above outlined study analyzed the correlation between synchronously measured ECG and PPG signals when arrhythmic heartbeats occurred. PP intervals obtained from the PPG can be considered equivalent to the RR interval obtained from ECG, provided that the physiological state is static. Suzuki et al., 2009 [119] noted that in the case of the irregular RR intervals caused by arrhythmia, the amplitude of PPG pulses also varies and it is important to consider the change of the pulse amplitude due to the irregular pulse when developing the irregular pulse detection algorithm. When the irregular interval is shorter than the normal interval, the amplitude of the irregular pulse is smaller than that of the normal pulse. This is because the duration of the ventricular diastole is shorter owing to the shorter RR interval thus causing blood volume in the ventricle to decrease, and consequently, decreasing the stroke volume. In contrast, when the irregular interval is longer than the normal interval, the amplitude of the irregular pulse is larger than that of the normal pulse. Irregularity in extracted PP interval series is detected by calculating the ratios of the preceding and current PP intervals. Another features used to distinguish between the irregular rhythm and the artifact is defined as AIR (amplitude and interval ratio):

$$AIR_j = \frac{a_j^f}{p_j}, \tag{3.1}$$

where a_j^f are the amplitudes of the falling edge, p_j are PP intervals.

In case of an irregular pulse, AIR is almost a constant value. In contrast, during artifacts, AIR varies, since artifacts have no regularity. Threshold values η_1 and η_2 were determined empirically, by using data obtained from three subjects. Therefore, premature beats are detected by employing a condition-based

beat classification:

$$\mathcal{O}_j = \begin{cases} 1, & \frac{p_{j-1}}{p_j} > \eta_1 \ \& \ AIR_j < \eta_2, \\ 0, & \text{otherwise}, \end{cases} \tag{3.2}$$

where $\eta_1 = 1.1$ and $\eta_2 = 0.55$ are the threshold values for the interval ratio $\frac{p_{j-1}}{p_j}$ and AIR_j, respectively.

The obtained results show that the irregular heartbeat detection algorithm can discriminate between the pulse wave of irregular heartbeat and the pulse wave with an artifact, e.g., body movement. Most of the artifact cases were related to rolling over during sleep. It was also observed that the irregular pulse detected by the algorithm is coincident with the irregular heartbeats detected by an ECG. However, the addressed limitation of the algorithm is related to irregular pulses with short intervals which could not be detected because their amplitude was too small to detect the pulse trigger. Nevertheless, in other cases, the algorithm is claimed to have a sufficiently high specificity and the feasibility to detect irregular heart beats without false alarms due to artifacts.

In order to test the performance of the algorithm and reveal the unaddressed drawbacks, this algorithm was implemented and tested with three common cases, namely, the PPG signal with premature beats, the PPG signal with the rhythm of bigeminy, and the PPG signal corrupted with artifacts. The case of successfully detected premature beats is demonstrated in Fig. 3.8:

Figure 3.9 shows synchronously recorded ECG and PPG signals during the transition from the sinus rhythm to the rhythm of bigeminy, where every second beat is premature beat.

In the case of the ECG signal during bigeminy, both short preceding and longer succeeding intervals associated with the premature beat are available. However, in the PPG signal, due to the low cardiac output of the early contractions, the PPG pulse, associated with the premature beat, is absent and the resulting interval is two times as long as the interval between two normal beats. Therefore, the algorithm fails to detect bigeminy in the PPG. This is due to the interval ratios, which were used to detect changes in the intervals. Since the intervals between the adjacent beats in both the sinus rhythm and the rhythm of bigeminy are of similar length, the ratios do not show any changes; they only demonstrate the transition from the sinus rhythm to bigeminy.

As described earlier, PPG is more prone to artifacts induced by body movement than the ECG signals. Suzuki et al., 2009 [119] claim that the algorithm reduces the influence of the body movement; therefore, for the testing purposes, the algorithm was applied on a PPG signal containing artifacts. Figure 3.10 shows the performance of the premature beat detector using the PPG signal partially contaminated with artifacts and containing no premature beats, as seen in the synchronously recorded ECG:

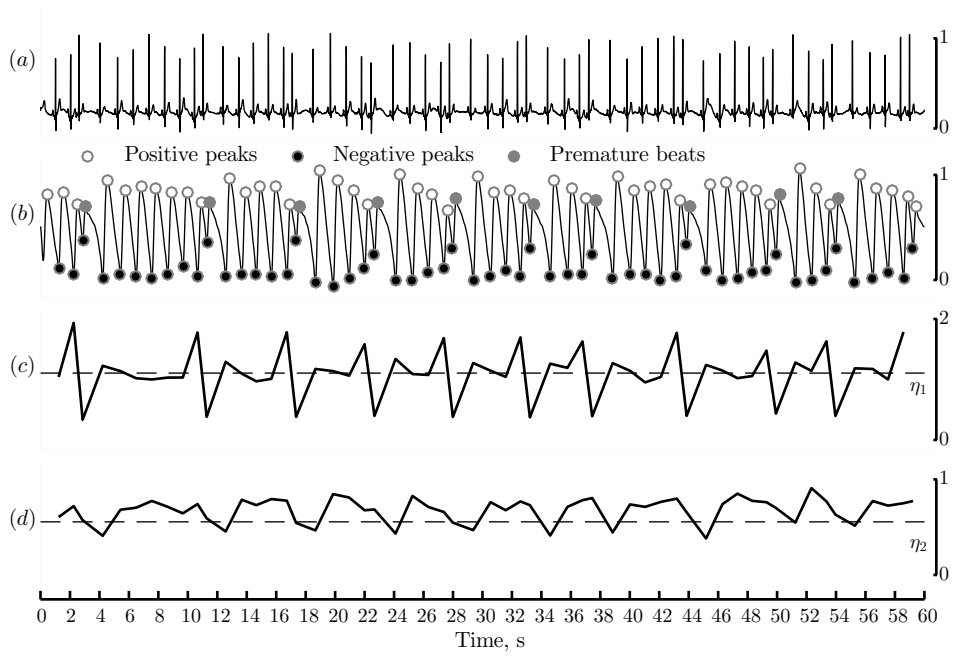

Fig. 3.8. Signals during premature beats: (*a*) ECG, (*b*) PPG, (*c*) interval ratios, and (*d*) amplitude and interval ratios (*AIR*).

Another attempt to detect premature beats was performed by Gil et al., 2013 [124]. This study did not directly focus on the detection of premature beats but rather used the detected premature beats to determine whether the PPG-based detection could be used as an alternative to ECG-based detection of the heart rate turbulence.

In contrast to Suzuki et al., 2009 [119], Gil et al., 2013 [124] concluded that the inclusion of the pulse amplitude features did not improve the classification performance significantly. The main reason is that the amplitude features are correlated with the temporal features since the change in the pulse amplitude is due to the change in the peak-to-peak interval, i.e., a short interval leads to the reduction of the amplitude, whereas a longer interval leads to the increase of the amplitude. The classification of PVCs was performed by applying a linear classifier.

The sensitivity/specificity of PVC classification was found to be 90.5 % / 99.9 %, with an accuracy of 99.3 % thus suggesting that the classification of PVCs can be reliably performed from PPG signals. A serious limitation of the algorithm, however, is that the PVCs which occurred within the 5 previous or 20 subsequent beats were excluded from further analysis. This suggests, that frequent PVCs, episodes of begeminy, trigeminy, etc. could not be detected by this approach.

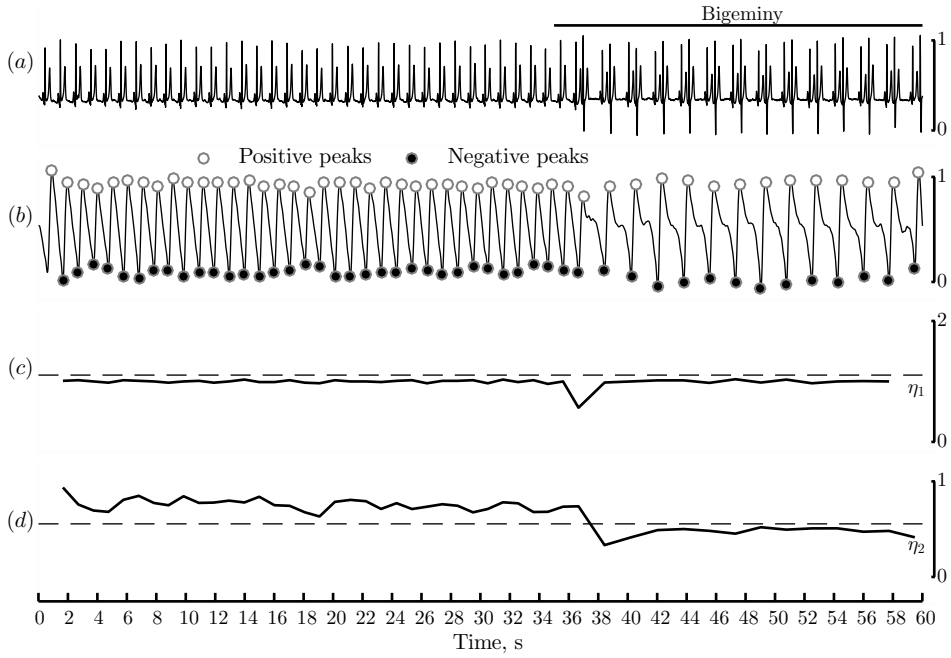

Fig. 3.9. Signals during bigeminy episode: (*a*) ECG, (*b*) PPG, (*c*) Interval ratios, and (*d*) Amplitude and interval ratios (AIR_k).

3.2.4 Automatic Detection of Atrial Fibrillation by using Photoplethysmography

To this day, very few photoplethysmogram-based atrial fibrillation detection methods have been developed. The first practical applications of PPG for AF detection were proposed in McManus et al., 2013 [128] and Lee et al., 2013 [28]. These methods make use of the rhythm-based features derived from PPG signals. The irregularity of the rhythm is estimated by applying the same basic methodologies used for the ECG derived features, namely, the root mean square of the successive difference ($RMSSD$), Shannon entropy (ShE), and sample entropy (SE) (Tateno et al., 2001 [142]; Dash et al., 2009 [143]). The normalized $RMSSD$ is defined as:

$$NRMSSD_k = \sqrt{\frac{1}{j-1}\sum_{j=1}^{l-1}(p_j - p_{j-1})^2}\frac{l}{\sum_{j=1}^{l} p_j}, \tag{3.3}$$

where l is the length of PP intervals and $p(j)$ is the j:th PP interval in the analysis window of length l, $j = 1, 2, ...$ Here $l = 64$ was used for the best AF detection accuracy. The normalization of $RMSSD$ is performed to account for the various heart rates.

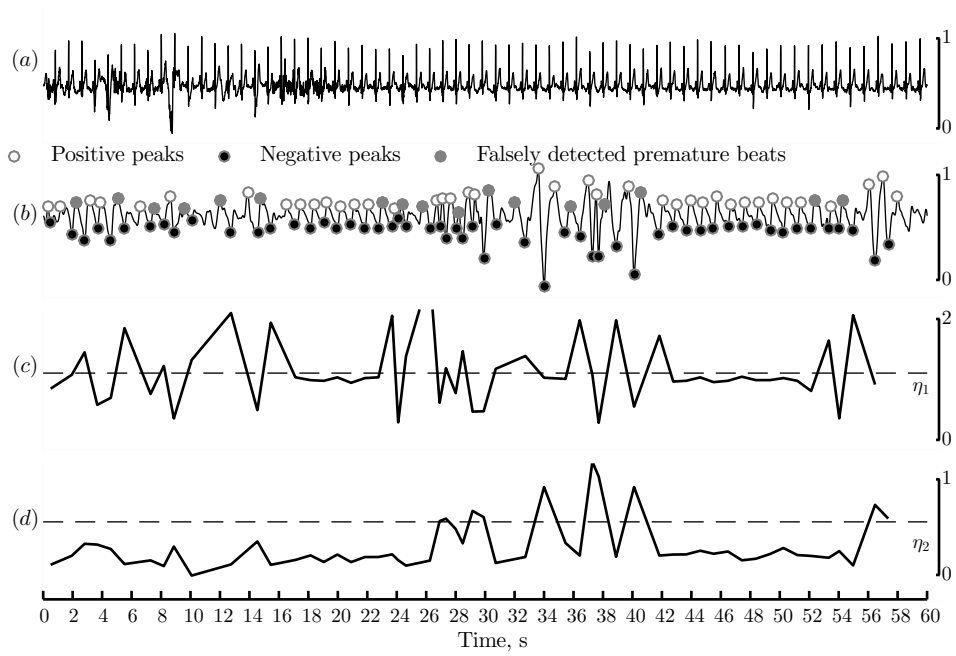

Fig. 3.10. Signals in case of artifacts: (a) ECG, (b) PPG, (c) Interval ratios, and (d) Amplitude and interval ratios (AIR_k).

The Shannon entropy is defined as:

$$ShEN_k = -\sum_{i=1}^{N} q_i \frac{\log(q_i))}{\log(\frac{1}{N})}, \qquad q_i = \frac{N_i}{l}, \tag{3.4}$$

where N is the number of bins, and N_i is the number of beats in the i:th bin. The best accuracy was obtained by using $N = 16$. The detection of AF is based on the simple logical conditions relaying on two statistical criteria, namely the fixed threshold values for $NRMSSD$ and ShE:

$$\mathcal{O}_k = \begin{cases} 1, \ NRMSSD_k > \eta_1 \ \& \ ShE_k > \eta_2, \\ 0, \ \text{otherwise}, \end{cases} \tag{3.5}$$

where $\eta_1 = 0.115$ and $\eta_2 = 0.55$ are the threshold values for $NRMSSD$ and ShE, respectively, which correspond to the largest area under the ROC curves.

In this study, PPG signals were obtained using a by smartphone camera on the subjects before (continuous AF) and after undergoing cardioversion (i.e., the rhythm is restored to the normal sinus rhythm). However, in order to test the described methodology for other potential cases of use, it was implemented and applied to a few different and highly common situations, i.e., the PPG signal during the normal sinus rhythm, the PPG signal during AF, the PPG

signals during ventricular bigeminy, and PPG corrupted with artifacts, which are presented in figures 3.11, 3.12, 3.13, and 3.14, respectively. Figure 3.11 demonstrates the output of the AF detector when only the normal sinus rhythm is present in the PPG segment:

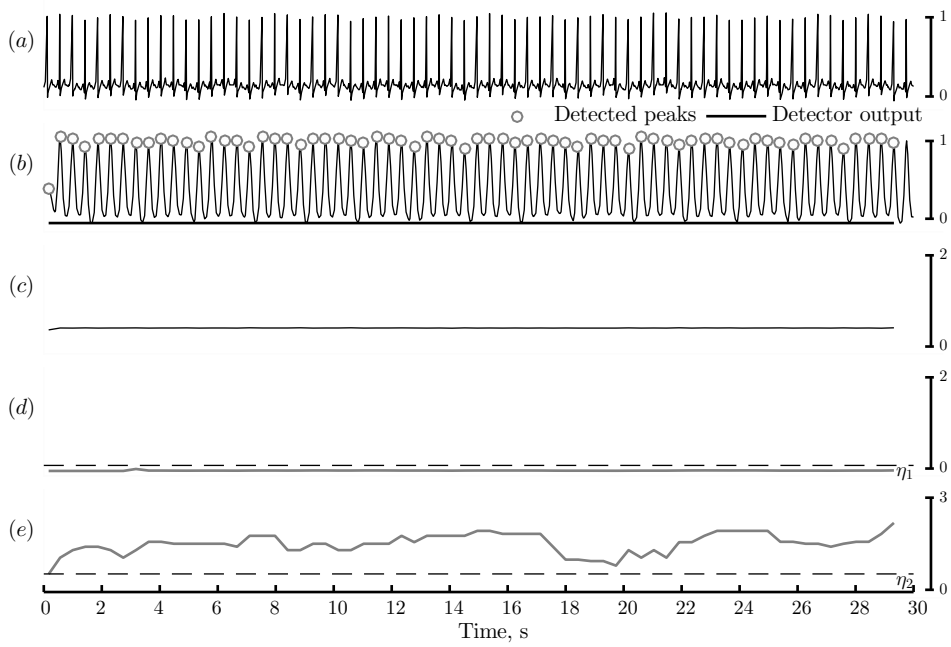

Fig. 3.11. Example of AF detector performance on PPG segment during the normal sinus rhythm: (*a*) ECG, (*b*) PPG, (*c*) peak-to-peak intervals in seconds, (*d*) $NRMSSD_k$, (*e*) ShE_k.

During the normal sinus rhythm, the intervals between successive beats are of relatively constant, no irregularity is detected and therefore the output of the AF detector remains bellow the detection threshold. However, notable differences between successive beats occur during arrhythmia, such as AF. Figure 3.12 shows the performance of the AF detector on the PPG segment during continuous AF:

In this case, AF was detected successfully. However, in addition to AF, other types of arrhythmia may also be present, therefore Fig. 3.13 shows the performance of the AF detector on PPG containing both sinus rhythm and episodes of ventricular begiminy:

Bigeminy introduces rhythm irregularity which force $NRMSSD_k$ and ShE_k values to raise above the threshold thus causing false alarms. However, the main source of false alarms when using PPG signals is artifacts. It is claimed that the use of a smartphones' camera to record the PPG signal partially bypasses the artifact problem since, during the recording, subjects were in the lying positions, breathing was assisted by the physician, and the recordings per se, were

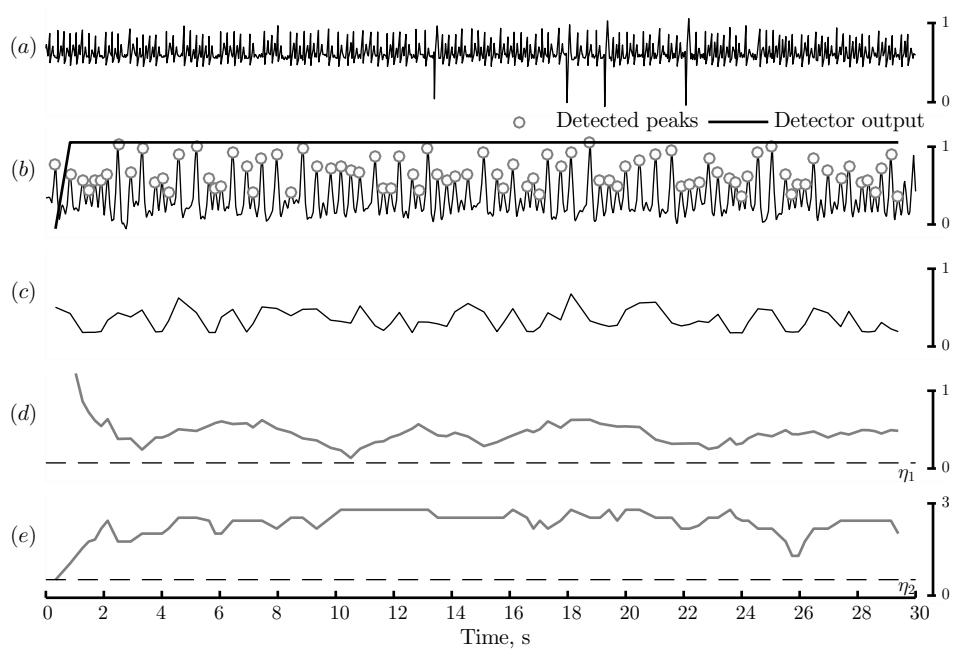

Fig. 3.12. An example of AF detector performance on PPG segment during AF: (*a*) ECG, (*b*) PPG, (*c*) Peak-to-peak intervals in seconds, (*d*) $NRMSSD_k$, (*e*) ShE_k.

quite short. If the subjects were prone to tremor, other potential recording sites were used instead of a finger, e.g., a leg or a forearm. However, there were no other measures taken to prevent false alarms in case of artifacts; therefore, the performance of the AF detector was also tested on a PPG segment corrupted with artifacts (see Fig. 3.14):

McManus et al., 2013 [128] claimed that the combination of $NRMSSD$ and ShE shows excellent sensitivity (Se), specificity (Sp), and accuracy (Ac) when using only the rhythm-derived features from the PPG signal. The comparison reference was the detection of AF by using a standard 12-lead ECG. However, as the results with PPG signals containing other arrhythmia and arifacts show, the method is only applicable when PPG signals are of good quality and if only two rhythm types are present, namely, the AF and the sinus rhythm. Another limitation of this study is due to the fact that $NRMSSD$ and ShE threshold values were obtained from the ECG RR intervals (Physionet MIT–BIH AF and MIT–BIH NSR databases) omitting the peculiarities because of a different origin of ECG and PPG signals. This is why such an approach could not be used for long-term screening of the AF.

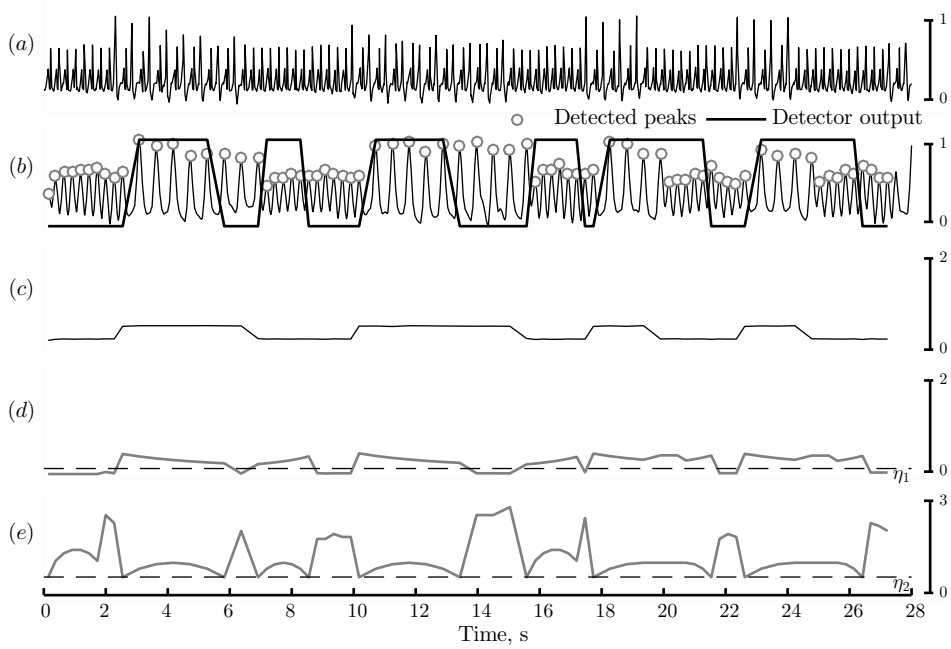

Fig. 3.13. Example of AF detector performance on PPG segment with bigeminy episodes: (*a*) ECG, (*b*) PPG, (*c*) peak-to-peak intervals in seconds, (*d*) $NRMSSD_k$, (*e*) ShE_k.

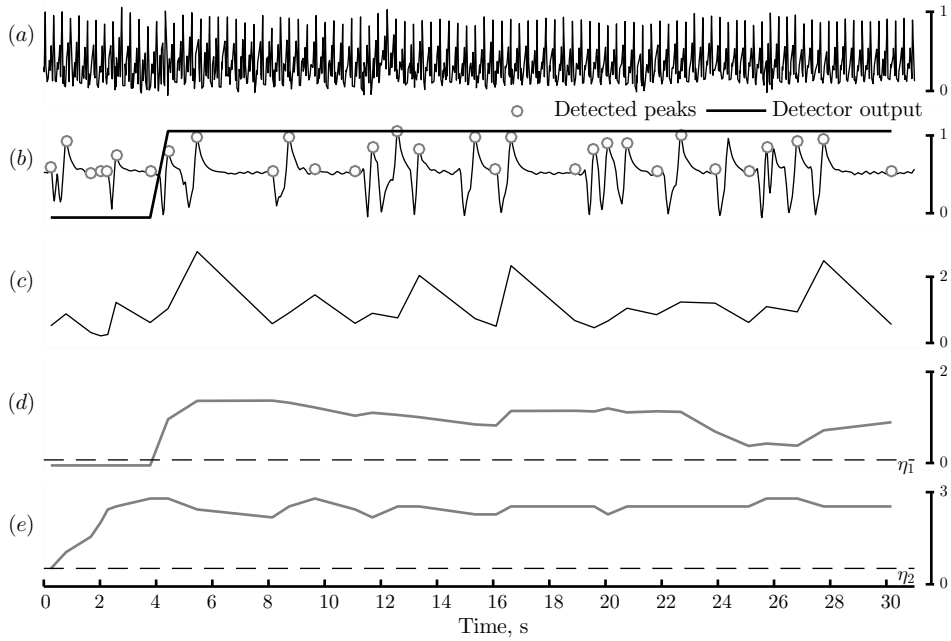

Fig. 3.14. Example of AF detector performance on PPG segment with artifacts: (*a*) ECG, (*b*) PPG, (c) peak-to-peak intervals in seconds, (*d*) $NRMSSD_k$, (*e*) ShE_k.

3.3 Conclusions of the Chapter

1. Photoplethysmography is a low cost, simple and portable technology, which is employed in a wide range of commercially available medical devices for measuring the oxygen saturation and the heart rate, for assessing the arterial compliance, etc. The latest investigations demonstrate great potential for the use of photoplethysmography in the detection of cardiac arrhythmias. However, the main challenges concerning the acquisition and analysis of photoplethysmogram signals are motion-induced artifacts.

2. Currently available photoplethysmogram-based algorithms for the detection of premature beats and atrial fibrillation are not suitable for ambulatory long-term screening due to lack of measures taken to reduce the rate of false alarms during occurrence of other types of arrhythmia, such as bigeminy and, especially, signals corruptions, such as artifacts.

3. Databases with synchronously recorded ECG and PPG signals are needed for testing and evaluation of PPG based arrhythmia detection algorithms.

4 PROPOSED METHODS FOR PPG MODELING AND PPG-BASED ARRHYTHMIA DETECTION

4.1 Modeling of PPG during cardiac arrhythmia

This chapter introduces a novel phenomenological model for simulating PPG signals during arrhythmia (Sološenko et al., 2017 [144]). The model uses the RR interval series as input for generating a PPG signal. The model accounts for the presence of premature beats by introducing the amplitude and time scale factors which modify the pulse width and amplitude, thus making it possible to simulate ectopic beats and certain rhythms such as bigeminy known to cause false alarms in RR interval-based AF detection.

The RR interval series obtained from an annotated ECG recording serves as the input to the proposed simulation model, see Fig. 4.1. The model consists of two main parts, namely, modeling of a single PPG pulse and concatenation of pulses into a connected signal.

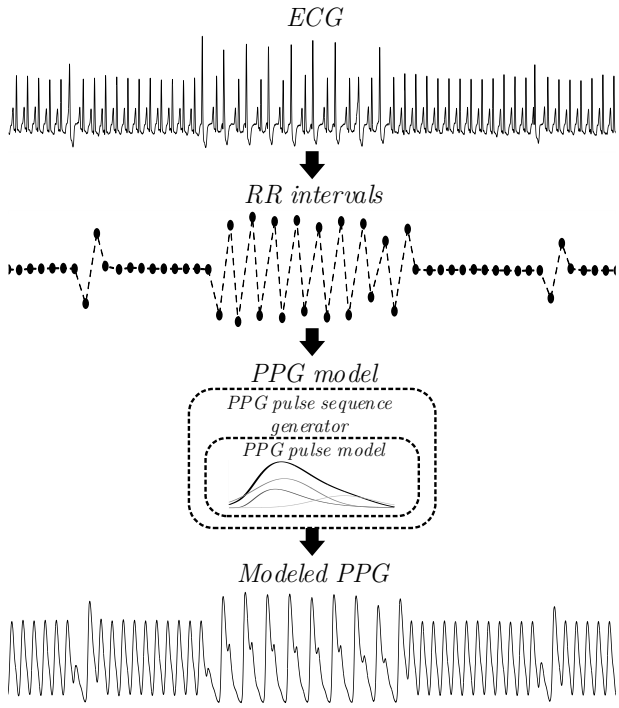

Fig. 4.1. Block diagram of the proposed model for simulation of PPG signals.

4.1.1 Modeling of a Single PPG Pulse

PPG pulse is modeled as a linear combination of three functions—one log-normal waveform and two Gaussians—together accounting for direct and reflected pulse waves (Baruch et al., 2011 [113]). Here, the log-normal function is defined as

$$\varphi_1(t; m, \sigma_1) = \begin{cases} \dfrac{1}{t\sqrt{2\pi\sigma_1^2}} e^{-\dfrac{(\ln(t/m))^2}{2\sigma_1^2}}, & t > 0, \\ 0, & t \leqslant 0, \end{cases} \tag{4.1}$$

where t is time, m is the scale parameter, and σ_1^2 is the shape parameter. The Gaussian waveform is defined by

$$\varphi_i(t; \sigma_i) = \frac{1}{\sqrt{2\pi\sigma_i^2}} e^{-\dfrac{t^2}{2\sigma_i^2}}, \quad i = 2, 3, \tag{4.2}$$

where σ_i^2 is the width parameter. Then, the PPG pulse is modeled as a linear combination of weighted, time-shifted, and time-scaled versions of $\varphi_1(t; m, \sigma_1)$, $\varphi_2(t; \sigma_2)$, and $\varphi_3(t; \sigma_3)$, i.e.,

$$\varphi(t; \boldsymbol{\theta}) = w_1\varphi_1(t - \tau_1; m, \sigma_1) + \sum_{i=2}^{3} w_i\varphi_i(t - \tau_i; \sigma_i) + a, \tag{4.3}$$

where a denotes the DC offset. For convenience, all the model parameters are merged into the vector

$$\boldsymbol{\theta} = [w_1, w_2, w_3, \tau_1, \tau_2, \tau_3, m, \sigma_1, \sigma_2, \sigma_3, a]. \tag{4.4}$$

The parameters of the PPG pulse are estimated by nonlinear least squares fitting (Coleman et al., 1996 [145]),

$$J(\boldsymbol{\theta}) = \int_{-\infty}^{\infty} (y(t) - \varphi(t; \boldsymbol{\theta}))^2 \, dt, \tag{4.5}$$

$$\hat{\boldsymbol{\theta}} = \arg\min_{\boldsymbol{\theta}} J(\boldsymbol{\theta}), \tag{4.6}$$

where $\hat{\boldsymbol{\theta}}$ is the vector minimizing the difference between the PPG pulse template $y(t)$ and the model PPG pulse $\varphi(t; \boldsymbol{\theta})$. Prior to minimization, each PPG template is normalized to unit amplitude.

Since pulse morphology varies considerably depending on such factors as age and medical condition, a set of template PPG pulses, displayed in Fig. 4.2 is employed.

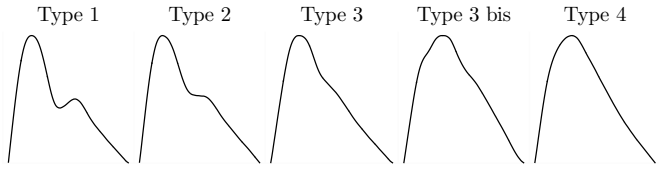

Fig. 4.2. Template PPG pulses according to Dawber et al. (Dawber et al., 1973 [146]).

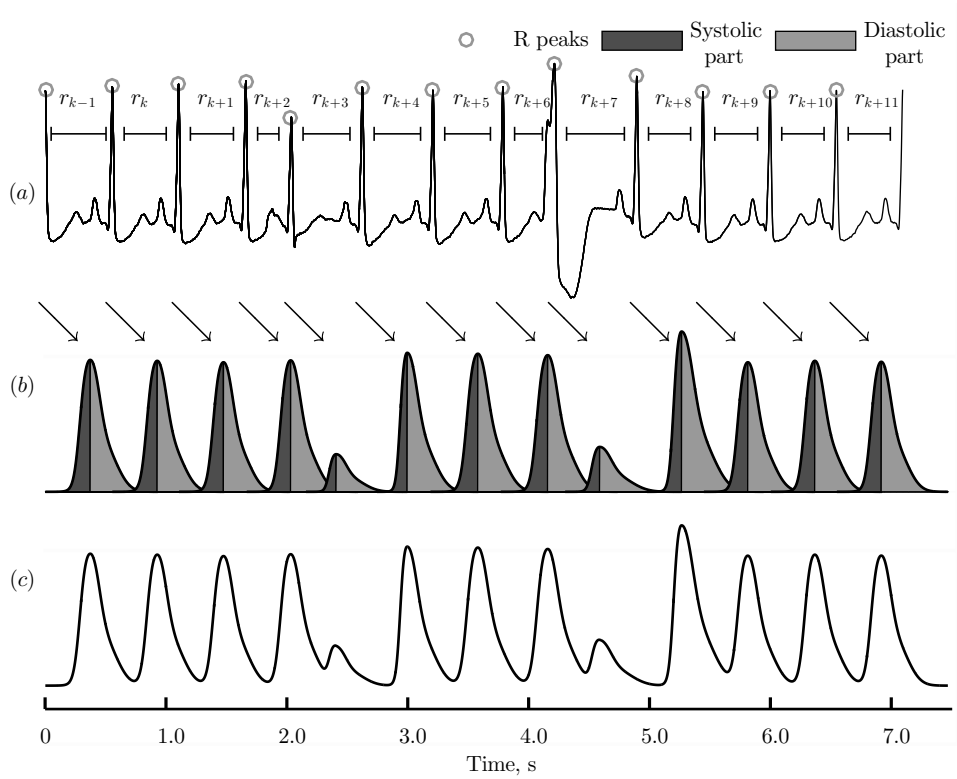

Fig. 4.3. Steps required to model a PPG signal. (*a*) ECG with detected R peaks and corresponding RR intervals, (*b*) modeled systolic and diastolic parts combined into a single pulse, and (*c*) the resulting, connected PPG signal. It should be noted that the two pulses with lower amplitudes relate to premature beats. Arrows point to pulses associated with R peaks.

4.1.2 Contextualization of a single PPG pulse

PPG pulse is composed of the systolic part and the diastolic part, where the width of each part depends on the adjacent RR intervals. For the k:th pulse, two time scale factors are introduced, both of which are inversely proportional

to RR intervals,

$$\beta_{s,k} = \begin{cases} \dfrac{1}{r_k}, & \dfrac{r_k}{r_{k-1}} \leqslant \eta_0, \\ \dfrac{1}{r_{k-1}}, & \text{otherwise}, \end{cases} \tag{4.7}$$

$$\beta_{d,k} = \begin{cases} \dfrac{1}{r_{k+1}}, & \dfrac{r_k}{r_{k-1}} \leqslant \eta_0, \\ \dfrac{1}{r_k}, & \text{otherwise}, \end{cases} \tag{4.8}$$

where r_k denotes the RR interval preceding the k:th pulse. Threshold η_0 determines whether the current beat is premature.

Another factor is the PPG pulse amplitude related to the ventricular filling time according to the length of the RR interval. For example, in the sinus rhythm, the ventricular filling time does not change much from beat to beat, which leads to negligible pulse amplitude variations. On the contrary, a premature beat causes the diastole to be shorter thus reducing the amplitude of the resulting pulse. The proposed model assumes that the amplitude of the premature pulse changes exponentially. Since a premature beat is followed by a compensatory pause, sufficiently long to fill the ventricles with extra blood, the subsequent pulse will have a larger amplitude.

The amplitude of the PPG pulse is assumed to be proportional to r_k unless the beat is premature when the relationship between the length of the current RR interval whereas the diastolic period can be characterized by an exponential function (Sarnari et al., 2009 [147]). The pulse amplitude is given by

$$\alpha_k = \begin{cases} 0.58 \cdot r_k^{1.32}, & \dfrac{r_k}{r_{k-1}} \leqslant \eta_0 \text{ or } \dfrac{r_{k+1}}{r_k} \geqslant \eta_1, \\ r_k, & \text{otherwise}. \end{cases} \tag{4.9}$$

where threshold η_1 determines whether the subsequent beat is premature thus allowing the decrease in amplitude.

The k:th PPG pulse denoted $s_{a,k}(t)$ is put into context by scaling the amplitude of $\varphi(t;\hat{\boldsymbol{\theta}})$ with α_k and the width with either $\beta_{s,k}$ or $\beta_{d,k}$:

$$s_{a,k}(t) = \begin{cases} \alpha_k \cdot \varphi(\beta_{s,k}(t-t_p);\hat{\boldsymbol{\theta}}), & -\infty < t < t_p, \\ \alpha_k \cdot \varphi(\beta_{d,k}(t-t_p);\hat{\boldsymbol{\theta}}), & t_p \leqslant t < \infty, \end{cases} \tag{4.10}$$

where t_p is the time for the largest positive peak in $\varphi(t; \hat{\boldsymbol{\theta}})$. Finally, the sampling of $s_{a,k}(t)$ is performed by

$$s_k(n) = s_{a,k}(t = nT), \quad n = 0, 1, \ldots \tag{4.11}$$

where T denotes the length of the sampling interval.

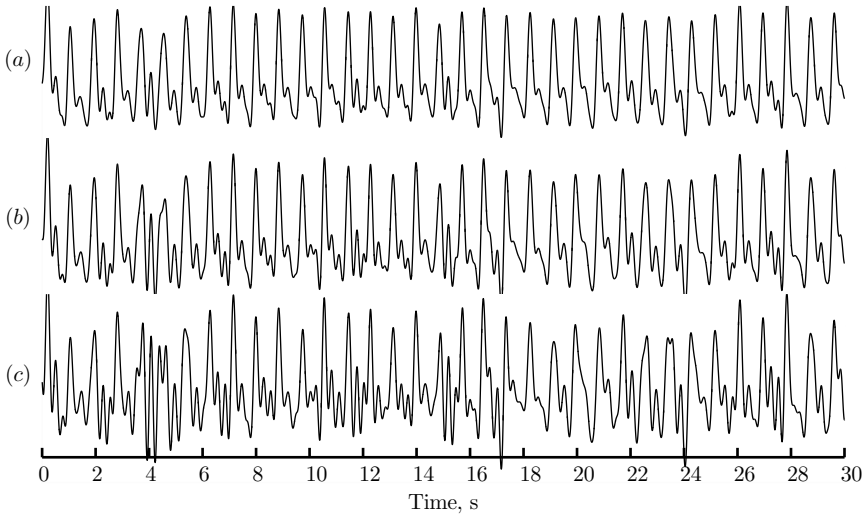

Fig. 4.4. Model PPG signal composed of Type 1 pulses (cf. Fig.4.2) at SNRs equal to (*a*) 20 dB, (*b*) 15 dB, and (*c*) 10 dB.

4.1.3 Modeling of a Connected PPG Signal

A connected, discrete-time model signal $x(n)$ is generated by placing contextualized PPG pulses at the heartbeat occurrence times δ_k obtained from the RR interval series and adding noise $v(n)$:

$$x(n) = \sum_{k=1}^{K} s_k(n - \delta_k) + v(n), \tag{4.12}$$

where K denotes the number of pulses in the connected signal. The steps required to produce a simulated signal are demonstrated in Fig. 4.3.

Noise $v(n)$ is generated by filtering the white noise, where the filter is determined by the spectral properties of the motion artifacts extracted from PPG signals in the MIMIC database. By using the above simulation model, a noise-free signal is generated from the RR intervals of the segment with the artifact. The artifact is extracted by canceling the model signal from the observed signal while using a normalized least-mean squares (NLMS) filter. Then, the extracted artifact serves as the desired input to the NLMS filter, whereas the white noise is the reference input. The filter output is a signal resembling the extracted artifact.

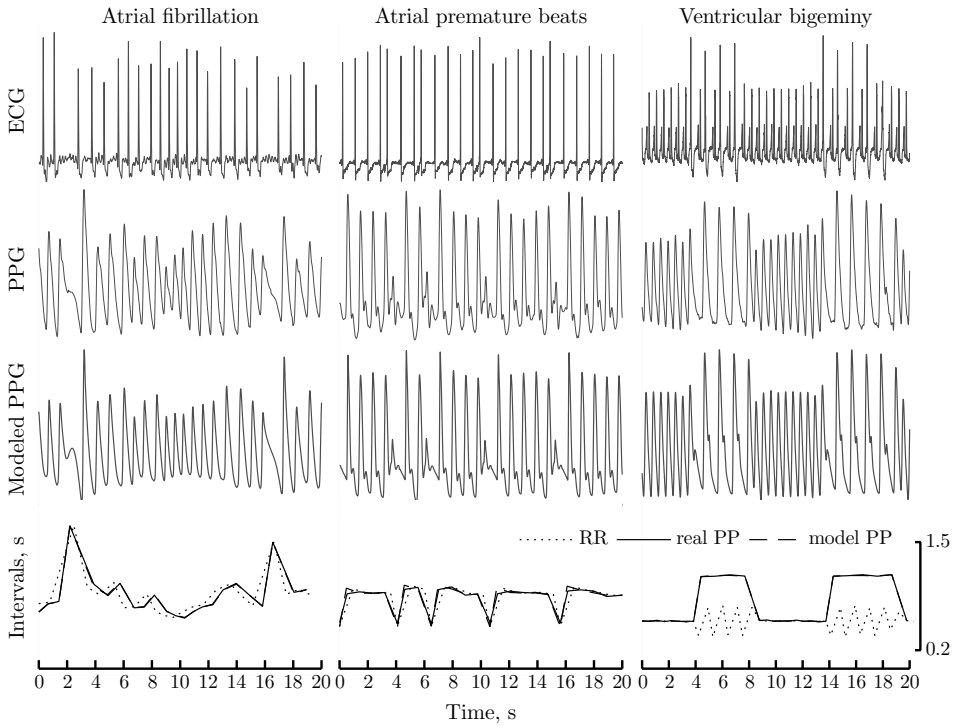

Fig. 4.5. Synchronously recorded ECG and PPG signals from the MIMIC database compared to the simulated PPG signals during atrial fibrillation, sinus rhythm with atrial premature beats, and sinus rhythm with ventricular bigeminy. The bottom row shows RR intervals and peak-to-peak (PP) intervals of the real and modeled PPG signals, respectively.

The resulting impulse response of the NLMS filter is used for producing $v(n)$. A connected model signal is displayed for different SNRs in Fig. 4.4.

Examples of model and real PPG signals during AF, premature atrial beats, and ventricular bigeminy are presented in Fig. 4.5. It is obvious that the model signals are similar to the real ones, also when rhythm disturbances occur. Furthermore, the difference between RR and the corresponding peak-to-peak (PP) intervals is observed, especially during the rhythm with ventricular bigeminy, while retaining the similarity between PP intervals in real and model PPGs.

4.2 PPG-based Detection of Premature Ventricular Contractions

In this chapter, a method involving PPG pulse power-derived features in addition to the temporal features for the detection of premature ventricular contractions is introduced. An important property of the proposed method is that the temporal features are normalized according to the preceding heart rate estimated by combining temporal preprocessing and spectral analysis. Hence, differently from the previous studies, this solution allows detecting PVCs even

during an episode of bigeminy. In addition, an artifact detector was implemented in order to reduce the number of false alarms.

It is well-known that the alternating part of the PPG is proportional to the peripheral blood volume changes (Peper et al., 2007 [148]). Premature contractions result in reduced ventricular filling diminishing the peripheral pulse amplitude (Zheng et al., 2008 [149]). Therefore, the PPG pulses during PVC may become hardly recognizable (Fig. 4.6 (a)), or may still have a sufficient amplitude for peak detection (Fig. 4.6 (b)). These two types of premature pulses in the PPG are denoted as P^1 and P^2, respectively.

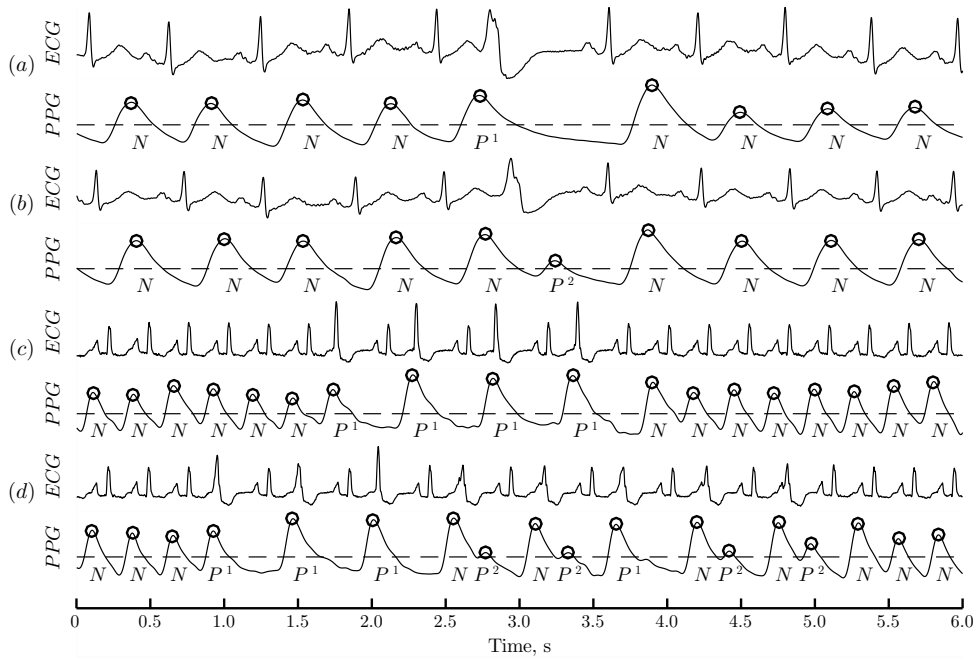

Fig. 4.6. Examples of PVC pulse types in PPG together with reference ECG: (*a*) PPG pulses during normal sinus rhythm (labeled as N) with a single PVC that is not followed by any observable pulse (labeled as P^1), (*b*) a single PVC characterized by a small pulse amplitude (labeled as P^2), (*c*), consecutive type P^1 pulses (bigeminy), (*d*) bigeminy with both PVC pulse types. In this particular example, ECGs and PPGs were preprocessed with zero-phase band-pass filters having cut-off frequencies of 0.05–150 Hz and 0.4–15 Hz, respectively.

The proposed method for PVC detection and classification exploits temporal (peak-to-peak) intervals (PPs) and power-derived (the power ratios, PRs) features obtained for each PPG pulse. The method is composed of 3 major parts: PPG preprocessing, feature extraction, and classification (see Fig. 4.7).

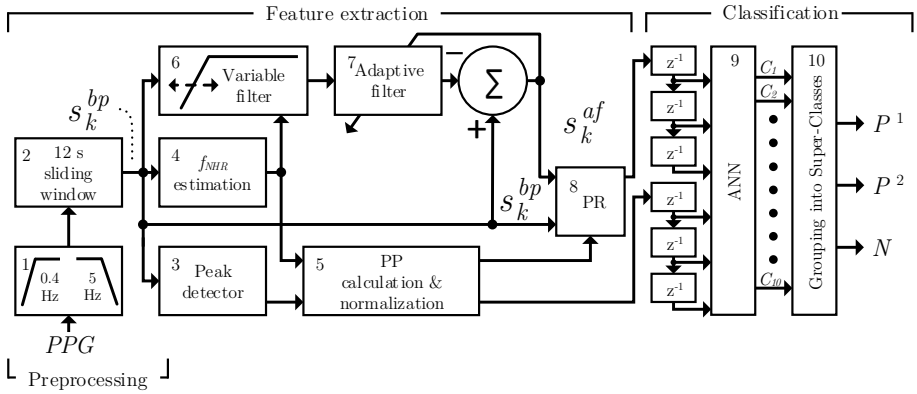

Fig. 4.7. Block diagram of the proposed method. Here, f_{NHR} is the normal heart rate, PP is the peak-to-peak interval, PR is a power ratio, ANN is the artificial neural network, s_k^{bp} is the preprocessed PPG, s_k^{af} is a PPG with higher frequency components removed.

4.2.1 Preprocessing and Feature Extraction

In order to minimize high frequency noise and baseline wandering, PPGs are preprocessed by using low-pass and high-pass finite impulse response (FIR) filters with 5 Hz and 0.4 Hz cut-off frequencies, respectively, thus resulting in signal s_k^{bp} (Fig. 4.7 block 1). These cut-off frequencies correspond to approximal maximal and minimal physiological heart rates. A 12 s sliding analysis window with 50% overlap is used for feature extraction (Fig. 4.7 block 2). Positive peaks of the preprocessed PPG are detected by using threshold crossing technique (Fig. 4.7 block 3). Then, a series of operations are applied (Fig. 4.7 block 4) for the estimation of a normal heart rate (f_{NHR}) (see Fig. 4.8).

Fig. 4.8. Block diagram of the normal heart rate estimator. Here, s_k^{bp} is a 12 s segment of the preprocessed PPG.

When estimating f_{NHR}, it is crucial to reduce the influence of the impulse noise, i.e., the noise of a higher amplitude than PPG, which may be falsely associated to f_{NHR} during spectral analysis. First, PPG is clipped in the empirically determined range of $\pm 0.7 std$ of the preprocessed PPG, and smoothed by applying a moving average filter. Then, the first derivative of the resulting PPG is calculated. The first derivative acts as a high pass filter that emphasizes higher frequency components of the PPG. In addition, the 1^{st} derivative is particularly useful when PPG segments contain bigeminy episodes which result in nearly 2 times lower PPG pulse rates compared to a normal rhythm (see Fig. 4.6 (c)).

Next, f_{NHR} is estimated by taking the frequency at the maximal amplitude of the power spectral density (PSD) function. Finally, outliers are removed by filtering the array of f_{NHR} using a 3^{rd} order median filter.

Normally, the heart rate is inversely related to PP intervals. However, for a specific PVC type (cf. Fig. 4.6 (a) and (c)), the length of PP can be approximately twice the length of the interval between the subsequent PPG pulses occurring during the normal rhythm. Therefore, in order to make the PPs heart rate independent, PP-related features are normalized before applying them to the classifier. One way to normalize PP intervals is to calculate the ratio of the current and the mean values of the intervals (Gil et al., 2013 [124]). However, the former normalization principle is sensitive to an erroneously detected PP value, i.e., during bigeminy or artifacts. Hence, PP-related features are normalized (Fig. 4.7 block 5) with respect to f_{NHR}:

$$PP_k = \frac{\left(p_{\,k} - p_{\,k-1}\right) f_{NHR}}{f_s}, \tag{4.13}$$

where k is the PP number, p_j is an array of the index value of the detected positive peaks, f_s is the sampling frequency (Hz), and f_{NHR} is the normal heart rate (Hz). Normalized PP intervals are close to 1 during the normal heart rhythm, yet they take either lower or higher values during PVCs.

The second high-pass FIR filter is characterized by a variable cut-off frequency (Fig. 4.7 block 6), and is employed for the purpose of extracting higher frequency components of PPG (from f_{NHR} to 5 Hz). The cut-off frequency is adjusted according to the current value of f_{NHR}. Then, the resulting signal is used as a reference input to a pre-whitened recursive least squares (RLS) adaptive filter (Fig. 4.7 block 7) (Douglas, 2000 [150]). The order and the forgetting factor of RLS filter were set to 10 and 0.999, respectively. Given that PPG pulses during PVCs are composed of lower frequency components compared to the normal rhythm, subtraction of higher frequencies produces signal s_k^{af} consisting solely of premature pulses. Therefore, the amplitude of PVCs is not affected, while the PPG pulses are suppressed considerably during the normal heart rate (see Fig. 4.9 (c)).

The power ratios (PRs) are computed in segments between two adjacent PPG pulses by involving both preprocessed PPG s_k^{bp} and signal s_k^{af}:

$$PR_k = \frac{\sum_{n=1}^{N} \left(s_k^{af}(n) - \overline{s_k^{af}}\right)^2}{\sum_{n=1}^{N} \left(s_k^{bp}(n) - \overline{s_k^{bp}}\right)^2}, \tag{4.14}$$

where k is the segment number, N is the segment length (total samples in the PP interval), $\overline{s_k^{af}}$ is the mean amplitude of samples in $s_k^{af}(n)$, and $\overline{s_k^{bp}}$ is the

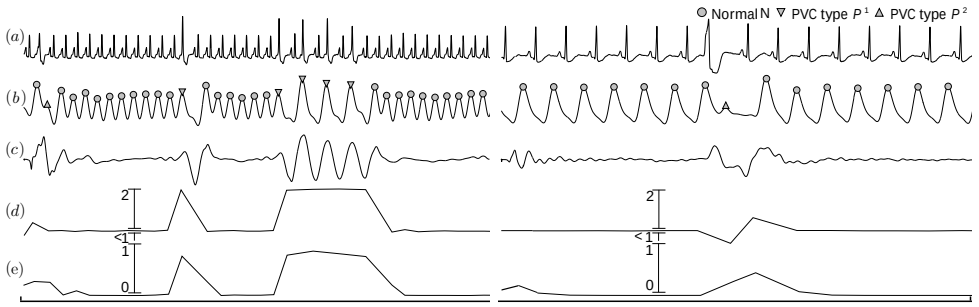

Fig. 4.9. Example of detected PVCs in PPG: (a) reference ECG, (b) preprocessed PPG with PVCs (s_k^{bp}), (c) output of the adaptive filter (s_k^{af}), (d) normalized peak-to-peak intervals (PPs), and (e) power ratios (PRs). The vertical lines in (d) and (e) denote the ranges of the normalized PP and PR values, respectively.

mean amplitude of samples in $s_k^{bp}(n)$. Since the PPG amplitude is markedly suppressed in normal beats, power ratios PR take lower values than those in PVCs.

4.2.2 Classification

Feed-forward artificial neural network (ANN) with either linear or non-linear outputs was investigated for the classification of individual PPG pulses (see Fig. 4.10).

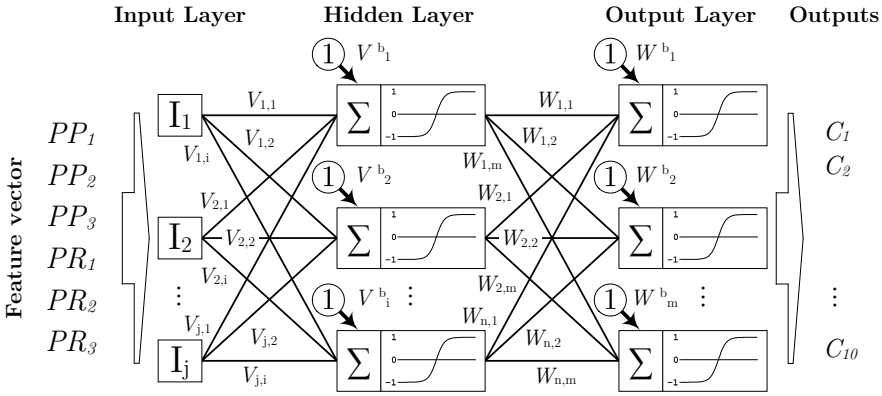

Fig. 4.10. Block diagram of the ANN-based PPG pulse classifier. Here, I stands for ANN inputs, V is the input and hidden layers connecting weights, V^b stands for the biases of hidden neurons, W represents the hidden and output layers connecting weights, W^b denotes the biases of the neurons in the output layer, and C stands for the outputs of ANN (classes).

Since each individual PPG pulse is described by 3 intervals (preceding, current and subsequent), various interval combinations are feasible, therefore it is reasonable to distinguish many classes (i.e., 10, see Table 4.1) in order to reduce

the misclassification rate. These 10 classes (Fig. 4.7 block 9) are further grouped into 3 super-classes denoted by P^1, P^2 and N, respectively (Fig. 4.7 block 10). The full list of classes and super-classes is presented in Table 4.1.

Table 4.1. PPG pulse classification into (a) 10 classes and (b) 3 super-classes

(a)	C_1 (*Normal*)	C_2 (*Normal* before P^1)	C_3 (*Normal* after P^1)	C_4 (*Normal* before P^2)	C_5 (*Normal* after P^2)	C_6 (*Bigeminy start*)	C_7 (*Bigeminy*)	C_8 (*Bigeminy end*)	C_9 (*Single* P^1)	C_{10} (*Single* P^2)
(b)	N					P^1				P^2

The number of neurons in a hidden layer of ANN was chosen empirically and was set to 40. The back-propagation method was used for training (Vogl et al., 1988 [151]). In order to cope with the overfitting, small random noise was added to each of the inputs (Piotrowski et al., 2013 [152]). Both ANN and back-propagation learning method were implemented in Mathworks, Inc. MATLAB^{TM} environment.

4.2.3 Artifact Detection

Motion and tissue deformation induced artifacts are a crucial issue hindering the development of arrhythmia detectors based on PPG. In order to reduce the number of false alarms due to falsely detected pulses, an artifact detector is implemented.

The process of artifact detection is illustrated in Fig. 4.11. In the analysis window, artifacts are flagged with respect to the ratio, obtained by dividing the clipped PPG by the preprocessed PPG (Fig. 4.11 (a)). Since the clipped PPG has a lower amplitude, the ratio approaches to 0 when artifacts occur. PPG is flagged as an artifact whenever the empirically determined threshold exceeds 0.3. In addition, four pulses before and after the artifact are excluded from the classification.

4.2.4 Implementation of Online Premature Ventricular Contraction Detector

An online version of the PVC detector was implemented as the application for the use in the Android operating system. A configuration of the algorithm employing PP features, ANN with non-linear outputs, and with blocks 6, 7 and 8 in Fig. 4.7 excluded, was selected for the implementation. PPG is transmitted to

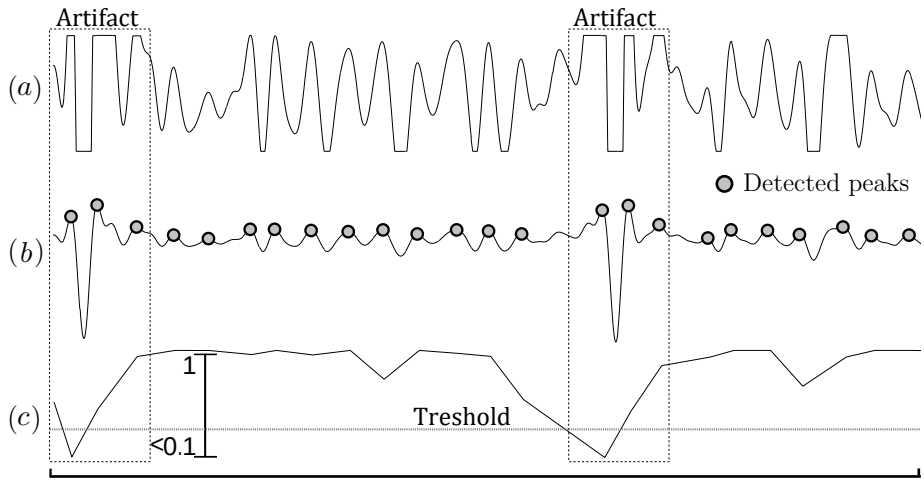

Fig. 4.11. Example of artifact detection in PPG: (a) clipped PPG, (b) preprocessed PPG, and (c) the ratio of the signals in (a) and (b). The vertical line denotes the ranges of the ratio values.

the smartphone via Bluetooth connection (see Fig. A3.1 in Appendix Appendix A3). The same PPG signals from the MIMIC database are transmitted via PC by using a National Instruments LabVIEW^{TM} application which has the capacity reading .mat files and transmits PPG signals in the sample-by-sample fashion. The PC and LabVIEW^{TM} application simulates a patient wearing a PPG sensor.

4.3 PPG-based Detection of Atrial Fibrillation

In this chapter, a photoplethysmography-based method for continuous screening for silent AF is proposed. The proposed detector offers a number of solutions to reduce the false alarm rate including blocks of ectopic filtering, bigeminy suppression, sinus arrhythmia suppression, and signal quality evaluation. Moreover, the proposed solutions can be applied to any RR interval analysis based AF detector. The base for the AF detection part is an improved and modified algorithm by Petrėnas et al., 2015 [32].

A block diagram of the PPG-based AF detector is presented in Fig. 4.12. The algorithm consists of four main parts, namely, preprocessing, feature extraction, artifact detection and AF detection which are described in detail below.

4.3.1 Preprocessing

PPG is mainly composed of lower frequency components, thus the higher frequency noise is removed by using a low-pass finite impulse response filter with

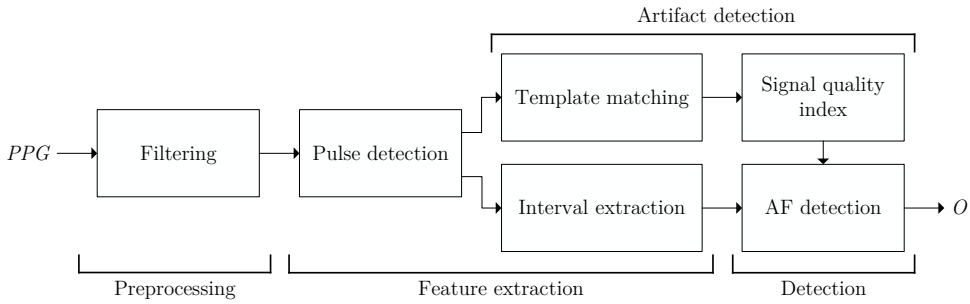

Fig. 4.12. Block diagram of the proposed AF detector.

a cut-off frequency of 5 Hz. The baseline wander is removed with a first order least mean squares adaptive filter (Laguna et al., 1992 [153]).

4.3.2 Peak detection

PPG peaks are detected by using a peak detector with an adaptive threshold (Aboy et al., 2005 [154]). The threshold is adapted by taking the P:th percentile of the PPG samples contained in a 2-s sliding window so as to cover at least one heart cycle. The delay time for the next peak search is adapted by filtering the extracted intervals with the third order median filter and multiplying the result with the experimentally determined multiplier M. The resulting time series are further referred to as *PP intervals*.

4.3.3 Signal Quality Index

Artifacts and misdetected pulses are identified via the signal quality index (SQI). SQI is based on the cross-correlation between the extracted PPG pulse and the signal quality-dependent template. Normally, a previous PPG pulse, extracted from the analyzed signal, is used to evaluate the quality of the current PPG pulse. However, if the quality of the previous PPG pulse is low, then the hardcoded pulse template is used instead. The template is resampled to match the number of samples to that of the current pulse. The cross-correlation function is defined by

$$R_{fg,k}(\tau) = \int_{-\infty}^{\infty} f_k(t) g_k(t-\tau) dt, \tag{4.15}$$

where $f_{k,n}$ is the current pulse, $g_{k,n}$ is a template, τ represents the lag, and k stands for the number of k:th pulse. Both the current pulse and the template are normalized by subtracting the mean and dividing by the standard deviation. The lag at the maximal cross-correlation is determined by

$$\tau_k = \arg\max_n R_{k,n}, \tag{4.16}$$

where k is the k:th lag value. The maximal cross-correlation is obtained by

$$c_k = R_{k,\tau_k}, \tag{4.17}$$

Template $g_{k,n}$ is updated by the previous pulse whenever cross-correlation c_k exceeds 0.95, and lag τ_k is within the range of ± 0.05 s. The template update is performed by

$$g_{k,n} = \begin{cases} f_{k,n}, & c_k \geqslant \mu \text{ and } \tau_{min} \leqslant \tau_k \leqslant \tau_{max} \\ g^h_{k,n}, & \text{otherwise,} \end{cases} \tag{4.18}$$

where μ is the cross-correlation threshold, τ_{min} and τ_{max} are thresholds of correlation lags between the extracted pulse and the template, $g^h_{k,n}$ is the hardcoded template. Finally, the signal quality index is derived by

$$Q_k = \begin{cases} 1, & c_k \geqslant \mu \\ 0, & \text{otherwise,} \end{cases} \tag{4.19}$$

where Q_k is approaching to 1 for a high quality pulse, while it is is much lower for pulses affected by motion artifacts. Figure 4.13 illustrates the main steps of the signal quality assessment.

4.3.4 Ectopic Beat Filtering

Premature heart contractions may result in irregular pulses or in complete absence of the ectopic pulse, thus it is desirable to minimize the false-positive rate due to ectopic activity-caused irregularity. We found that a 3-point median filter is useful for rejecting outlier PP intervals due to, for instance, irregular or missed pulses. Higher-order median filters are less beneficial since they smooth the pulse series to such a degree that AF episodes with low PP irregularity remain undetected. The median filter is defined by

$$p_{m,k} = \text{median}\{p_{k-1}, p_k, p_{k+1}\}, \tag{4.20}$$

where p_k denotes the duration of the k:th PP interval in seconds.

Normally AF is associated with the increased heart rate, thus the mean RR interval can be employed as a feature in the AF detector, cf. Lake et al., 2011 [155]; Langley et al., 2012 [156]. Here, the exponential averager is used to track the 'trend' in the RR interval series. The exponential averager is defined by

$$p_{t,k} = p_{t,k-1} + \alpha(\Gamma(p_{m,k}) - p_{t,k-1}), \tag{4.21}$$

where α $(0 < \alpha < 1)$ determines the degree of smoothing, and $K(\cdot)$ is a saturated linear transfer function produced by

$$K(p_{m,k}) = \begin{cases} 0, & p_{m,k} < 0 \\ p_{m,k}, & 0 < p_{m,k} < 1 \\ 1, & p_{m,k} \geqslant 1. \end{cases} \tag{4.22}$$

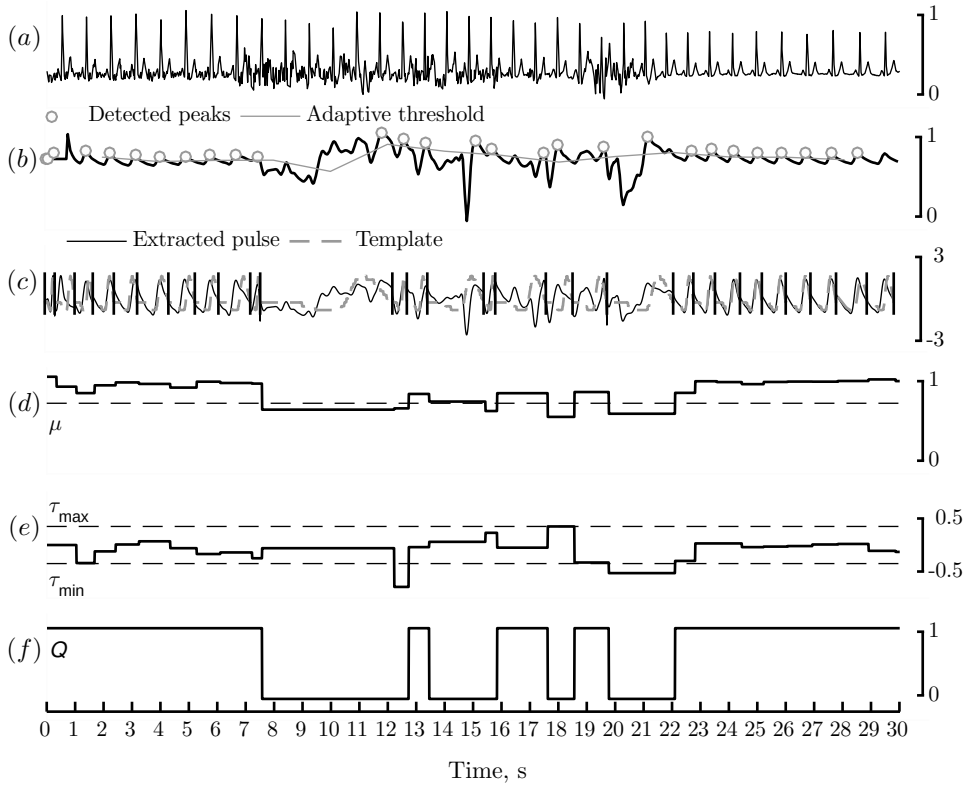

Fig. 4.13. Steps of the signal quality assessment: synchronously recorded (*a*) reference ECG and (*b*) PPG signals, (*c*) template matching, where the vertical lines denote the boundaries of the extracted PPG pulses, (*d*) cross-correlation between the extracted pulse and the template, (*e*) cross-correlation lags, and (*f*) the resulting SQI.

limiting of low pulse rates while using a saturated linear transfer function is useful for detecting AF episodes of a very low pulse rate (<60 bpm).

4.3.5 Sinus arrhythmia suppression

Regular but highly variable pulse rates, for example, during sinus arrhythmia, may also cause false-positives (Cheung et al., 2015 [157]). Sinus arrhythmia is identified by finding a number of turning points in detection window z_k. For regular pulses, z_k takes values close to 0, yet it increases for irregular pulses.

4.3.6 PP interval irregularity

In a sliding detection window of length N, located at time k, the number of all pairwise PP interval combinations differing more than γ seconds is determined

and normalized with its maximum value $N(N-1)/2$, i.e.,

$$I_{t,k} = \begin{cases} 2\frac{\sum_{i=0}^{N-2}\sum_{j=i+1}^{N-1} H(|p_{k-i}-p_{k-j}|-\gamma)}{N(N-1)\cdot p_{t,k}}, & z_k > 2, \\ 0, \text{ otherwise} \end{cases} \tag{4.23}$$

where $H(\cdot)$ is the Heaviside step function. The division by $p_{t,k}$ is motivated by the wish to emphasize PP irregularity at higher heart rates. $I_{t,k}$ is close to 0 for regular rhythms since the difference between pairs of PP intervals is usually smaller than γ, whereas $I_{t,k}$ is approaching 1 during AF.

4.3.7 Bigeminy Suppression

Episodes of bigeminy might be incorrectly detected as AF when detection relies only on PP intervals. Since a premature pulse usually merges with the preceding pulse, bigeminy in PPG signals might take different patterns from those observed in ECG. Therefore, the bigeminy suppression block, originally proposed in Petrėnas et al., 2015 [32], is modified to account for PPG properties. The bigeminy suppression measure is defined by

$$B_k = \left(\frac{\sum_{j=0}^{N-1} b_{k-j}}{\sum_{j=0}^{N-1} b_{m,k-j}} - 1 \right)^2, \tag{4.24}$$

where N is an even-valued integer, b_k and $b_{m,k}$ are median filtered ratios of successive PP intervals p_k and median filtered intervals $p_{m,k}$, given by

$$b_k = \text{median}\left\{ \frac{p_{k-1}}{p_k}, \frac{p_k}{p_{k+1}}, \frac{p_{k+1}}{p_{k+2}} \right\}, \tag{4.25}$$

$$b_{m,k} = \text{median}\left\{ \frac{p_{m,k-1}}{p_{m,k}}, \frac{p_{m,k}}{p_{m,k+1}}, \frac{p_{m,k+1}}{p_{m,k+2}} \right\}. \tag{4.26}$$

The use of PP interval ratios is motivated by the observation that the original implementation of bigeminy filtering does not work properly due to the constant PP interval length. Median filtering is intended to smoothen the resulting spikes during pulse transition from normal to bigeminy, and vice versa (see Fig. 4.14). For bigeminy and regular pulse, the ratio in (4.24) is approximately 1 since $p_{m,k}$ and p_k are similar, and thus $B_{t,k}$ is approximately 0, see Fig. 4.14.

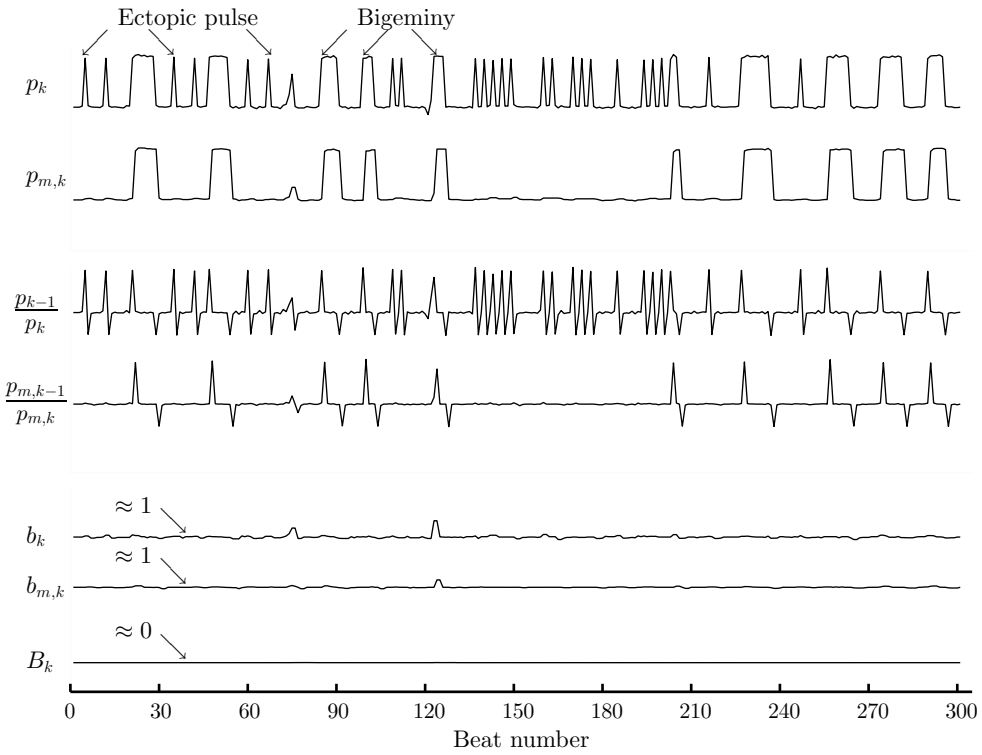

Fig. 4.14. The steps to obtain bigeminy suppression measure by processing PP intervals.

4.3.8 Signal Fusion and Detection

Simple signal fusion is employed to produce decision function $\mathcal{O}_k$,

$$\mathcal{O}_k = \begin{cases} I_{t,k}, & B_{t,k} \geqslant \delta \\ B_{t,k}, & B_{t,k} < \delta. \end{cases} \tag{4.27}$$

$\mathcal{O}_k$ is identical to $B_{t,k}$, unless $B_{t,k}$ exceeds fixed threshold δ. Otherwise, $\mathcal{O}_k$ is equal to $I_{t,k}$.

Figure 4.15 illustrates the outputs of both PPG-optimized and original AF detectors $\mathcal{O}_k$ and ${}^*\mathcal{O}_k$ together with corresponding intervals p_k for PPG signals with an AF episode surrounded by ectopic beats, sinus rhythm with the episodes of bigeminy and a segment with artifacts. It is obvious, that during an episode of AF, outputs of both the PPG-optimized and original algorithms exceed threshold values η and ${}^*\eta$, respectively. However, unlike the original algorithm, the output of the PPG-optimized algorithm does not exceed threshold value η during the PPG segment with episodes of bigeminy and artifacts, therefore, resulting in no false alarms. It is obvious that median filtering removes the PP intervals related to ectopic pulses so that an AF episode could be correctly detected and false alarms could be avoided.

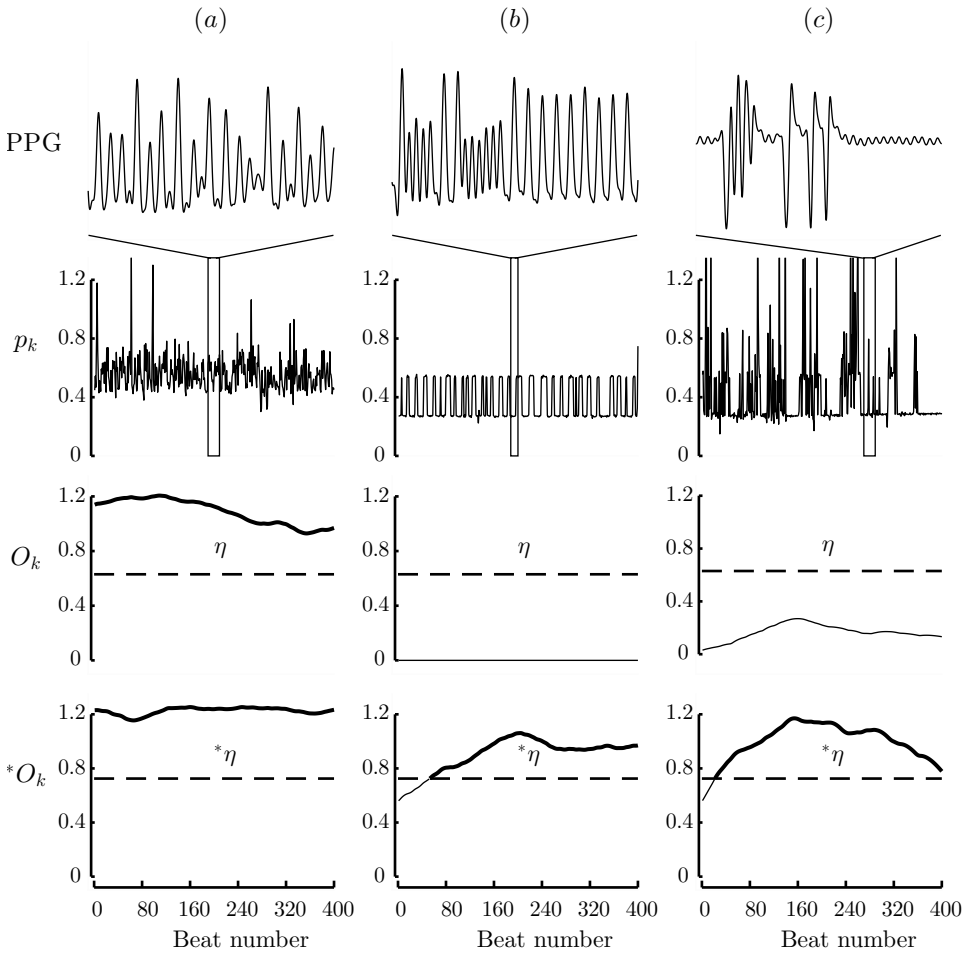

Fig. 4.15. Intervals p_k and outputs of PPG-optimized (O_k) and original ($^*O_k$) AF detection algorithms together with corresponding detection thresholds η and $^*\eta$ while using PPG signals during: (a) atrial fibrillation, (b) bigeminy, and (c) artifacts.

4.3.9 Implementation of Online Atrial Fibrillation Detector

The online version of the AF detector was implemented as the application for the use in the Android operating system. As in the case with PVC detector, the PPG signal is transmitted to the smartphone via wireless Bluetooth connection (see Fig. A3.2 in Appendix Appendix A3).

4.4 Conclusion of the Chapter

1. A phenomenological model for simulating PPG during sinus rhythm and arrhythmias has been developed. The model accepts RR interval series as input for generating simulated PPG signals. The model may be employed

for the development and assessment of PPG-based arrhythmia detection algorithms.

2. A PPG-based algorithm for the detection of PVCs has been developed. The proposed detector relies on temporal, frequency domain features and artificial neural network classifier for the detection of PVCs. The rate of false alarms is reduced by employing an artifact detector. The algorithm can be implemented for online PVC detection.

3. A real-time PPG-based algorithm for the detection of AF relying on an improved and modified low-complexity AF detection algorithm and signal quality assessment has been proposed. The algorithm employs solutions allowing to reduce the influence of sources of false alarms, such as the ectopic beats, bigeminy, sinus arrhythmia and artifacts. The algorithm can be implemented for online AF detection.

5 PERFORMANCE EVALUATION OF THE DEVELOPED METHODS

5.1 Modeling of the PPG during Cardiac Arrhythmia

5.1.1 Data

The proposed model is evaluated on PPG signals from the Physionet MIMIC Database, the University of Queensland Vital Sign Database (UQVSD), and the MIT–BIH Atrial Fibrillation Database (AFDB).

ECG and PPG signals in the MIMIC database were originally sampled at 500 Hz and 125 Hz, respectively, both with 12-bit precision. The sampling rate of PPG was then digitally increased to match that of ECG. Records with both ECG and PPG signals and varying morphology (56 records in total, see Table A1.1 in Appendix) were selected and divided into 60-s segments. Only segments of ECG and PPG free of excessive noise and artifacts were included for further analysis. PPGs were preprocessed with a bandpass finite impulse response (FIR) filter with 0.5 and 15 Hz as cut-off frequencies and scaled to develop the unit amplitude. Each segment was manually assigned to one of the following three rhythm types: sinus rhythm, sinus rhythm with premature beats, and AF, resulting in 510, 1198, and 377 segments, respectively. For single PPG pulse modeling, 56 pulses of distinctive morphologies, free from noise and artifacts were extracted from one of the 60-s segment and grouped according to the pulse types shown in Fig. 4.2.

The University of Queensland Vital Signs Dataset contains data recorded during 32 surgical cases from patients who underwent anaesthesia at the Royal Adelaide Hospital (see Table A1.2 in Appendix). All the signals in the UQVSD were recorded at 10 ms temporal resolution. Each case contains from 2 to 30 records of 10 minutes with a varying quality of both ECG and PPG signals. Only 60-s segments free of excessive noise in both ECG and PPG were selected: 341 segments with sinus rhythm, 78 segments of sinus rhythm with premature beats, and 33 segments with AF. For single PPG pulse modeling, 32 pulses of distinctive morphologies, free from noise and artifacts, were extracted and grouped according to the pulse types shown in Fig. 4.2. The ECG signals in AFDB were sampled at 250 Hz with 12-bit precision. The annotated RR interval series were used to generate model PPG signals.

5.1.2 AF Detection

The significance of the proposed PPG model is studied in terms of AF detection performance. A low-complexity AF detector based on RR interval information is investigated; it has been designed to detect brief AF episodes

(< 30 s). The detector is described in detail in (Petrėnas et al., 2015 [32]). Important features of the detector are the short sliding detection window (8 beats) and the low-power consumption due to few arithmetical operations, making the detector particularly well-suited for use in a wearable system. By controlling the cut-off frequency of the exponential trend filters, the detector can be tuned to detect AF episodes as short as 8 beats.

The model PPG signal subject to AF detection is further preprocessed by using an FIR bandpass filter with cut-off frequencies at 0.5 and 5 Hz aimed at removing noise components not overlapping with the spectrum of the PPG signal. Then, a real-time peak detector based on Aboy et al., 2005 [154] is applied to the preprocessed signal so that the intervals between successive pulses can be determined and used as input to the AF detector. In the peak detector, an adaptive threshold is used in relation to the 55:th percentile of the samples in a 2-s sliding window.

5.1.3 Performance Evaluation

A number of parameter values need to be set in the simulation model. For a single PPG pulse, the initial values of the involved parameters are, prior to fitting, manually defined within reasonable ranges so that the direct wave of the pulse precedes the two reflection waves.

Therefore, interval ratio thresholds η_0 and η_1 in (4.7)–(4.9) are set to 0.8 and 1.4, respectively. Suitable threshold values are investigated in the Results section (see Fig. 5.3).

Sampling interval T in (4.11) is set to d/F_s, where d is the duration of a time interval used to obtain parameters for model PPG pulses, and F_s represents the sampling rate, e.g., 500 Hz for MIMIC signals.

The adequacy of the proposed PPG model is evaluated by comparison to PPGs from the MIMIC and UQVSD databases. The root mean square error (E) between the real and model signals is the primary measure intended to evaluate the performance defined by

$$E = \frac{1}{M} \sum_{m=1}^{M} \sqrt{\frac{1}{N} \sum_{n=1}^{N} (u_m(n) - x_m(n))^2}, \tag{5.1}$$

where M is the total number of segments, m is the segment number, N is the total number of samples in a segment, n is the sample number, and $u_m(n)$ is the real signal. Prior to computing E, both real and modeled signals are normalized to the unit amplitude. In order to avoid issues related to signal misalignment, crosscorrelation was used to align the two involved signals.

In order to test the AF detector, all the 25 annotated RR interval series from the AFDB database were used. Since the morphology of PPG pulses

depends on many factors including the age and the medical condition, the evaluation is performed with PPGs modeled by utilizing the five PPG pulse types in Fig. 4.2; thus a total of 125 model PPGs are analyzed. The performance of the peak detector and the AF detector are evaluated separately in terms of precision (P), sensitivity (Se) and specificity (Sp), respectively, at various SNRs ranging from 0 to 30 dB. Precision is defined as

$$P = \frac{TP}{TP + FP} \cdot 100\%, \tag{5.2}$$

where TP is the number of correctly detected peaks and FP is the number of falsely detected peaks. Accuracy is obtained by

$$Se = \frac{TP}{TP + FP} \cdot 100\%, \tag{5.3}$$

where TP is the number of beats correctly identified as AF, whereas FP is the number of beats that are falsely detected as AF.

$$Sp = \frac{TN}{FN + TN} \cdot 100\%, \tag{5.4}$$

where TN is the number of beats correctly identified as non-AF, and FN is the number of beats, falsely detected as non-AF.

In order to extract the artifact from the real PPG segment, the NLMS adaptation step size $\mu = 1 \times 10^{-3}$ and filter order 20 was used. The impulse response of an extracted artifact was determined by setting the values for the adaptation step size and the filter order to 1×10^{-7} and 200, respectively. This allows for slower adaptation and a larger number of coefficients for capturing the impulse response of the artifact.

5.1.4 Results

Modeling of single PPG pulses. The proposed PPG pulse model was compared with the relative models based on gamma and two Gaussian waveforms (Huang et al., 2013 [136]), three log-normal waveforms (Huotari et al., 2011 [137]), and three Gaussian waveforms (Wang et al., 2013 [134]; Liu et al., 2014 [135]) (see Fig. 5.1). The initial set of pulse fitting parameters is provided in Table A2.1 (see Appendix Appendix A2).

The top chart in Fig. 5.2 shows the average RMS errors stemming from using different PPG pulse models, together with 56 PPG pulses from the MIMIC database (see table A1.1 in Appendix Appendix A1 for details), grouped into 3 PPG pulse types; types 2 and 3 bis pulses were not present in the database. The smallest error was obtained for the log-normal waveform combined with two Gaussians. The middle chart in Fig. 5.2 shows the average RMS errors that result from using different PPG pulse models, together with 32 PPG pulses from the

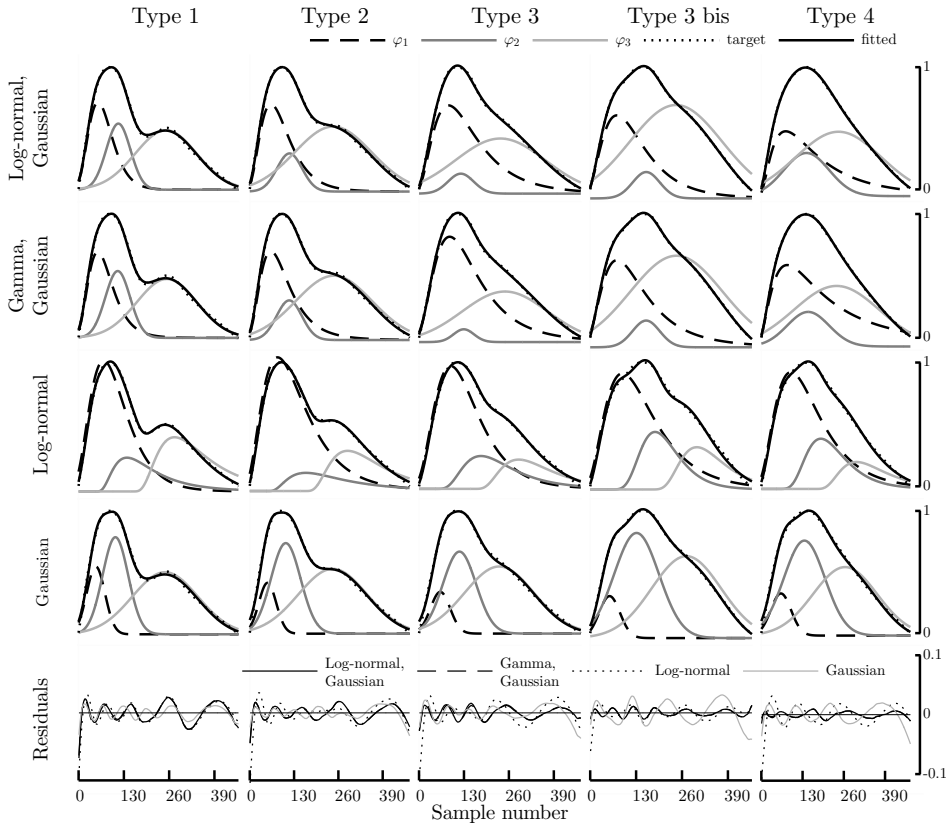

Fig. 5.1. Examples of model PPG pulses. The top row shows the PPG pulses obtained by combining log-normal and Gaussian waveforms, the second row shows the PPG pulse obtained on the basis of gamma and Gaussian waveforms, the third row shows the log-normal waveform-based approach and the fourth row shows PPG pulses modeled by using Gaussian waveforms. The bottom row shows residuals between templates and model PPG pulses.

UQVSD database (see table A1.2 in Appendix Appendix A1 for details) also grouped into 3 PPG pulse types; types 2 and 3 bis pulses were not present in the database. The largest error was obtained for the model with three Gaussians, while the smallest error for Type 3 and Type 4 pulses was obtained for the log-normal waveform combined with two Gaussians. The bottom chart in Fig. 5.2 shows the RMS errors obtained from the five different PPG pulse types shown in Fig. 4.2. A similar error was obtained for the log-normal waveform combined with two Gaussians and for the gamma waveform combined with two Gaussians, while the largest error was obtained for the model with three Gaussians.

Modeling of connected PPG signals. Figure 5.3 shows the RMS error between modeled and real PPG signals as a function of η_0 and η_1 thresholds, used in (4.7)–(4.9). The results suggest that suitable values for η_0 and η_1 are 0.8 and 1.4,

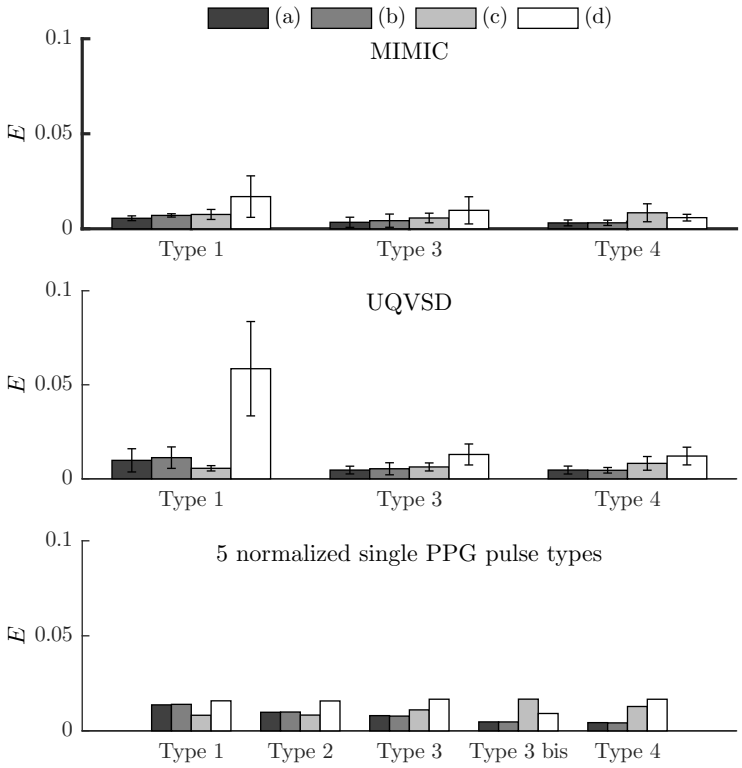

Fig. 5.2. From top to bottom. The RMS error for 56 normalized PPG pulses (3 - Type 1, 40 - Type 3, and 13 - Type 4) from the MIMIC database, the RMS error for 32 normalized PPG pulses (3 - Type 1, 20 - Type 3, and 9 - Type 4) from the UQVSD database, and the RMS error for 5 normalized single PPG pulse types (see Fig. 4.2) while using different modeling approaches: (a) log-normal and Gaussian, (b) gamma and Gaussian, (c) log-normal, (d) Gaussian.

respectively. The increase in the RMS error for $\eta_0 > 0.8$ is due the rules in (4.7) and (4.8), applying to beats associated with small interval variation but which are not premature. Threshold η_1 ensures that the ratio of a compensatory pause r_{k+1} and premature r_k is associated only with a premature beat when determining the pulse amplitude in (4.9) since, in cases when r_{k-1} is compensatory pause and r_k is a normal interval, the ratio may also be below 0.8 and, accordingly, falsely associated with a premature pulse. Therefore, a larger threshold than $\eta_1 = 1.4$ leads to an increase in the RMS error, due to which, premature beats are associated with normal beats. As expected, η_0 and η_1 have no effect during the sinus rhythm since the difference between successive intervals is insignificant.

Figure 5.4 shows that the lowest RMS error is obtained for PPGs with sinus rhythm and sinus rhythm with premature beats, whereas E increases to 0.1 for AF.

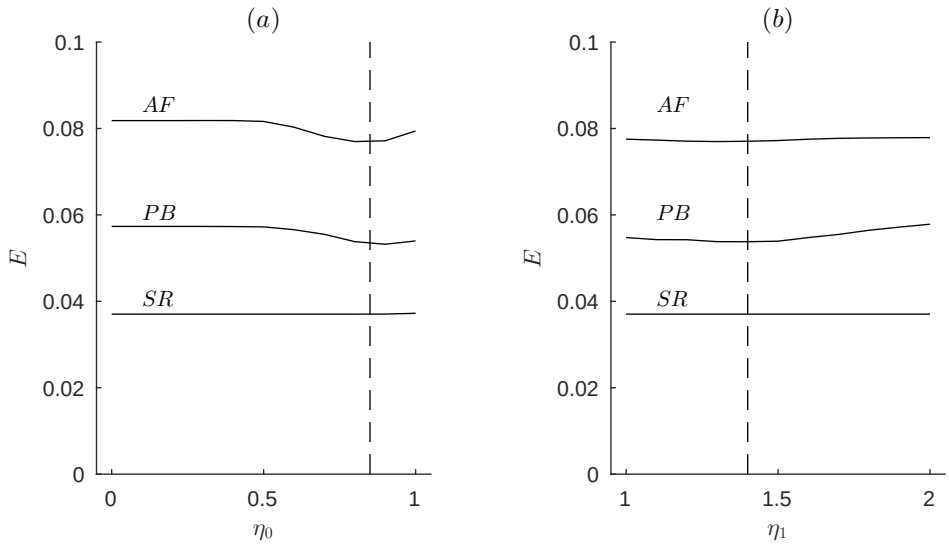

Fig. 5.3. RMS error between 1-min connected model signals and real PPG signals as a function of the thresholds (*a*) η_0, (*b*) η_1 in (4.7)–(4.9). Dashed horizontal lines show ratio thresholds for various rhythm types: atrial fibrillation (AF), sinus rhythm with premature beats (PB), and sinus rhythm (SR).

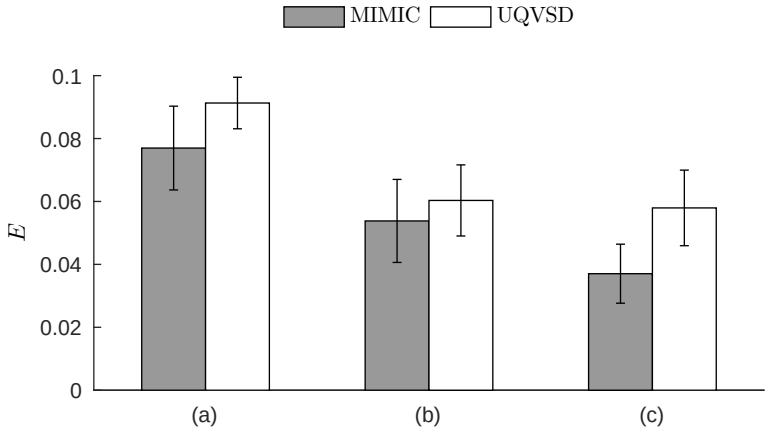

Fig. 5.4. The RMS error for 1-min continuous PPG signals with (*a*) atrial fibrillation, (*b*) sinus rhythm with premature beats, and (*c*) sinus rhythm. PPG signals are simulated by using the log-normal and Gaussian pulse modeling approach.

Figure 5.5 presents the precision (P) of the peak detector and both sensitivity (Se) and specificity (Sp) of the AF detector as a function of SNR for the five pulse types. It is obvious that the detection performance of both peak and AF detectors drops rather quickly below a certain SNR which is strongly dependent on the pulse type. Signals composed of Type 1 pulses cause the detection accuracy to drop at a higher SNR than the other four types of pulses do. The

increase in Se at low SNRs is due to the detection of extra random noise-induced peaks, resulting in irregular intervals causing the AF detector to produce false alarms.

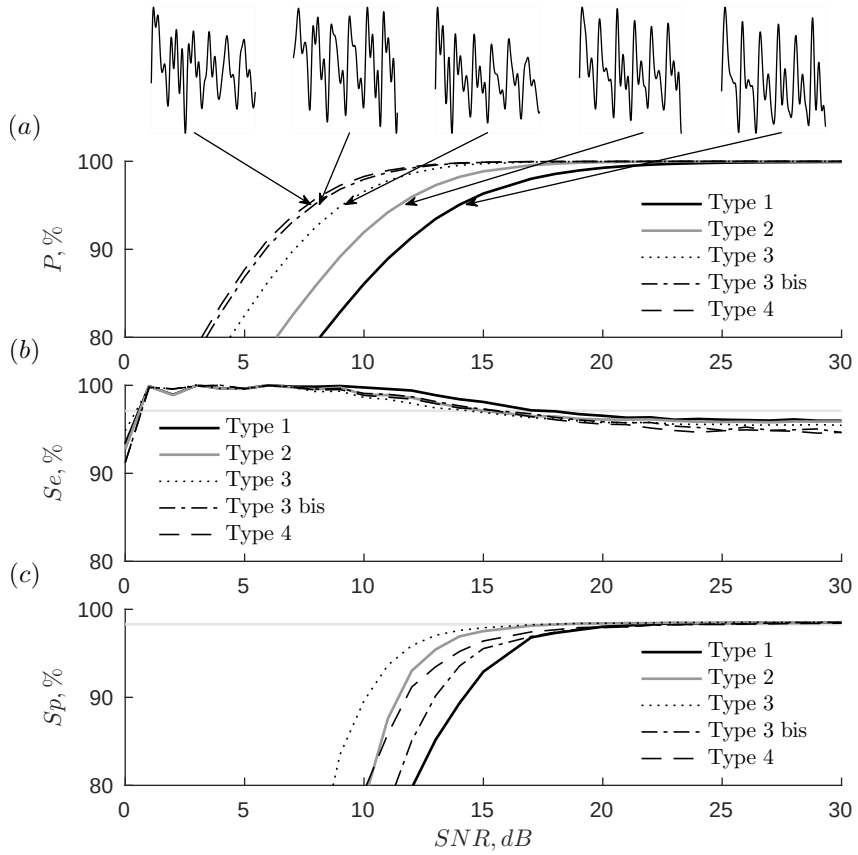

Fig. 5.5. (a) Precision of peak detection, (b) sensitivity of AF detection and (c) specificity of AF detection. The PPG signal, corresponding to the SNR at a precision of P =95 %, is displayed above the corresponding curve. The sensitivity and specificity resulting from RR-based detection in AFDB (97.1 % and 98.3 %, respectively) are displayed as horizontal lines.

5.1.5 Discussion

The aim of this work is to develop a phenomenological model for simulating PPG signals with paroxysmal AF. With the emerging technologies, capable of acquiring PPG (wristbands with integrated PPG sensors, smartphone camera), there is still lack of algorithms which could provide diagnostic information, i.e., detect arrhythmic episodes. Lack of annotated PPG databases with arrhythmic episodes is a major limitation hindering the development of such algorithms.

An important advantage of the proposed model for PPG signals is that

annotated ECG databases with AF episodes, e.g., MIT–BIH Arrhythmia, MIT–BIH Atrial Fibrillation, Long Term AF database, or generators of RR interval series, e.g., McSharry et al., 2003 [158]; Lian et al., 2007 [159], can be used for generating annotated PPG signals—a principle which makes it possible to compare the performance of a PPG-based detector to that of an ECG-based detector. Since the ECG and PPG signals have different origins, i.e., electrical and hemodynamic, their properties are quite different as well. For example, the PPG pulse related to a premature beat may not be observable, which leads to the consequence that the peak-to-peak interval is approximately twice as long as is the corresponding RR interval (see Fig.4.5). Therefore, it is desirable that PPG-based AF detectors are developed and evaluated on PPG signals, rather than on ECG signals (Lee et al., 2013 [28]) so that PPG-specific changes in morphology are taken into account.

Various approaches to simulating hemodynamic signals have been proposed, however, none of them have been directly intended for simulation of arrhythmia (Clifford et al., 2004 [138]; Nabar et al., 2011 [139]; Martin-Martinez et al., 2013 [140]; Scarsoglio et al., 2014 [141]). Therefore, an important objective of the present study was to develop a simulator accounting for PPG morphology during AF and premature beats, as well as during transitions from the sinus rhythm to AF, or vice versa.

This study proposes a combination of a log-normal function and two Gaussian functions for the modeling of different types of PPG pulses. However, other approaches may also be considered since negligible differences are observed in PPG sequences generated by different models therefore making no significant impact on the morphology of the simulated signals, and no influence on the AF detection performance, either. While the Hermite functions originally proposed for modeling QRS complexes (Sörnmo et al., 1981 [160]), are well-suited for simulating subtle changes in the PPG, i.e., dicrotic notch, they are less-suited for modeling the reflected blood volume waves due to negative polarity; therefore, these functions were not further pursued.

The modeling of the PPG pulse amplitude has received little, if any, attention in the scholarly literature. Since the amplitude depends on numerous factors, such as age, arterial compliance, and permeability (Allen et al., 2003 [161]), we have, for the sake of simplicity, assumed that the pulse amplitude is inversely proportional to the length of the RR interval. Given that a simulator has been developed for modeling the PPG during AF, the model does not account for amplitude modulation induced by respiration, nor for the modulation of the pulse width. Therefore, the simulation model is not suitable for evaluating the performance of the methods which derive the respiratory rate from PPG, e.g., the one developed in (Lázaro et al., 2013 [162]).

The performance of the AF detector is heavily dependent on the accuracy of the PPG pulse detector since the series with peak-to-peak intervals serves as

the input to the AF detector: the number of false positives increases considerably at lower SNRs due to the incorrect peak detection. The results in Fig. 5.5 show that PPG signals composed of Type 1 pulses are particularly vulnerable to noise as the risk to falsely detect the dicrotic pulse as a systolic peak increases.

The PPG is much more prone to noise and artifacts than the ECG, therefore, the synchronously recorded ECG is indispensable for high-precision annotation of the PPG. Therefore, the MIMIC (Moody et al., 1996 [130]) and MIMIC II (Saeed et al., 2011 [132]) databases are usually applied for the development and testing of PPG-based algorithms. Yet, the MIMIC and MIMIC II databases are unannotated, and would require substantial time to manually annotate.

The idea to use an annotated ECG database as the basis for simulation of PPG signals may also be considered when other physiological signals are of interest to model, e.g., impedance plethysmography or continuous arterial blood pressure. The proposed simulator may also be explored for reconstructing noise-corrupted PPG signals when a synchronously recorded ECG is available or for other noise cleaning approaches, such as Banerjee et al., 2015 [163].

A limitation of the present study is that simulator performance was not investigated on other types of arrhythmias such as atrial flutter or supraventricular tachycardia since these types are lacking in the MIMIC database. Although such arrhythmias may be present in the comprehensive MIMIC II database, signals are generally of lower quality due to the lower sampling rate, artifacts, and missing signals. Another limitation of the present study is that the model is not tested on a PPG-specific AF detector. The development of PPG-specific AF detectors is highly needed; hopefully, it will be prompted by the present model PPG signals.

5.2 PPG-based Detection of Premature Ventricular Contractions

5.2.1 Data

Clinical signals. The algorithm was developed on 18 PPGs (a training set) sampled at 125 Hz, which were taken from the PhysioNet MIMIC II database (Goldberger et al., 2000 [131]; Saeed et al., 2011 [132]). Twenty-five 1–2 h PPGs sampled at 250 Hz (the MIMIC database (Moody et al., 1996 [130])), and one 100-min-long signal sampled at 250 Hz (recorded at Kaunas Biomedical Engineering Institute, referred to as BMEI) were used for testing. In order to reduce the errors that may occur during the feature extraction, all the signals were resampled to 500 Hz.

PVCs in the PPG were annotated with respect to a synchronously recorded reference ECG. At first, PVCs in the ECG were detected by using an automated RR interval detection algorithm (Benitez et al., 2001 [164]). Then, RR intervals were used for manual evaluation of ECG morphology so that to ensure that the

particular beat is PVC. Finally, PVC-related PPG pulses were labeled as P^1 or P^2 according to the previously described procedure. The remaining PPG pulses were assigned to normal N.

Since the signals in both databases (MIMIC and MIMIC II) contain severe signal corruptions or various pathologies, several of them were excluded from the study. The criteria for discarding the signals was the absence of usable information in either ECG or PPG, therefore resulting in difficulties to correctly annotate the signals. The list of the test signals is presented in Table 5.1.

Table 5.1. Test PPGs obtained from the MIMIC database (No. 1–25) and recorded at KTU BME institute (No. 26)

No.	Record	$\#P^1$	$\#P^2$	No.	Record	$\#P^1$	$\#P^2$
1	039	0	0	14	404	0	268
2	041	0	0	15	408	9	2
3	055	1	0	16	439	12	3
4	211	0	0	17	442	1288	366
5	212	159	30	18	444	7	10
6	218	0	0	19	449	7	2
7	221	11	0	20	466	3	4
8	224	0	0	21	471	1	0
9	225	0	11	22	474	2	4
10	230	0	4	23	482	48	88
11	237	40	14	24	484	69	20
12	252	0	0	25	485	754	16
13	253	0	0	26	BMEI	25	2
	Total:	211	59		Total:	2225	785

Simulated signals. The simulated PPG signals were produced by applying the PPG model proposed in Sološenko et al., 2017 [144]. Since the PPG model accepts RR interval series as its input, the RR interval series generator is used to supply them (McSharry et al., 2003 [158]). The generator of RR interval series is capable of simulating both the RR series during the normal sinus rhythm and during cardiac ectopy at various heart rates. The settings used for generating the RR interval series are presented in Table 5.2.

5.2.2 Performance Evaluation

The performance of the method was evaluated in terms of the sensitivity (Se), specificity (Sp) and accuracy (Ac). Due to the a considerable difference regarding a number of normal pulses and PVCs, the Matthews correlation co-

Table 5.2. Parameter settings used in RR interval generator

No.	Parameter	Value
1	Mean heart rate	[60, 240] bpm
2	Standard deviation	[0.5, 3] bpm
3	Mayer wave frequency, F_1	0.1 Hz
4	Respiratory rate, F_2	[0.2, 0.5] Hz
5	Standard deviation of F_1, $\sigma_{V,1}$	0.01 Hz
6	Standard deviation of F_2, $\sigma_{V,2}$	0.01 Hz
7	Low-frequency/high-frequency ratio, P_1/P_2	[0.5, 2]
8	Rate of atrial ectopic beats	0.05

efficient was employed as an additional performance measure (Mc) (Gorodkin, 2004 [165]).

The method was tested by using ANN with either linear and non-linear outputs. The full feature set (3 PP and 3 PR) was applied for training the ANN. In addition, the performance was also tested with a reduced feature set, consisting of just 3 PP inputs. Since, the weights in the ANN are initialized randomly, the training process was repeated 3 times, and then the averaged performance values were taken as the overall performance measure.

It should be noted that the initial testing was carried out without involving artifact detection. Then, both the best performing, and the most computationally efficient (with PP features, linear outputs, and blocks 6, 7 and 8 excluded in Fig. 4.7) configurations were used for repeated testing but with the artifact detector involved.

5.2.3 Results

Clinical signals. The results of clinical signals are presented in Tables 5.3–5.6. Table 5.3 shows that the performance of ANN does not depend on the type of neurons in the output layer, although slightly better results were obtained when an ANN with the linear outputs is used. On the other hand, the ANN employing only a PP feature set is associated with a higher accuracy when non-linear outputs are used (Table 5.4).

The ANN with non-linear outputs and the full feature set was further reinvestigated – but with the artifact detector included. The inclusion of the artifact detector allowed reducing the number of false positives by approximately 60 %. Thus, Sp for PVC types P^1 and P^2 increased from 99.6 %/99.8 % to 99.9 %/99.9 %, respectively. However, the inclusion of the artifact detector resulted in a slight decrease in Se from 94.2 %/93.1 % to 93.2/92.4 %, respectively (Table 5.5). The decrease in sensitivity can be explained by the fact that some of the premature pulses have a similar morphology to that of artifacts, and

Table 5.3. The classification results obtained while using both PP and PR features as input to ANN: (*a*) performance measures, (*b*) confusion matrices.

		Linear output ANN			Non-linear output ANN		
	Class ⇒	N	P^1	P^2	N	P^1	P^2
(*a*)	$Se, \%$	99.4	94.2	93.1	99.3	93.2	91.6
	$Sp, \%$	94.2	99.6	99.8	93.1	99.5	99.8
	$Ac, \%$	99.3	99.5	99.8	99.3	99.5	99.8
	$Mc, \%$	78.3	79.3	75.2	78.0	77.5	75.2
	Class ⇒	N	P^1	P^2	N	P^1	P^2
(*b*)	N	255002	133	57	254867	156	70
	P^1	1122	2295	1	1236	2271	1
	P^2	496	8	786	468	9	773

Table 5.4. The classification results obtained while using solely PP-based features: (*a*) performance measures, (*b*) confusion matrices.

		Linear output ANN			Non-linear output ANN		
	Class ⇒	N	P^1	P^2	N	P^1	P^2
(*a*)	$Se, \%$	99.3	90.5	84.0	99.0	91.2	91.0
	$Sp, \%$	89.1	99.6	99.8	92.6	99.4	99.7
	$Ac, \%$	99.2	99.5	99.7	99.0	99.3	99.7
	$Mc, \%$	74.4	77.1	66.8	71.7	73.5	66.5
	Class ⇒	N	P^1	P^2	N	P^1	P^2
(*b*)	N	255069	222	134	253302	186	53
	P^1	1134	2205	1	1499	2237	0
	P^2	610	9	709	768	13	746

therefore were removed from further analysis.

The most computationally efficient configuration is associated with a slightly worse performance compared to the best performing configuration (see Tables 5.5 and 5.6). By combining this configuration with the artifact detector, the number of false positives decreased by approximately 63 % compared to the level achieved without employing the artifact detector. Moreover, Sp for the P^1 PVC type increased from 99.6 % to 99.9 %. In contrast, Sp for P^2 PVC type remained unchanged. According to the previous explanation, a slight decrease in Se is observed for both PVC pulse types, i.e., from 90.5 %/84.0 % to 89.5 %/83.2 % for

Table 5.5. Classification results obtained while using non-linear output ANN classifier, both PP and PR features and artifact detector: (*a*) performance measures, (*b*) confusion matrices.

(*a*)

Class ⇒	N	P^1	P^2
$Se, \%$	99.8	93.2	92.4
$Sp, \%$	93.3	99.9	99.9
$Ac, \%$	99.7	99.8	99.8
$Mc, \%$	87.7	91.3	78.7

(*b*)

Class ⇒	N	P^1	P^2
N	255891	158	63
P^1	262	2270	1
P^2	373	8	780

Table 5.6. Classification results obtained while using linear output ANN, PP features and artifact detector: (*a*) performance measures, (*b*) confusion matrices.

(*a*)

Class ⇒	N	P^1	P^2
$Se, \%$	99.7	89.5	83.2
$Sp, \%$	88.2	99.9	99.8
$Ac, \%$	99.5	99.8	99.7
$Mc, \%$	81.9	87.5	68.3

(*b*)

Class ⇒	N	P^1	P^2
N	254696	246	137
P^1	362	2181	1
P^2	523	9	683

P^1 and P^2, respectively.

Online version with simulated signals. Figure 5.6 presents PVC detection results obtained on simulated PPG signal database at various SNRs ranging from 0 dB to 30 dB.

Here, the algorithm configuration relying on PP intervals and ANN with non-linear output was used as a compromise between the detection sensitivity, specificity and algorithm complexity. The results show that in most cases, PVCs can be reliably detected up to 20 dB SNR at 60 bpm with the sensitivity and specificity as high as 94.4±3.1 % and 99.98±0.01 %, respectively. At higher heart rates, ranging from 120 bpm to 240 bpm, PVCs can be reliably detected

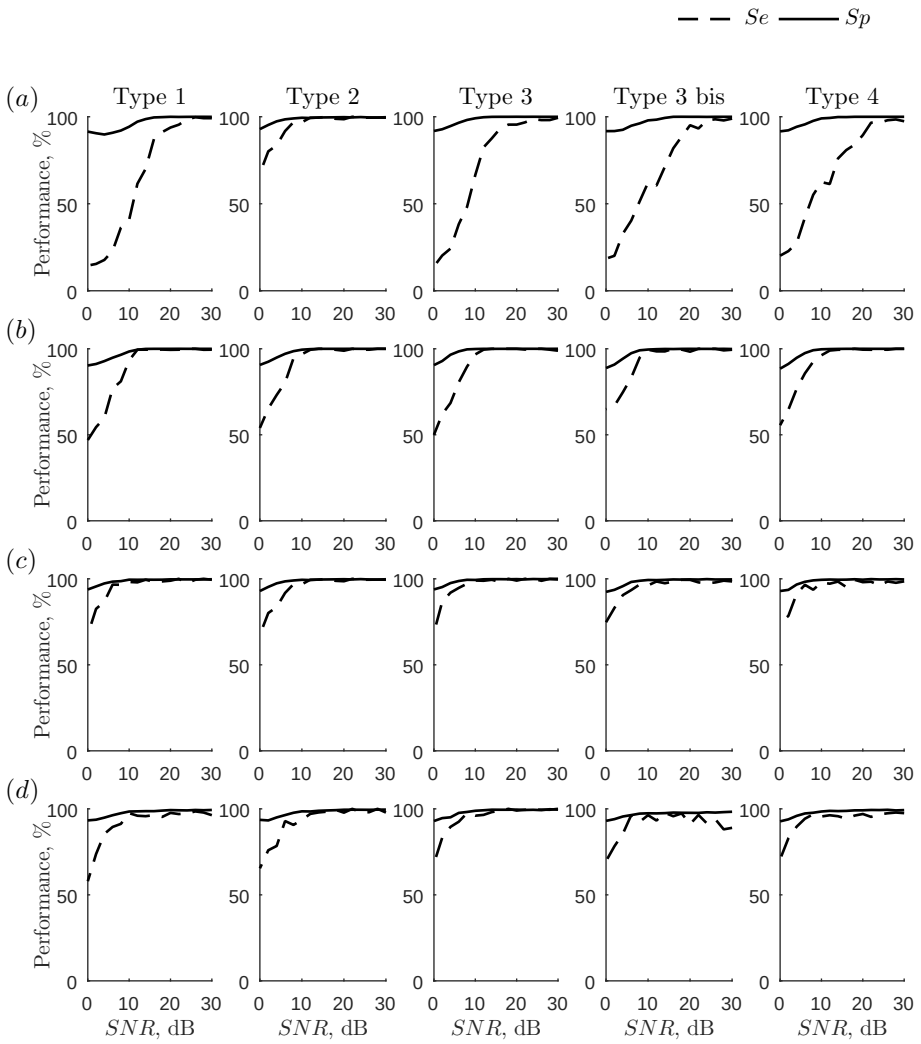

Fig. 5.6. PVC detection sensitivity (Se) and specificity (Sp) as a function of SNR on simulated PPG signals with five PPG pulse types and at different heart rates: (a) 60 bpm, (b) 120 bpm, (c) 180 bpm, and (d) 240 bpm.

at SNR as low as 10 dB. In this case, the mean sensitivity and specificity values for all the pulse types are 96.6±0.9 % and 99.06±0.6 %, respectively. At 0 dB SNR, the mean specificity of 91.9±1.6 % is obtained. The performance drop at the normal heart rate is explained by the fact that the spectrum of the applied noise is in the lower frequency ranges and distorts the fundamental components of the PPG signal more than in the range of 180–240 bpm.

5.2.4 Discussion

The goal of this work was to develop a method for the detection of premature ventricular contractions by relying solely on photoplethysmography signal analysis. Our first attempt to detect premature contractions by using PPG was presented in an earlier study (Sološenko et al., 2013 [166]). Besides that, a pilot study was performed on the basis of only 9 PPG signals; the previous algorithm, in contrast to the proposed one, had limited capabilities of detecting successive premature pulses, such as bigeminy.

In contrast to ECG, the PPG can be acquired in a single spot of the body, let alone the fact that no adhesive electrodes are required. Considering these points, PPG-based arrhythmia detection is an attractive solution for both short-term screening and long-term arrhythmia monitoring when unobtrusiveness for the user is of special importance.

The proposed PVC detector, due to the blocks of adaptive feature extraction and artifact detection, allowed to achieve superior performance in comparison to that obtained by Gil et al., 2013 [124]. Even though, Gil et al., 2013 [124] excluded those PVCs which had occurred within 5 previous or 20 subsequent beats, our method was more accurate (99.8 % vs. 99.3 %).

The study revealed that the main challenge is to distinguish between PVCs and artifacts, since the distorted PPG pulse can be erroneously assigned to the class of premature beats. Thus high amplitude artifacts may distort a group of nearby pulses and introduce residual distortions in a shape of further pulses. Nevertheless, even the simplified configuration of the algorithm showed sufficient performance to detect PVCs in artifact-distorted PPGs (see Table 5.4 (a)). Therefore, the simplified (computationally efficient) configuration can be considered for the implementation in a mobile device.

Although the algorithm shows nearly perfect specificity (99.9 %), the specificity can be further improved by computing PRs in several discrete ranges of each PP rather than by obtaining PRs across the entire PP interval. Additional improvement in the specificity may be achieved by upgrading the artifact detector since the current artifact detector is effective only in those cases when artifacts are denoted by a higher amplitude than the normal PPG pulse.

In this study, high-pass and low-pass FIR filters were used to pre-process the PPG. However, more advanced signal processing techniques can be employed either to eliminate PPG distortions, such as baseline wandering (Laguna et al., 1992 [153]; Wang et al., 2014 [167]), or to assess the PPG quality (Patterson et al., 2011 [168]; Li et al., 2012 [169]). Initial tests showed that a single-layer perceptron classifier does not converge during training, owing to the fact that the PPG features used in the present study are not linearly separable. Hence, a multi-layer perceptron (i.e., ANN) was chosen due to its universal characteristics and ability to approximate linear and non-linear functions. In addition, the performance of PPG pulse classification largely depends on the estimated normal

heart rate (parameter f_{NHR}) which influences the normalization process.

The presented study has several limitations. Firstly, the signals were not annotated by medical experts. Secondly, the method has not been tested on the signals recorded during active motion, such as walking or jogging. Finally, for some rare PVC types (e.g., interpolated PVCs) (Reilly et al., 1992 [170]), PVCs can not be detected by the algorithm because PPG is not sensitive enough to hemodynamic changes during such cardiac events.

5.3 PPG-based Detection of Atrial Fibrillation

5.3.1 Dataset and Performance Evaluation

Simulated signals. The algorithm was developed on the Long Term Atrial Fibrillation Database (LTAFDB) (Petrutiu et al., 2007 [171]; Goldberger et al., 2000 [131]). LTAFDB is composed of 84 ECG recordings from patients with paroxysmal or persistent AF, most recordings extending over 24-h duration. The entire database consists of nearly 9 million beats, of which, 59 % occur during AF.

The MIT–BIH Atrial Fibrillation Database (AFDB) (Moody et al., 1983 [172]; Goldberger et al., 2000 [131]), the MIT–BIH Arrhythmia Database (MITDB) (Goldberger et al., 2000 [131]) and the MIT–BIH Normal Sinus Rhythm Database (NSRDB) (Goldberger et al., 2000 [131]) were used for performance evaluation. The AFDB database includes 25 AF recordings of approximately 10-h duration; in total, it contains more than 1 million beats, of which, 43 % occur during AF. The MITDB consists of 48 half-hour ECG recordings with a total of approximately 109,000 beats. The NSRDB contains 18 ECG recordings of approximately 24-h duration, with a total of almost 2 million beats. Since no significant arrhythmias are present, it is well-suited for the evaluation of the detector specificity.

Simulated PPG signals for the PPG-based AF detector evaluation were generated by applying the RR interval series with annotations from the LTAFDB and AFDB to the input of the PPG signal simulator proposed in (Sološenko et al., 2017 [144]).

Clinical signals. The clinical dataset was collected from signals recorded at Kulautuva Rehabilitation Hospital of Kaunas Clinics, Lithuania. Two groups of participants were involved at Kulautuva Rehabilitation Hospital of Kaunas Clinics, Lithuania. The first group consisted of 15 patients with AF, 72.9±8.9 years old, with the body-mass index of 28.3±5.9 kg/m^2, and the total monitoring time of 316.2 hours (21±3.8 hours per patient). The second group consisted of 19 patients without AF, 67.5±10 years old, with the body-mass index of 28±5 kg/m^2, and the total monitoring time of 411.1 hours (21.6±3.1 hours per patient). The signal recording was approved by Kaunas Region Biomedical Research Ethics Committee (No. BE-2-20).

Performance measures. The performance was investigated in terms of sensitivity (Se), specificity (Sp), accuracy (Ac) and Matthews correlation coefficient (Mc). Sensitivity is defined by the number of correctly detected AF beats divided by the total number of AF beats, whereas specificity is defined by the number of correctly detected non-AF beats divided by the total number of non-AF beats. Accuracy is defined as the ratio of correctly detected both AF and non-AF beats with the total number of beats. All the other types of rhythm, including atrial flutter, were labeled as non-AF.

5.3.2 Results

Parameter settings Figure 5.7 displays the ROC curves of the original and PPG-optimized algorithms with LTAFDB. Detection threshold η was changed from the original value of 0.725 to 0.630. As in the previous study, the threshold value was chosen at the point of the ROC curve where both sensitivity and specificity on the LTAFDB were equal, i.e., 95 %.

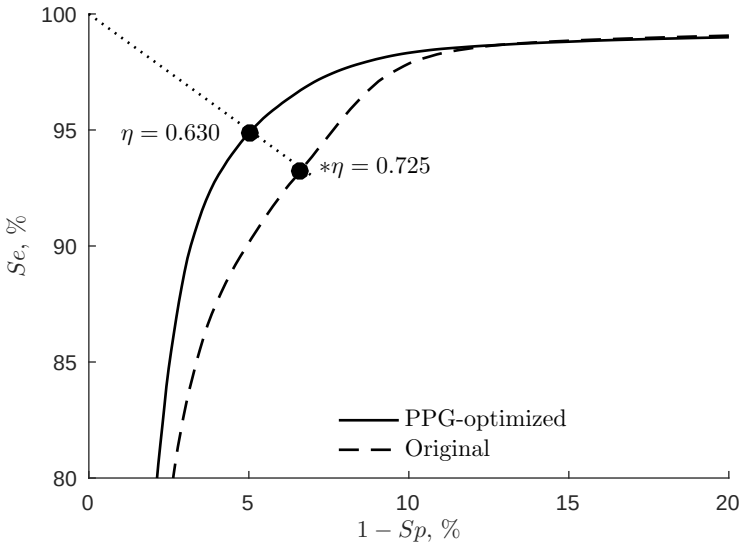

Fig. 5.7. ROC curves of both the original and PPG-optimized AF detectors.

Figure 5.8 shows AF detection performance as a function of peak detection threshold percentile. The highest AF detection accuracy is in the range between 55:th and 65:th percentiles.

Figure 5.9 shows the peak detection performance as a function of the peak detection interval multiplier. The highest AF detection accuracy is obtained at $M = 0.45$.

Figure 5.10 shows the PPG-based AF detection algorithm performance on the SQI threshold. The threshold was determined by using a simulated PPG signal generated by using RR intervals from LTAFDB. AF detection Ac does not

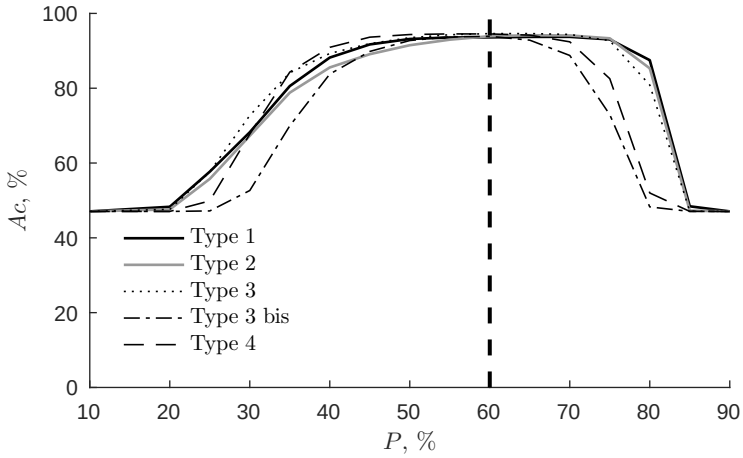

Fig. 5.8. AF detection accuracy on peak detection percentile P with different PPG pulse types.

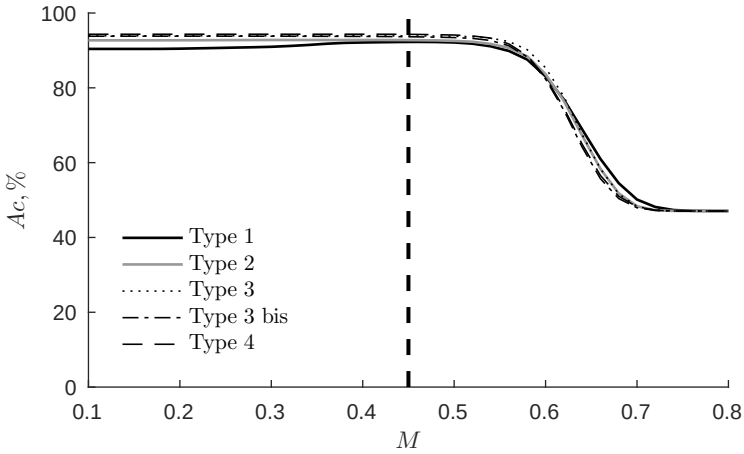

Fig. 5.9. AF detection accuracy on peak detection interval multiplier M with different PPG pulse types.

change up to correlation threshold value $\mu = 0.7$, when positive and negative correlation lags τ_{min} and τ_{max} are set to ± 0.35 ms, respectively.

The remaining parameters were kept the same as in the original AF detector: $\gamma = 0.03\ s$, $N = 8$, $\delta = 2 \times 10^{-4}$, and $\alpha = 0.02$.

Results with ECG RR intervals. Table 5.7 presents the performance of the PPG-optimized AF detection part on the ECG RR interval series from various public databases. The results show that modifications and improvements do not degrade the performance of the detector on the RR interval series from AFDB ($Se = 97.1$ % and $Sp = 98.4$ %); however, substantial improvement in specificity

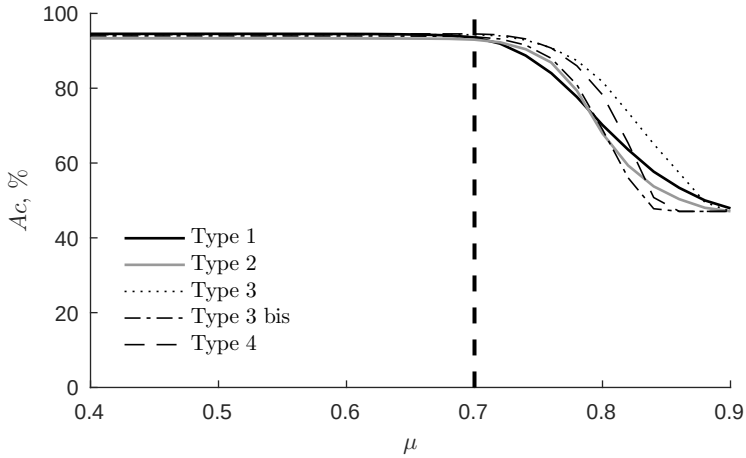

Fig. 5.10. AF detection accuracy (Ac) as a function of the SQI threshold and the type of the PPG pulse.

is noticed in MIDTB and NSRDB databases, at 91.3 % and 99.2 %, respectively.

Table 5.7. Sensitivity (Se), specificity (Sp), accuracy (Ac), and Mathews correlation coefficient (Mc) of the PPG-optimized and original AF detectors, evaluated on RR interval series from the MIT–BIH Atrial Fibrillation (AFDB), MIT–BIH Arrhythmia (MITDB), and MIT–BIH Normal Sinus Rhythm (NSRDB) databases.

Database	**AFDB**				**MITDB**				**NSRDB**			
Performance, %	*Se*	*Sp*	*Ac*	*Mc*	*Se*	*Sp*	*Ac*	*Mc*	*Se*	*Sp*	*Ac*	*Mc*
PPG-optimized	97.1	98.4	97.8	95.5	96.8	91.3	92.6	71.9	NA	99.2	NA	NA
Original	97.1	98.3	97.8	95.5	97.8	86.4	87.6	61.8	NA	98.6	NA	NA

Detection on the simulated database. Figure 5.11 shows the results of the proposed as well as the original algorithms at various SNR levels ranging from 0 dB to 30 dB for five PPG pulse types are shown. The proposed algorithm retains a high specificity of nearly 100 % even at SNR values in the range from 0 dB to 10 dB, whereas the specificity of the original algorithm declines starting from the SNR value of 10dB.

Detection on the clinical database. Figure 5.12 shows the performance of the algorithm while using real PPG signals at different values of correlation threshold μ ranging from 0.4 % to 0.8 %. As in case with simulated PPG signals, the AF detection is based on triggering AF detection part of the algorithm only when no

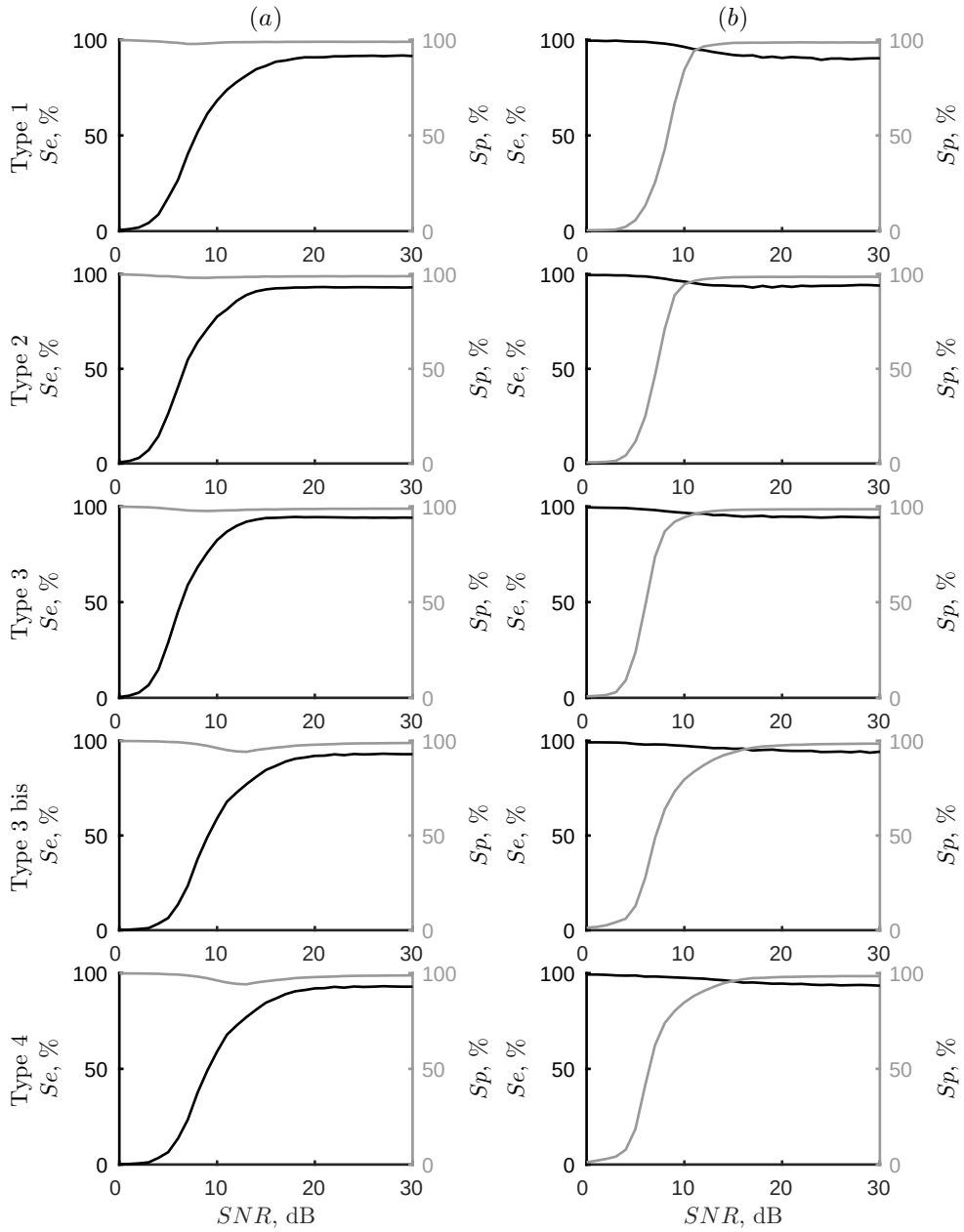

Fig. 5.11. Sensitivity (Se) and specificity (Sp) of (a) proposed and (b) original RR interval-based AF detection algorithms at various SNR values and for different PPG pulse types.

artifacts are detected, e.g., $SQI = 0$ and vice versa. Compared to the method based on the acceleration data, resulting in up to 65.4±5.7 % of motion-free data, $Se = 99.9$ %, and $Sp = 91.5$ %, the proposed method at threshold $\mu = 0.7$ results

in $Se = 69.42$ %, and $Sp = 99.76$ %. The percentage of the informative signal and Sp can be considerably increased by lowering SQI threshold μ however, at the expense of reduced Se, which is undesirable in long-term monitoring applications due to a large number of false-positives (Fig. 5.12 c).

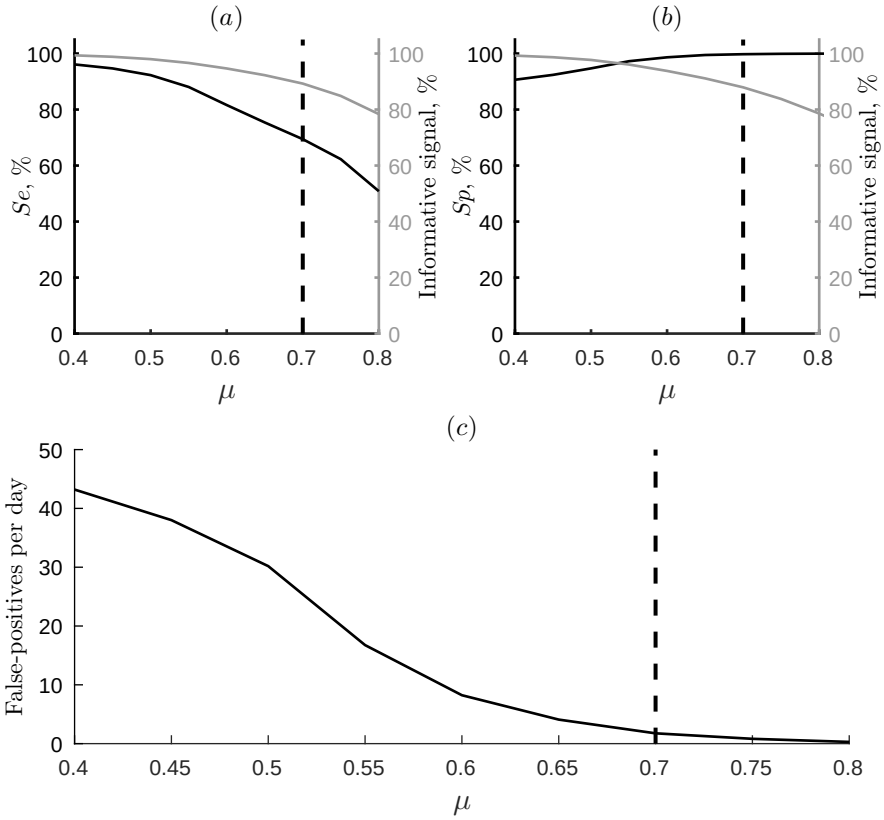

Fig. 5.12. Detection performance on a clinical PPG database for different SQI thresholds: (*a*) sensitivity on PPG signals with persistent AF, (*b*) specificity on PPG signals with no AF, and (*c*) the average number of false-positives per day.

5.3.3 Discussion

The proposed algorithm for AF screening is developed while having high specificity at low SNRs in mind.

Various studies stated that cardiac event recorders are prone to false alarms due to ectopic beats since they share similar symptoms to those of AF. For example, a study of 48 participants (50 % with AF) showed that while using an external loop recorder *3100 BT* by Vitaphone (*3100 BT*, Vitaphone, Mannheim, Germany) each patient in sinus rhythm on average had more than 5 false-positive ECG recordings (Müller et al., 2009 [173]). Comparable performance of this device was reported in another study where 2,923 ECG events were collected

in 108 patients Velthuis et al., 2013 [174]. Roughly 1200 detected events were classified as AF by the automatic algorithm, however, only 56 were confirmed to be AF after manual revision.

For screening in the community or for personal use, a drop in sensitivity may be a necessary trade-off to achieve very high specificity. This is particularly important if large numbers of people are screened or when multiple recordings are requested for each person, as might be the case with a PPG-based application. In this situation even small reductions in specificity could lead to very large numbers of false-positive results, which would require verification with a separate ECG (Freedman, 2016 [31]). A study by Desteghe et al., 2016 [175] showed that even a commercial ECG-based AliveCor system composed of the ECG recording device and a mobile application has a relatively low sensitivity (55 %) at an expense of high specificity. It was made intentionally in order to decrease the number of false alarms, especially when a large population is monitored. Moreover, as opposed to ECG, no diagnosis could be made out of PPG signals, therefore high specificity in PPG-based AF detectors is of utmost importance since even a small decrease in specificity may produce a large number of false alarms (Freedman, 2016 [31]).

The currently used ECG-based screening devices are developed to exhibit high sensitivity. This is due to short recording time and the ability to confirm the diagnosis in ECG recordings by a physician. On the other hand, a PPG-based continuous screening device would have a different purpose, because currently there are no clinical guidelines on how to interpret arrhythmias in PPG. Thus the device should have high specificity so that to reduce the number of false alarms as much as possible. If AF is detected by a PPG-based device then standard techniques should be prescribed, i.e., Holter monitoring. Such an approach would allow implementing low-price mass-screening of the target population.

When developing PPG-based AF detection algorithms, the peculiarities of PPG signals have to be taken into account. Other authors applied ECG-based AF detection methods on PPG signals without any specific modifications and adaptations, and although they do work, there are differences between ECG and PPG-derived features, particularly during arrhythmic events.

Even though an accelerometer can provide information on motion, there are certain activities which may not involve motion as such, e.g., curling fingers into the palm, which is sufficient to compromise the quality of the PPG signal due to the movement of the internal tissues.

The modifications of the ECG RR interval-based AF detection algorithm not only accounts for the differences between PPG and ECG derived features but also for the improved AF detection accuracy on ECG signals.

In order to improve sensitivity in long-term PPG-based AF monitoring without compromising the specificity, the quality of the recorded signal has to be improved.

5.4 Conclusions of the Chapter

1. A phenomenological model for simulating PPG signals during AF, as well as other regular and irregular rhythms, is introduced. In quantitative terms, the simulated signals bear close resemblance to a wide range of signals taken from databases. The possibility to simulate connected PPG signals, composed of different types of PPG pulses at different SNRs is valuable when developing and testing PPG-based AF detectors.

2. A photoplethysmography-based method for the detection of premature ventricular contractions has been developed. Considering its high performance, the proposed PVC detector is expected to have both non-clinical (e.g., sleep monitoring) and clinical (e.g., in hemodialysis procedures) relevance when moderate physical activity is involved.

3. The present study shows that the proposed PPG signal-based AF detection algorithm offers not only good accuracy at moderate SNR levels but also excellent specificity at low SNR levels.

6 CONCLUSIONS

1. The increase in arrhythmia prevalence is due to the ageing population, usually associated with cardiovascular diseases, lifestyle and the constantly improving ability to suspect and diagnose arrhythmia. Currently, there are various strategies and equipment available for arrhythmia detection, however, most of them are electrocardiogram-based, requiring no fewer than two electrodes attached to the body or hand-held either for long-term or for intermediate monitoring, respectively. New, more convenient and cost-effective approaches employing alternative signals e.g., photoplethysmogram, are being developed and investigated. However, in order to reduce the influence of motion-induced artifacts on arrhythmia detection specificity, such approaches are only used for short recordings, e.g., by attaching a finger to the smartphone camera. Therefore, signal processing methods and algorithms for long-term arrhythmia screening in photoplethymogram signals are required.

2. There is lack of annotated databases for testing of photoplethysmogram-based arrhythmia detection algorithms. Therefore, a photoplethysmogram model capable of simulating both normal rhythm and various types of arrhythmia, namely, premature contractions and atrial fibrillation, has been developed. The model makes use of rhythm-based information obtained either from annotated electrocardiogram signals or rhythm simulators aimed generate simulated photoplethysmogram signals. The obtained results show that simulated signals visually resemble the real photoplethysmogram signals with the root mean square error between both normalized simulated and real signals not exceeding 0.1. Currently, this is the only photoplethysmogram model intended for arrhythmia simulation so far. The model is well-suited for the development and assessment of photoplethysmogram-based arrhythmia detection algorithms.

3. An algorithm for the detection of premature ventricular contractions relying solely on photoplethysmogram-based feature analysis has been developed. Characteristics of the proposed algorithm, such as the normalization of extracted rhythm-based features according to an estimated normal sinus rhythm, false alarm suppression with artifact detection and the use of neural network classifier for beat classification into normal and premature ones allows the detection of not only single premature ventricular contractions but also for the rhythm of bigeminy. When compared to already known algorithms, the proposed one shows substantial performance improvement, e.g., $Se = 94.4 \pm 3.1$ % and $Sp = 99.98 \pm 0.01$ % with simulated signals and up to $Se = 92.8$ % and $Sp = 99.9$ % on clinical signals, respectively, and

could be used for continuous ambulatory screening of premature ventricular contractions. The online version is implemented as an application for Android OS, thus making it suitable for wearable systems, such as PPG-capable smartwatches or smartphones.

4. A photoplethysmogram-based method combining heart rhythm analysis and signal quality assessment algorithms for reliable atrial fibrillation detection has been developed. The detection part relies on a modified and improved low-complexity atrial fibrillation detector, adapted for photoplethysmogram-based features. The photoplethysmogram quality assessment part employs correlation technique for distinguishing photoplethysmogram pulses between normal and noise-corrupted ones. The results show that atrial fibrillation detection supplemented by signal quality assessment allows achieving hight detection sensitivity, e.g., nearly 90 %, up to 20 dB SNR with simulated signals composed of Type 1 pulses and up to 98.6 % with clinical signals. Exceptionally high specificity is possible even at relatively low SNRs, e.g., nearly 100 % at 0–10dB with simulated signals and up to 99.9 % with clinical signals. The proposed algorithm has a potential to be applied for continuous ambulatory screening of atrial fibrillation. The algorithm is suitable for the implementation in the wearable systems, e.g., smartwatches or smartphones, therefore, the online version is implemented as an Android OS application.

REFERENCES

1. J. B. KOSTIS et al. "Premature ventricular complexes in the absence of identifiable heart disease". In: *Circulation* vol. 63 no. 6 (1981), pp. 1351–1356 (cit. on pp. 10, 22, 23).

2. C. T. JANUARY et al. "2014 AHA/ACC/HRS Guideline for the Management of Patients With Atrial Fibrillation: Executive Summary: A Report of the American College of Cardiology/American Heart Association Task Force on Practice Guidelines and the Heart Rhythm Society". In: *Journal of the American College of Cardiology* vol. 64 no. 21 (2014), pp. 2246–2280 (cit. on p. 10).

3. H. L. KENNEDY, J. A. WHITLOCK, and M. K. SPRAGUE. "Long-Term Follow-up of Asymptomatic Healthy Subjects with Frequent and Complex Ventricular Ectopy". In: *New England Journal of Medicine* vol. 312 no. 4 (1985), pp. 193–197 (cit. on pp. 10, 20).

4. G. A. NG. "Treating patients with ventricular ectopic beats". In: *Heart* vol. 92 no. 11 (2006), pp. 1707–1712 (cit. on pp. 10, 20, 21, 31, 32).

5. G. EPHREM et al. "The Prognostic Significance of Frequency and Morphology of Premature Ventricular Complexes during Ambulatory Holter Monitoring". In: *Annals of Noninvasive Electrocardiology* vol. 18 no. 2 (2013), pp. 118–125. ISSN: 1542-474X (cit. on p. 10).

6. F. ATAKLTE et al. "Meta-Analysis of Ventricular Premature Complexes and Their Relation to Cardiac Mortality in General Populations". In: *The American Journal of Cardiology* vol. 112 no. 8 (2013), pp. 1263–1270 (cit. on pp. 10, 21).

7. F. SANTORO et al. "Ventricular Fibrillation Triggered by PVCs from Papillary Muscles: Clinical Features and Ablation". In: *Journal of Cardiovascular Electrophysiology* vol. 25 no. 11 (2014), pp. 1158–1164. ISSN: 1540-8167 (cit. on p. 10).

8. H. WATANABE, N. TANABE, and Y. MAKIYAMA. "*ST*-segment abnormalities and premature complexes are predictors of new-onset atrial fibrillation: The Niigata Preventive Medicine Study". In: *American Heart Journal* vol. 152 no. 4 (2006), pp. 731–735. ISSN: 0002-8703 (cit. on pp. 10, 22).

9. S. K. AGARWAL et al. "Premature ventricular complexes and the risk of incident stroke: the Atherosclerosis Risk In Communities (ARIC) Study." In: *Stroke; a journal of cerebral circulation* vol. 41 (2010), pp. 588–593. ISSN: 1524-4628 (cit. on p. 10).

10. H. HIROSE et al. "Cardiac mortality of premature ventricular complexes in healthy people in Japan". In: *Journal of Cardiology* vol. 56 no. 1 (2010), pp. 23–26. ISSN: 0914-5087 (cit. on p. 10).

11. X. JOUVEN, M. ZUREIK, and M. DESNOS. "Long-Term Outcome in Asymptomatic Men with Exercise-Induced Premature Ventricular Depolarizations". In: *New England Journal of Medicine* vol. 343 no. 12 (2000), pp. 826–833 (cit. on p. 10).

12. J. P. FROLKIS, C. E. POTHIER, and E. H. BLACKSTONE. "Frequent Ventricular Ectopy after Exercise as a Predictor of Death". In: *New England Journal of Medicine* vol. 348 no. 9 (2003), pp. 781–790 (cit. on p. 10).

13. B. ZARET, L. COHEN, and M. MOSER. *Yale University School of Medicine Heart Book*. William Morrow and Co., 1992. ISBN: 9780688097196 (cit. on p. 10).

14. M. J. REED and A. GRAY. "Collapse query cause: the management of adult syncope in the emergency department". In: *Emerg Med J* vol. 23 no. 8 (2006), pp. 589–594. ISSN: 1472-0205 (cit. on p. 10).

15. A. GARCIA-TOUCHARD et al. "Ventricular ectopy during REM sleep: implications for nocturnal sudden cardiac death". In: *Nat Clin Pract Cardiovasc Med* vol. 4 no. 5 (2007), pp. 284–288. ISSN: 1743-4297 (cit. on p. 10).

16. K. M. SHAMSEDDIN and P. S. PARFREY. "Sudden cardiac death in chronic kidney disease: epidemiology and prevention". In: *Nature Reviews Nephrology* no. 3 (2011), pp. 145–154 (cit. on p. 10).

17. M. HAIM et al. "Prospective national study of the prevalence, incidence, management and outcome of a large contemporary cohort of patients with incident non-valvular atrial fibrillation". In: *Journal of the American Heart Association* vol. 4 no. 1 (2015), e001486 (cit. on p. 10).

18. S. COLILLA et al. "Estimates of current and future incidence and prevalence of atrial fibrillation in the U.S. adult population". In: *American Journal of Cardiology* vol. 112 no. 8 (2013), pp. 1142–1147 (cit. on pp. 10, 24).

19. J. S. HEALEY et al. "Subclinical Atrial Fibrillation and the Risk of Stroke". In: *New England Journal of Medicine* vol. 366 no. 2 (2012), pp. 120–129 (cit. on p. 10).

20. N. LOWRES et al. "Screening to identify unknown atrial fibrillation. A systematic review". In: *Thrombosis and Haemostasis* vol. 110 no. 2 (2013), pp. 213–222 (cit. on pp. 10, 11, 26).

21. G. Y. LIP et al. "Prognosis and treatment of atrial fibrillation patients by European cardiologists: one year follow-up of the EURObservational Research Programme-Atrial Fibrillation General Registry Pilot Phase (EORP-AF Pilot registry)". In: *European Heart Journal* vol. 35 no. 47 (2014), pp. 3365–3376 (cit. on pp. 10, 11).

22. A. KISHORE et al. "Detection of atrial fibrillation after ischemic stroke or transient ischemic attack: a systematic review and meta-analysis". In: *Stroke* vol. 45 no. 2 (2014), pp. 520–526 (cit. on p. 11).

23. E. J. BENJAMIN et al. "Impact of Atrial Fibrillation on the Risk of Death". In: *Circulation* vol. 98 no. 10 (1998), pp. 946–952. ISSN: 0009-7322 (cit. on p. 11).

24. N. LOWRES, L. NEUBECK, and S. B. FREEDMAN. "Can screening for atrial fibrillation be implemented at scale?" In: *EP Europace* vol. 18 no. 10 (2016), p. 1449 (cit. on p. 11).

25. P. KIRCHHOF. "Integrated care of patients with atrial fibrillation: the 2016 ESC atrial fibrillation guidelines". In: *Heart* (2017). ISSN: 1355-6037 (cit. on p. 11).

26. S. Z. ROSERO et al. "Ambulatory ECG Monitoring in Atrial Fibrillation Management". In: *Progress in Cardiovascular Diseases* vol. 52 no. 2 (2013), pp. 143–152 (cit. on pp. 11, 37).

27. E. I. CHARITOS et al. "A comprehensive evaluation of rhythm monitoring strategies for the detection of atrial fibrillation recurrence: insights from 647 continuously monitored patients and implications for monitoring after therapeutic interventions". In: *Circulation* vol. 126 no. 7 (2012), pp. 806–814 (cit. on p. 11).

28. J. LEE et al. "Atrial Fibrillation Detection Using an iPhone 4S". In: *IEEE Transactions on Biomedical Engineering* vol. 60 no. 1 (2013), pp. 203–206. ISSN: 0018-9294 (cit. on pp. 11, 43, 51, 55, 87).

29. D. D. MCMANUS et al. "PULSE-SMART: Pulse-Based Arrhythmia Discrimination Using a Novel Smartphone Application". In: *Journal of Cardiovascular Electrophysiology* vol. 27 no. 1 (2016), pp. 51–57 (cit. on p. 11).

30. P.-H. CHAN et al. "Diagnostic Performance of a Smartphone-Based Photoplethysmographic Application for Atrial Fibrillation Screening in a Primary Care Setting". In: *Journal of the American Heart Association* vol. 5 no. 7 (2016) (cit. on pp. 11, 51).

31. B. FREEDMAN. "Screening for Atrial Fibrillation Using a Smartphone: Is There an App for That?" In: *Journal of the American Heart Association* vol. 5 no. 7 (2016) (cit. on pp. 11, 39, 51, 101).

32. A. PETRĖNAS, V. MAROZAS, and L. SÖRNMO. "Low-complexity detection of atrial fibrillation in continuous long-term monitoring". In: *Computers in Biology and Medicine* vol. 65 (2015), pp. 184–191. ISSN: 0010-4825 (cit. on pp. 13, 72, 76, 81).

33. M. E. MANGONI and J. NARGEOT. "Genesis and Regulation of the Heart Automaticity". In: *Physiological Reviews* vol. 88 no. 3 (2008), pp. 919–982 (cit. on p. 17).

34. Z. F. ISSA, J. M. MILLER, and D. P. ZIPES. "Chapter 3 - Electrophysiological Mechanisms of Cardiac Arrhythmias". In: *Clinical Arrhythmology and Electrophysiology: A Companion to Braunwald's Heart Disease (Second Edition)*. Ed. by Z. F. ISSA, J. M. MILLER, and D. P. ZIPES. Second Edition. Philadelphia: W.B. Saunders, 2012, pp. 36–61. ISBN: 978-1-4557-1274-8 (cit. on p. 17).

35. M. ZONI-BERISSO et al. "Epidemiology of atrial fibrillation: European perspective". In: *Clinical Epidemiology* (2014), p. 213 (cit. on pp. 20, 24).

36. F. GAITA et al. "Long-term follow-up of right ventricular monomorphic extrasystoles". In: *Journal of the American College of Cardiology* vol. 38 no. 2 (2001), pp. 364–370 (cit. on pp. 20, 21).

37. M. von ROTZ et al. “Risk factors for premature ventricular contractions in young and healthy adults”. In: *Heart* vol. 103 no. 9 (2016), pp. 702–707 (cit. on p. 20).

38. F. C. MESSINEO. “Ventricular ectopic activity: Prevalence and risk”. In: *The American Journal of Cardiology* vol. 64 no. 20 (1989), pp. 53–56 (cit. on p. 21).

39. D. P. SOUTHALL et al. “24-hour electrocardiographic study of heart rate and rhythm patterns in population of healthy children”. In: *British Heart Journal* vol. 45 no. 3 (1981), pp. 281–291 (cit. on p. 21).

40. M. von ROTZ et al. “Risk factors for premature ventricular contractions in young and healthy adults”. In: *Heart* vol. 103 no. 9 (2017), pp. 702–707. ISSN: 1355-6037 (cit. on p. 21).

41. A. J. CAMM et al. “The rhythm of the heart in active elderly subjects”. In: *American Heart Journal* vol. 99 no. 5 (1980), pp. 598–603 (cit. on p. 21).

42. A. MORSHEDI-MEIBODI. “Clinical Correlates and Prognostic Significance of Exercise-Induced Ventricular Premature Beats in the Community: The Framingham Heart Study”. In: *Circulation* vol. 109 no. 20 (2004), pp. 2417–2422 (cit. on p. 21).

43. M. BIKKINA, M. G. LARSON, and D. LEVY. “Prognostic implications of asymptomatic ventricular arrhythmias: the Framingham Heart Study”. In: *Annals of Internal Medicine* vol. 117 no. 12 (1992), pp. 990–996 (cit. on p. 21).

44. I. S. ABDALLA et al. “Relation between ventricular premature complexes and sudden cardiac death in apparently healthy men”. In: *American Journal of Cardiology* vol. 60 no. 13 (1987), pp. 1036–1042 (cit. on p. 21).

45. S. K. AGARWAL et al. “Premature Ventricular Complexes on Screening Electrocardiogram and Risk of Ischemic Stroke”. In: *Stroke* vol. 46 no. 5 (2015), pp. 1365–1367 (cit. on p. 21).

46. D. F. DUFFEE, W. K. SHEN, and H. C. SMITH. “Suppression of frequent premature ventricular contractions and improvement of left ventricular function in patients with presumed idiopathic dilated cardiomyopathy”. In: *Mayo Clinic Proceedings* vol. 73 no. 5 (1998), pp. 430–433 (cit. on p. 21).

47. J. F. SARRAZIN et al. “Impact of radiofrequency ablation of frequent post-infarction premature ventricular complexes on left ventricular ejection fraction”. In: *Heart Rhythm* vol. 6 no. 11 (2009), pp. 1543–1549 (cit. on p. 21).

48. B. N. SINGH. “Controlling cardiac arrhythmias: an overview with a historical perspective”. In: *American Journal of Cardiology* vol. 80 no. 8A (1997), 4G–15G (cit. on p. 21).

49. R. K. YARLAGADDA et al. “Reversal of cardiomyopathy in patients with repetitive monomorphic ventricular ectopy originating from the right ventricular outflow tract”. In: *Circulation* vol. 112 no. 8 (2005), pp. 1092–1097 (cit. on p. 21).

50. S NIWANO et al. “Prognostic significance of frequent premature ventricular contractions originating from the ventricular outflow tract in patients with normal left ventricular function”. In: *Heart* vol. 95 no. 15 (2009), pp. 1230–1237 (cit. on pp. 21, 22, 32).

51. J. M. WORTHINGTON, M. GATTELLARI, and D. Y. LEUNG. “"Where Theres Smoke...": Are Premature Ventricular Complexes a New Risk Factor for Stroke?” In: *Stroke* vol. 41 no. 4 (2010), pp. 572–573 (cit. on p. 22).

52. S. K. AGARWAL et al. “Relation of Ventricular Premature Complexes to Heart Failure (from the Atherosclerosis Risk In Communities [ARIC] Study)”. In: *The American Journal of Cardiology* vol. 109 no. 1 (2012), pp. 105–109 (cit. on p. 22).

53. M. W. MASSING et al. “Usefulness of Ventricular Premature Complexes to Predict Coronary Heart Disease Events and Mortality (from the Atherosclerosis Risk In Communities Cohort)”. In: *The American Journal of Cardiology* vol. 98 no. 12 (2006), pp. 1609–1612 (cit. on p. 22).

54. M. JESERICH et al. “Patients with exercise-associated ventricular ectopy present evidence of myocarditis”. In: *Journal of Cardiovascular Magnetic Resonance* vol. 17 no. 1 (2015), p. 100. ISSN: 1532-429X (cit. on p. 22).

55. B. A. KOPLAN and W. G. STEVENSON. “Ventricular tachycardia and sudden cardiac death”. In: *Mayo Clinic Proceedings* vol. 84 no. 3 (2009), pp. 289–297 (cit. on p. 22).

56. S. S. CHUGH et al. “Epidemiology of sudden cardiac death: clinical and research implications”. In: *Progress in Cardiovascular Diseases* vol. 51 no. 3 (2008), pp. 213–228 (cit. on p. 23).

57. Y. PARK et al. “Frequent Premature Ventricular Complex Is Associated with Left Atrial Enlargement in Patients with Normal Left Ventricular Ejection Fraction”. In: *Pacing and Clinical Electrophysiology* vol. 37 no. 11 (2014), pp. 1455–1461 (cit. on p. 23).

58. H. SHIRAISHI et al. “A Case of Cardiomyopathy Induced by Premature Ventricular Complexes”. In: *Circulation Journal* vol. 66 no. 11 (2002), pp. 1065–1067 (cit. on p. 23).

59. B. BELHASSEN. “Radiofrequency ablation of "benign" right ventricular outflow tract extrasystoles.” In: *Journal of the American College of Cardiology* vol. 45 no. 8 (2005), pp. 1266–1268 (cit. on pp. 23, 32).

60. J. BALL et al. “Atrial fibrillation: Profile and burden of an evolving epidemic in the 21st century”. In: *International Journal of Cardiology* vol. 167 no. 5 (2013), pp. 1807–1824. ISSN: 0167-5273 (cit. on p. 23).

61. T. M. MUNGER, L. Q. WU, and W. K. SHEN. “Atrial fibrillation”. In: *Journal of Biomedical Research* vol. 28 no. 1 (2014), pp. 1–17 (cit. on pp. 23, 33).

62. S. S. CHUGH et al. “Worldwide Epidemiology of Atrial Fibrillation: A Global Burden of Disease 2010 Study”. In: *Circulation* vol. 129 no. 8 (2013), pp. 837–847 (cit. on pp. 23, 24, 26).

63. M. NAGHAVI et al. “Global, regional, and national age-sex specific all-cause and cause-specific mortality for 240 causes of death, 1990-2013: a systematic analysis for the Global Burden of Disease Study 2013”. In: *Lancet* vol. 385 no. 9963 (2015), pp. 117–171 (cit. on p. 23).

64. Y. MIYASAKA et al. “Secular trends in incidence of atrial fibrillation in Olmsted County, Minnesota, 1980 to 2000, and implications on the projections for future prevalence”. In: *Circulation* vol. 114 (2006), pp. 119–125 (cit. on pp. 23, 24).

65. B. P. KRIJTHE et al. “Projections on the number of individuals with atrial fibrillation in the European Union, from 2000 to 2060”. In: *European Heart Journal* vol. 34 no. 35 (2013), pp. 2746–2751 (cit. on p. 23).

66. V. L. ROGER et al. "Heart Disease and Stroke Statistics–2012 Update: A Report From the American Heart Association". In: *Circulation* vol. 125 no. 1 (2011), e2–e220 (cit. on pp. 23, 25).

67. A. R. MENEZES et al. "Atrial Fibrillation in the 21st Century: A Current Understanding of Risk Factors and Primary Prevention Strategies". In: *Mayo Clinic Proceedings* vol. 88 no. 4 (2013), pp. 394–409 (cit. on pp. 23, 25).

68. V. FUSTER et al. "[ACC/AHA/ESC 2006 guidelines for the management of patients with atrial fibrillation–excutive summary]". In: *Revista Portuguesa de Cardiologia* vol. 26 no. 4 (2007), pp. 383–446 (cit. on p. 24).

69. A. S. GO, E. M HYLEK, and K. A. PHILLIPS. "Prevalence of diagnosed atrial fibrillation in adults: National implications for rhythm management and stroke prevention: the anticoagulation and risk factors in atrial fibrillation (atria) study". In: *JAMA* vol. 285 no. 18 (2001), pp. 2370–2375 (cit. on p. 24).

70. A. J. CAMM et al. "Guidelines for the management of atrial fibrillation". In: *European Heart Journal* vol. 31 no. 19 (2010), pp. 2369–2429. ISSN: 0195-668X (cit. on p. 24).

71. C. MARINI et al. "Contribution of Atrial Fibrillation to Incidence and Outcome of Ischemic Stroke". In: *Stroke* vol. 36 no. 6 (2005), pp. 1115–1119. ISSN: 0039-2499 (cit. on pp. 24, 25).

72. V. BARRIOS et al. "Patients With Atrial Fibrillation in a Primary Care Setting: Val-FAAP Study". In: *Revista Espanola de Cardiologia* vol. 65 no. 01 (2012), pp. 47–53 (cit. on p. 24).

73. E. J. BENJAMIN et al. "Independent risk factors for atrial fibrillation in a population-based cohort. The Framingham Heart Study". In: *JAMA* vol. 271 (1994), pp. 840–844 (cit. on pp. 24, 25).

74. J. HEERINGA et al. "Prevalence, incidence and lifetime risk of atrial fibrillation: The Rotterdam study". In: *European Heart Journal* vol. 27 (2006), pp. 949–953 (cit. on p. 24).

75. D. M. LLOYD-JONES. "Lifetime Risk for Development of Atrial Fibrillation: The Framingham Heart Study". In: *Circulation* vol. 110 no. 9 (2004), pp. 1042–1046 (cit. on p. 24).

76. B. N. JUSTIN, M. TUREK, and A. M. HAKIM. *Heart disease as a risk factor for dementia.* 2013 (cit. on p. 25).

77. A. F. GROSS and T. A. STERN. "The Cognitive Impact of Atrial Fibrillation". In: *The Primary Care Companion For CNS Disorders* (2013) (cit. on p. 25).

78. S. E. WOLOWACZ et al. "The cost of illness of atrial fibrillation: a systematic review of the recent literature". In: *Europace* vol. 13 no. 10 (2011), pp. 1375–1385 (cit. on p. 25).

79. M. H. KIM et al. "Estimation of Total Incremental Health Care Costs in Patients With Atrial Fibrillation in the United States". In: *Circulation: Cardiovascular Quality and Outcomes* vol. 4 no. 3 (2011), pp. 313–320 (cit. on p. 25).

80. A. RINGBORG et al. "Costs of atrial fibrillation in five European countries: results from the Euro Heart Survey on atrial fibrillation". In: *Europace* vol. 10 (2008), pp. 403–411 (cit. on p. 25).

81. R. R. HUXLEY et al. "Absolute and Attributable Risks of Atrial Fibrillation in Relation to Optimal and Borderline Risk Factors: The Atherosclerosis Risk in Communities [ARIC] Study". In: *Circulation* vol. 123 no. 14 (2011), pp. 1501–1508 (cit. on p. 25).

82. D. A FITZMAURICE et al. "Screening versus routine practice in detection of atrial fibrillation in patients aged 65 or over: cluster randomised controlled trial". In: *BMJ* vol. 335 no. 7616 (2007), pp. 383–383 (cit. on p. 26).

83. N. LOWRES et al. "Feasibility and cost-effectiveness of stroke prevention through community screening for atrial fibrillation using iPhone ECG in pharmacies". In: *Thrombosis and Haemostasis* vol. 111 no. 6 (2014), pp. 1167–1176 (cit. on p. 26).

84. L. GAZTAÑAGA, F. E. MARCHLINSKI, and B. P. BETENSKY. "Mechanisms of Cardiac Arrhythmias". In: *Revista Española de Cardiología (English Edition)* vol. 65 no. 2 (2012), pp. 174–185 (cit. on p. 26).

85. J. F. HUIZAR et al. "Left ventricular systolic dysfunction induced by ventricular ectopy: a novel model for premature ventricular contraction-

induced cardiomyopathy". In: *Circulation: Arrhythmia and Electrophysiology* vol. 4 no. 4 (2011), pp. 543–549 (cit. on p. 26).

86. H. HACHIYA et al. "How to diagnose, locate, and ablate coronary cusp ventricular tachycardia". In: *Journal of Cardiovascular Electrophysiology* vol. 13 no. 6 (2002), pp. 551–556 (cit. on p. 27).

87. D. P. ZIPES. "Mechanisms of Clinical Arrhythmias". In: *Journal of Cardiovascular Electrophysiology* vol. 14 no. 8 (2003), pp. 902–912 (cit. on p. 27).

88. A. J. CAMM, T. F. LÜSCHER, and P. W. SERRUYS. *The ESC Textbook of Cardiovascular Medicine*. Oxford, UK, 2009 (cit. on p. 28).

89. A. J. CAMM et al. "Chapter 15 - Atrial Tachycardia, Flutter, and Fibrillation". In: *Electrophysiological Disorders of the Heart*. Ed. by S. SAKSENA et al. Philadelphia: Churchill Livingstone, 2005, 283 –cp1 (cit. on p. 28).

90. G. K. MOE, W. C. RHEINBOLDT, and J. ABILDSKOV. "A computer model of atrial fibrillation". In: *American Heart Journal* vol. 67 no. 2 (1964), pp. 200–220. ISSN: 0002-8703 (cit. on p. 28).

91. M. A. ALLESSIE et al. "Experimental evaluation of Moe's multiple wavelet hypothesis of atrial fibrillation". In: *Cardiac Electrophysiology and Arrhythmias*. Ed. by D. P. ZIPES and J. JALIFE. Grune & Stratton, 1985, pp. 265–276 (cit. on p. 29).

92. S. NATTEL, B. BURSTEIN, and D. DOBREV. "Atrial remodeling and atrial fibrillation: mechanisms and implications". In: *Circulation: Arrhythmia and Electrophysiology* vol. 1 no. 1 (2008), pp. 62–73 (cit. on p. 29).

93. M. HAÏSSAGUERRE et al. "Spontaneous Initiation of Atrial Fibrillation by Ectopic Beats Originating in the Pulmonary Veins". In: *New England Journal of Medicine* vol. 339 no. 10 (1998), pp. 659–666 (cit. on p. 29).

94. M. ALLESSIE, J. AUSMA, and U. SCHOTTEN. "Electrical, contractile and structural remodeling during atrial fibrillation". In: *Cardiovascular Research* vol. 54 no. 2 (2002), p. 230 (cit. on p. 29).

95. M. C. WIJFFELS et al. "Atrial fibrillation begets atrial fibrillation. A study in awake chronically instrumented goats". In: *Circulation* vol. 92 (1995), pp. 1954–1968 (cit. on p. 29).

96. A. K. BHANDARI et al. "Correlation of symptoms with occurrence of paroxysmal supraventricular tachycardia or atrial fibrillation: A transtelephonic monitoring study". In: *American Heart Journal* vol. 124 no. 2 (1992), pp. 381–386 (cit. on p. 29).

97. Y. KANEI et al. "Frequent premature ventricular complexes originating from the right ventricular outflow tract are associated with left ventricular dysfunction." In: *Annals of noninvasive electrocardiology : the official journal of the International Society for Holter and Noninvasive Electrocardiology, Inc* vol. 13 (1 2008), pp. 81–85 (cit. on p. 31).

98. M. S. AHN. "Current Concepts of Premature Ventricular Contractions". In: *Journal of Lifestyle Medicine* vol. 3 no. 1 (2013), pp. 26–33 (cit. on p. 32).

99. J. M. ANUMONWO and J. KALIFA. "Risk factors and genetics of atrial fibrillation". In: *Heart Failure Clinics* vol. 12 no. 2 (2016), pp. 157–166 (cit. on p. 33).

100. M. L. OISHI and S. XING. "Atrial fibrillation: management strategies in the emergency department". In: *Emergency Medicine Practice* vol. 15 no. 2 (2013), pp. 1–26 (cit. on p. 33).

101. M. JUN et al. "The association between kidney function and major bleeding in older adults with atrial fibrillation starting warfarin treatment: population based observational study". In: *British Medical Journal* vol. 350 (2015), h246 (cit. on p. 34).

102. H. HEIDBUCHEL et al. "Updated European Heart Rhythm Association Practical Guide on the use of non-vitamin K antagonist anticoagulants in patients with non-valvular atrial fibrillation." In: *Europace : European pacing, arrhythmias, and cardiac electrophysiology : journal of the working groups on cardiac pacing, arrhythmias, and cardiac cellular electrophysiology of the European Society of Cardiology* vol. 17 (10 2015), pp. 1467–507 (cit. on p. 34).

103. J. V. AMERENA et al. "Update on the management of atrial fibrillation". In: *Med. J. Aust.* Vol. 199 no. 9 (2013), pp. 592–597 (cit. on p. 34).

104. C. FERGUSON et al. "Atrial fibrillation: Stroke prevention in focus". In: *Australian Critical Care* vol. 27 no. 2 (2014), pp. 92–98 (cit. on p. 34).

105. E. HOEFMAN, P. J. BINDELS, and H. C. van WEERT. "Efficacy of diagnostic tools for detecting cardiac arrhythmias: systematic literature search". In: *Netherlands Heart Journal* vol. 18 no. 11 (2010), pp. 543–551 (cit. on p. 35).

106. R. SUBBIAH et al. "Cardiac monitoring in patients with syncope: making that elusive diagnosis". In: *Current Cardiology Reviews* vol. 9 no. 4 (2013), pp. 299–307 (cit. on p. 35).

107. C. de ASMUNDIS et al. "Comparison of the patient-activated event recording system vs. traditional 24 h Holter electrocardiography in individuals with paroxysmal palpitations or dizziness". In: *EP Europace* vol. 16 no. 8 (2014), pp. 1231–1235. ISSN: 1099-5129 (cit. on p. 37).

108. A. D. KRAHN et al. "Insertable loop recorder use for detection of intermittent arrhythmias". In: *Pacing Clin Electrophysiol* vol. 27 no. 5 (2004), pp. 657–664 (cit. on p. 39).

109. S. DAVIS et al. "Implantable loop recorders are cost-effective when used to investigate transient loss of consciousness which is either suspected to be arrhythmic or remains unexplained." In: *Europace* vol. 14 (3 2012), pp. 402–409 (cit. on p. 39).

110. P. GARABELLI, S. STAVRAKIS, and S. PO. "Smartphone-based arrhythmia monitoring". In: *Current Opinion in Cardiology* vol. 32 no. 1 (2017), pp. 53–57 (cit. on p. 39).

111. K. MATSUMURA et al. "iPhone 4s Photoplethysmography: Which Light Color Yields the Most Accurate Heart Rate and Normalized Pulse Volume Using the iPhysioMeter Application in the Presence of Motion Artifact?" In: *PLoS ONE* vol. 9 no. 3 (2014), e91205 (cit. on p. 43).

112. A. N. BASHKATOV et al. "Optical properties of human skin, subcutaneous and mucous tissues in the wavelength range from 400 to 2000 nm". In: *Journal of Physics D: Applied Physics* vol. 38 no. 15 (2005), pp. 2543–2555 (cit. on p. 43).

113. M. C. BARUCH et al. "Pulse Decomposition Analysis of the digital arterial pulse during hemorrhage simulation". In: *Nonlinear Biomedical Physics* vol. 5 no. 1 (2011), pp. 1–15. ISSN: 1753-4631 (cit. on pp. 44, 62).

114. M. ELGENDI. “On the analysis of fingertip photoplethysmogram signals”. In: *Curr Cardiol Rev* vol. 8 no. 1 (2012), pp. 14–25 (cit. on p. 47).

115. K. M. WARREN et al. “Improving Pulse Rate Measurements during Random Motion Using a Wearable Multichannel Reflectance Photoplethysmograph”. In: *Sensors (Basel)* vol. 16 no. 3 (2016) (cit. on p. 48).

116. R. W. WIJSHOFF, M. MISCHI, and R. M. AARTS. “Reduction of Periodic Motion Artifacts in Photoplethysmography”. In: *IEEE Transactions on Biomedical Engineering* vol. 64 no. 1 (2017), pp. 196–207 (cit. on p. 48).

117. K. H. SHELLEY. “Photoplethysmography: beyond the calculation of arterial oxygen saturation and heart rate”. In: *Anesthesia and Analgesia* vol. 105 no. 6 Suppl (2007), pp. 31–36 (cit. on p. 50).

118. J. ALLEN. “Photoplethysmography and its application in clinical physiological measurement”. In: *Physiological Measurement* vol. 28 no. 3 (2007), pp. 1–39 (cit. on p. 50).

119. T. SUZUKI, K.-I. KAMEYAMA, and T. TAMURA. “Development of the irregular pulse detection method in daily life using wearable photoplethysmographic sensor”. In: (2009), pp. 6080–6083. ISSN: 1557-170X (cit. on pp. 50, 52–54).

120. L. WANG, B. LO, and G.-Z. YANG. “Multichannel Reflective PPG Earpiece Sensor With Passive Motion Cancellation”. In: *Biomedical Circuits and Systems, IEEE Transactions on* vol. 1 no. 4 (2007), pp. 235–241. ISSN: 1932-4545 (cit. on p. 50).

121. T. TAMURA et al. “Wearable Photoplethysmographic Sensors—Past and Present”. In: *Electronics* vol. 3 no. 2 (2014), pp. 282–302 (cit. on p. 50).

122. K. LI and S. WARREN. “A Wireless Reflectance Pulse Oximeter With Digital Baseline Control for Unfiltered Photoplethysmograms”. In: *Biomedical Circuits and Systems, IEEE Transactions on* vol. 6 no. 3 (2012), pp. 269–278. ISSN: 1932-4545 (cit. on p. 50).

123. R. HAAHR et al. “An Electronic Patch for Wearable Health Monitoring by Reflectance Pulse Oximetry”. In: *Biomedical Circuits and Systems, IEEE Transactions on* vol. 6 no. 1 (2012), pp. 45–53. ISSN: 1932-4545 (cit. on p. 50).

124. E. GIL et al. "Heart Rate Turbulence Analysis Based on Photoplethysmography". In: *IEEE Transactions on Biomedical Engineering* vol. 60 no. 11 (2013), pp. 3149–3155. ISSN: 0018-9294 (cit. on pp. 50, 54, 69, 94).

125. L. DRIJKONINGEN et al. "Validation of a smartphone based photoplethysmographic beat detection algorithm for normal and ectopic complexes". In: *Computing in Cardiology 2014*. 2014, pp. 845–848 (cit. on p. 50).

126. L. F. POLANIA et al. "Method for classifying cardiac arrhythmias using photoplethysmography". In: *2015 37th Annual International Conference of the IEEE Engineering in Medicine and Biology Society (EMBC)*. IEEE, 2015 (cit. on p. 50).

127. M. LEWIS et al. "Screening for atrial fibrillation: sensitivity and specificity of a new methodology." In: *British Journal of General Practice* vol. 61 no. 582 (2011), pp. 38–39 (cit. on p. 51).

128. D. D. MCMANUS et al. "A novel application for the detection of an irregular pulse using an iPhone 4S in patients with atrial fibrillation". In: *Heart Rhythm* vol. 10 no. 3 (2013), pp. 315–319 (cit. on pp. 51, 55, 58).

129. S. R. STEINHUBL et al. "Rationale and design of a home-based trial using wearable sensors to detect asymptomatic atrial fibrillation in a targeted population: The mHealth Screening To Prevent Strokes (mSToPS) trial". In: *American Heart Journal* vol. 175 (2016), pp. 77–85 (cit. on p. 51).

130. G. MOODY and R. MARK. "A database to support development and evaluation of intelligent intensive care monitoring". In: *Computers in Cardiology* vol. 23 (1996), pp. 657–660. ISSN: 0276-6547 (cit. on pp. 51, 88).

131. A. L. GOLDBERGER et al. "PhysioBank, PhysioToolkit, and PhysioNet: Components of a New Research Resource for Complex Physiologic Signals". In: *Circulation* vol. 101 no. 23 (2000), pp. 215–220 (cit. on pp. 51, 88, 95).

132. M. SAEED et al. "Multiparameter Intelligent Monitoring in Intensive Care II (MIMIC-II): A public-access intensive care unit database". In: *Critical Care Medicine* vol. 39 (2011), pp. 952–960 (cit. on pp. 51, 88).

133. D. LIU, M. GORGES, and S. A. JENKINS. "University of Queensland vital signs dataset: development of an accessible repository of anesthesia patient monitoring data for research". In: *Anesthesia and Analgesia* vol. 114 no. 3 (2012), pp. 584–589 (cit. on p. 51).

134. L. WANG et al. "Multi-Gaussian fitting for pulse waveform using Weighted Least Squares and multi-criteria decision making method". In: *Computers in Biology and Medicine* vol. 43 no. 11 (2013), pp. 1661–1672 (cit. on pp. 51, 82).

135. C. LIU et al. "Modelling arterial pressure waveforms using Gaussian functions and two-stage particle swarm optimizer". In: *Biomed Research International* vol. 2014 (2014), p. 923260. ISSN: 2314-6133 (cit. on pp. 51, 82).

136. S. C. HUANG et al. "Decomposition Analysis of Digital Volume Pulse Signal Using Multi-Model Fitting". In: *XIII Mediterranean Conference on Medical and Biological Engineering and Computing 2013*. IFMBE Proceedings vol. 41 (2013). Ed. by L. M. ROA ROMERO, pp. 635–638 (cit. on pp. 51, 82).

137. M. HUOTARI et al. "Photoplethysmography and its detailed pulse waveform analysis for arterial stiffness". In: *Journal of Structural Mechanics* vol. 44 no. 4 (2011), pp. 345–362 (cit. on pp. 51, 82).

138. G. D. CLIFFORD and P. E. MCSHARRY. "A realistic coupled nonlinear artificial ECG, BP, and respiratory signal generator for assessing noise performance of biomedical signal processing algorithms". In: *Proceedings of SPIE* vol. 5467 (2004), pp. 290–301 (cit. on pp. 51, 87).

139. S. NABAR et al. "Resource–efficient and Reliable Long Term Wireless Monitoring of the Photoplethysmographic Signal". In: WH '11 (2011), 9:1–9:10 (cit. on pp. 51, 87).

140. D. MARTIN-MARTINEZ et al. "Stochastic Modeling of the PPG Signal: A Synthesis-by-Analysis Approach With Applications". In: *IEEE Transactions on Biomedical Engineering* vol. 60 no. 9 (2013), pp. 2432–2441. ISSN: 0018-9294 (cit. on pp. 51, 87).

141. S. SCARSOGLIO et al. "Impact of atrial fibrillation on the cardiovascular system through a lumped-parameter approach". In: *Medical & Biological Engineering & Computing* (2014), pp. 905–920 (cit. on pp. 51, 87).

142. K. TATENO and L. GLASS. "Automatic detection of atrial fibrillation using the coefficient of variation and density histograms of RR and deltaRR intervals". In: *Medical & Biological Engineering & Computing* vol. 39 (2001), pp. 664–671 (cit. on p. 55).

143. S. DASH et al. "Automatic Real Time Detection of Atrial Fibrillation". In: *Annals of Biomedical Engineering* vol. 37 no. 9 (2009), pp. 1701–1709 (cit. on p. 55).

144. A. SOLOŠENKO et al. "Modeling of the Photoplethysmogram During Atrial Fibrillation". In: *Computers in Biology and Medicine* vol. 81 (2017), pp. 130–138. ISSN: 0010-4825 (cit. on pp. 61, 89, 95).

145. T. F. COLEMAN and Y. LI. "An Interior Trust Region Approach for Nonlinear Minimization Subject to Bounds". In: *SIAM Journal on Optimization* vol. 6 no. 2 (1996), pp. 418–445 (cit. on p. 62).

146. T. R. DAWBER, H. E. THOMAS, and P. M. MCNAMARA. "Characteristics of the dicrotic notch of the arterial pulse wave in coronary heart disease". In: *Angiology* vol. 24 no. 4 (1973), pp. 244–255 (cit. on p. 63).

147. R. SARNARI et al. "Doppler Assessment of the Ratio of the Systolic to Diastolic Duration in Normal Children: Relation to Heart Rate, Age and Body Surface Area". In: *Journal of the American Society of Echocardiography* vol. 22 no. 8 (2009), pp. 928–932 (cit. on p. 64).

148. E. PEPER et al. "Is there more to blood volume pulse than heart rate variability respiratory sinus arrhythmia, and cardiorespiratory synchrony?" In: *Biofeedback* vol. 35 no. 2 (2007), pp. 54–61 (cit. on p. 67).

149. D. ZHENG, J. ALLEN, and A. MURRAY. "Determination of aortic valve opening time and left ventricular peak filling rate from the peripheral pulse amplitude in patients with ectopic beats". In: *Physiological Measurement* vol. 29 no. 12 (2008), pp. 1411–1419 (cit. on p. 67).

150. S. DOUGLAS. "Numerically-robust O(N^2) RLS algorithms using least-squares prewhitening". In: *Acoustics, Speech, and Signal Processing, 2000. ICASSP '00. Proceedings. 2000 IEEE International Conference on.* Vol. 1. 2000, pp. 412–415 (cit. on p. 69).

151. T. VOGL et al. "Accelerating the convergence of the back-propagation method". In: *Biological Cybernetics* vol. 59 no. 4-5 (1988), pp. 257–263. ISSN: 0340-1200 (cit. on p. 71).

152. PIOTROWSKI et al. "A comparison of methods to avoid overfitting in neural networks training in the case of catchment runoff modelling". In: *Journal of Hydrology* vol. 476 (2013), pp. 97–111 (cit. on p. 71).

153. P. LAGUNA, R. JANÉ, and P. CAMINAL. "Adaptive filtering of ECG baseline wander". In: *Engineering in Medicine and Biology Society, 1992 14th Annual International Conference of the IEEE*. Vol. 2. 1992, pp. 508–509 (cit. on pp. 72, 94).

154. M. ABOY et al. "An automatic beat detection algorithm for pressure signals". In: *IEEE Transactions on Biomedical Engineering* vol. 52 no. 10 (2005), pp. 1662–1670. ISSN: 0018-9294 (cit. on pp. 73, 81).

155. D. E. LAKE and J. R. MOORMAN. "Accurate estimation of entropy in very short physiological time series: The problem of atrial fibrillation detection in implanted ventricular devices". In: *American Journal of Physiology: Heart and Circulatory Physiology* vol. 300 no. 1 (2011), pp. 319–325 (cit. on p. 74).

156. P. LANGLEY et al. "Accuracy of algorithms for detection of atrial fibrillation from short duration beat interval recordings". In: *Medical Engineering and Physics* vol. 34 no. 10 (2012), pp. 1441–1447. ISSN: 1350-4533 (cit. on p. 74).

157. A. J. CHEUNG and B. M. Y. CHEUNG. "False detection of atrial fibrillation in children by a blood pressure monitor with atrial fibrillation detection function". In: *BMJ Case Reports* vol. 2015 (2015) (cit. on p. 75).

158. P. MCSHARRY et al. "A dynamical model for generating synthetic electrocardiogram signals". In: *IEEE Transactions on Biomedical Engineering* vol. 50 no. 3 (2003), pp. 289–294. ISSN: 0018-9294 (cit. on pp. 87, 89).

159. J. LIAN et al. "Open source model for generating RR intervals in atrial fibrillation and beyond". In: *Biomedical Engineering Online* vol. 6 (2007), p. 9 (cit. on p. 87).

160. L. SÖRNMO et al. "A Method for Evaluation of QRS Shape Features Using a Mathematical Model for the ECG". In: *IEEE Transactions on Biomedical Engineering* vol. BME-28 no. 10 (1981), pp. 713–717. ISSN: 0018-9294 (cit. on p. 87).

161. J. ALLEN and A. MURRAY. "Age-related changes in the characteristics of the photoplethysmographic pulse shape at various body sites". In: *Physiological Measurement* vol. 24 no. 2 (2003), p. 297 (cit. on p. 87).

162. J. LÁZARO et al. "Deriving respiration from photoplethysmographic pulse width". In: *Medical & Biological Engineering & Computing* vol. 51 no. 1 (2013), pp. 233–242. ISSN: 1741-0444 (cit. on p. 87).

163. R. BANERJEE et al. "Noise cleaning and Gaussian modeling of smart phone photoplethysmogram to improve blood pressure estimation". In: *2015 IEEE International Conference on Acoustics, Speech and Signal Processing (ICASSP)*. 2015, pp. 967–971 (cit. on p. 88).

164. D. S. BENITEZ et al. "The use of the Hilbert transform in ECG signal analysis." In: *Computers in Biology and Medicine* vol. 31 no. 5 (2001), pp. 399–406 (cit. on p. 88).

165. J. GORODKIN. "Comparing two K-category assignments by a K-category correlation coefficient". In: *Computational Biology and Chemistry* vol. 28 no. 5-6 (2004), pp. 367–374. ISSN: 1476-9271 (cit. on p. 90).

166. A. SOLOŠENKO and V. MAROZAS. "Automatic Extrasystole Detection Using Photoplethysmographic Signals". In: *XIII Mediterranean Conference on Medical and Biological Engineering and Computing 2013*. Vol. 41. IFMBE Proceedings. 2013, pp. 985–988. ISBN: 978-3-319-00845-5 (cit. on p. 94).

167. H. WANG et al. "Shape-Preserving Preprocessing for Human Pulse Signals Based on Adaptive Parameter Determination". In: *Biomedical Circuits and Systems, IEEE Transactions on* vol. 8 no. 4 (2014), pp. 594–604. ISSN: 1932-4545 (cit. on p. 94).

168. J. PATTERSON and G.-Z. YANG. "Ratiometric Artifact Reduction in Low Power Reflective Photoplethysmography". In: *Biomedical Circuits and Systems, IEEE Transactions on* vol. 5 no. 4 (2011), pp. 330–338. ISSN: 1932-4545 (cit. on p. 94).

169. K. LI, S. WARREN, and B. NATARAJAN. "Onboard Tagging for Real-Time Quality Assessment of Photoplethysmograms Acquired by a Wireless Reflectance Pulse Oximeter". In: *Biomedical Circuits and Systems, IEEE Transactions on* vol. 6 no. 1 (2012), pp. 54–63. ISSN: 1932-4545 (cit. on p. 94).

170. J. REILLY and H. ANTONI. *Electrical Stimulation and Electropathology*. Cambridge University Press, 1992. ISBN: 9780521417914 (cit. on p. 95).

171. S. PETRUTIU, A. V. SAHAKIAN, and S. SWIRYN. "Abrupt changes in fibrillatory wave characteristics at the termination of paroxysmal atrial fibrillation in humans". In: *Europace* vol. 9 (2007), pp. 466–470 (cit. on p. 95).

172. G. B. MOODY and R. G. MARK. "A new method for detecting atrial fibrillation using R-R intervals". In: *Computers in Cardiology* vol. 10 (1983), pp. 227–230 (cit. on p. 95).

173. A. MÜLLER et al. "Reliability of an external loop recorder for automatic recognition and transtelephonic ECG transmission of atrial fibrillation". In: *Journal of Telemedicine and Telecare* vol. 15 no. 8 (2009), pp. 391–396 (cit. on p. 100).

174. B. O. VELTHUIS et al. "Performance of an External Transtelephonic Loop Recorder for Automated Detection of Paroxysmal Atrial Fibrillation". In: *Annals of Noninvasive Electrocardiology* vol. 18 no. 6 (2013), pp. 564–570. ISSN: 1542-474X (cit. on p. 101).

175. L. DESTEGHE and H. HEIDBUCHEL. "'Performance of handheld electrocardiogram devices to detect atrial fibrillation in a cardiology and geriatric ward setting: authors' response"'. In: *Europace* (2016) (cit. on p. 101).

LIST OF PUBLICATIONS

Publications indexed in the Web of Science with impact factor

1. Sološenko A.; Petrėnas A.; Marozas V.; Sörnmo S. (2017). Modeling of the photoplethysmogram during atrial fibrillation. In: *Computers in Biology and Medicine.* Amsterdam: Elsevier, ISSN: 0010-4825, vol. 81, pp. 130–138. [IF: 1.521].

2. Sološenko A.; Petrėnas A.;, Marozas V. (2015). Photoplethysmography-based method for automatic detection of premature ventricular contractions. *IEEE Transactions on Biomedical Circuits and Systems.* IEEE, vol. 9, no. 5, ISSN: 1932-4545, pp. 662–669. [IF: 2.482].

Publications indexed in the Web of Science without impact factor

1. Stankevičius D.; Petrėnas A.; Sološenko A.; Grigutis M.; Januškevičius T.; Rimševičius L.; Marozas V. (2016). Photoplethysmography-based system for atrial fibrillation detection during hemodialysis. In: *XIV Mediterranean Conference on Medical and Biological Engineering and Computing 2016, MEDICON'2016. IFMBE Proceedings*, vol. 57. Berlin, Heidelberg: Springer. ISBN 1680-0737, Paphos, Cyprus. 2016, pp. 79–82.

2. Sološenko A.; Marozas V. (2014). Automatic premature ventricular contraction detection in photoplethysmographic signals. In: *In Proceedings of the 2014 IEEE/CAS-EMB Biomedical Circuits and Systems Conference, edition 2014. BioCAS'2014, EPFL, IEEE.* Lausanne, Switzerland. 2014, pp. 49–52.

3. Sološenko A.; Marozas V. Automatic extrasystole detection using photoplethysmographic signals. (2014). In: *XIII Mediterranean Conference on Medical and Biological Engineering and Computing 2013, MEDICON'2013. IFMBE Proceedings*, vol. 41. Berlin, Heidelberg: Springer. ISSN: 1680-0737, Seville, Spain. 2014, pp. 985–988.

Other peer-reviewed scientific publications

Articles in periodicals

1. Januškevičius T.; Grigutis M.; Rimševičiu L.; Sološenko A.; Stankevičius D.; Miglinas M. (2015). Sword of Damocles: cardiac events during dialysis. (lt.: Damoklo kardas: Širdies įvykiai dializės metu) In: *Theory and*

Practice in Medicine (Medicinos teorija ir praktika) / Vilnius medical society (Vilniaus medicinos draugija), vol. 21, no. 2.2. ISSN: 1392-1312, pp. 251–255.

Publications in proceedings of the international scientific conferences

1. Patašius, M.; Sološenko, A.; Marozas, V.; Lukoševičius, A. (2014) Extensible system for gathering and storing of biomedical signals. In: *Biomedical engineering 2014: Proceedings of the 18th international conference, Kaunas University of Technology, Biomedical Engineering Institute, Kaunas, Lithuania.* Kaunas: Technologija, ISSN: 2029-3380. pp. 89–92.

2. Sološenko A.; Marozas V. (2014). Smartphone based application for online premature ventricular contraction detection. In: *Biomedical Engineering 2014: Proceedings of the 18th International Conference, Kaunas University of Technology Biomedical Engineering Institute, Kaunas, Lithuania.* Technologija, ISSN: 2029-3380. pp. 174–177.

3. Vizbara V.; Sološenko A.; Stankevičius D.; Marozas V. (2013). Comparison of green, blue and infrared light in wrist and forehead photoplethysmography. In: *Biomedical Engineering 2013: Proceedings of the 17th International Conference, Kaunas University of Technology Biomedical Engineering Institute, Kaunas, Lithuania.* Kaunas: Technologija. ISSN: 2029-3380. pp. 78–81.

Abstracts in scientific conferences

1. Sološenko A.; Marozas, V. (2014). Automatic detection of ventricular extrasystoles (lt.: Automatinis skilvelių ekstrasistolių atpažinimas). In: *Science for Health 2014: 7th National Conference for Doctoral Students (Mokslas–sveikatai: Nacionalinė doktorantų mokslinė konferencija).* Lithuanian University of Health Sciences, Kaunas, Lithuania, pp. 85–86.

2. Sološenko A.; Petrėnas, A.; Marozas, V. (2017). Investigation of premature beat detection using photoplethysmogram (lt.: Priešlaikinių širdies susitraukimų atpažinimo fotopletizmogramoje tyrimas). In: *Interdisciplinary Research in Physical and Technological Sciences: 7th Conference of Young Scientists (Fizinių ir technologijos mokslų tarpdalykiniai tyrimai: 7-oji jaunųjų mokslininkų konferencija).* Lithuanian Academy of Sciences, Vilnius, Lithuania, pp. 62–63.

Abstracts in exhibitions-contests

1. Sološenko, A.; Grigutis, M.; Januškevičius, T.; Stankevičius, D.; Petrėnas, A.; Rimševičius, L.; Marozas, V. (2015). Real-time system for atrial fibrillation detection during haemodialysis (lt.: Realaus laiko sistema prieširdžių

virpėjimui atpažinti hemodializės metu). Kaunas, Lithuania *KTU Technorama 2015*. Santaka Valley, Kaunas, Lithuania, pp. 62–63.

2. Stankevičius, D.; Sološenko, A.; Petrėnas, A.; Daukantas, S.; Mickus, T.; Skibarkienė, J.; Marozas, V.; Kubilius, R. (2016). Patient-unobtrusive long-term patient monitoring system for detection of myocardial infarction-induced episodes of atrial fibrillation (lt.: Pacientui netrukdanti ilgalaikės stebėsenos sistema miokardo infarkto sukeltiems prieširdžių virpėjimo epizodams atpažinti). *KTU Technorama 2016*. Santaka Valley, Kaunas, Lithuania, pp. 130–131.

SL344. 2017-12-22, 13,5 leidyb. apsk. l. Tiražas 16 egz. Užsakymas 397.
Išleido Kauno technologijos universitetas, K. Donelaičio g. 73, 44249 Kaunas
Spausdino leidyklos „Technologija“ spaustuvė, Studentų g. 54, 51424 Kaunas

Appendix A1 DATABASES AND SIGNALS

Tables A1.1 and A1.2 present the signals included from the MIMIC and UQSVD databases, respectively, together with the corresponding rhythm types.

Table A1.1. Signals from MIMIC database for model evaluation. Numbers correspond to the record names in the database. One pulse is extracted from each of the 56 records.

Record	*AF*	*PB*	*SR*	Record	*AF*	*PB*	*SR*
055	N	N	Y	404	Y	Y	Y
208	Y	N	N	410	Y	Y	Y
209	Y	N	N	411	N	Y	Y
210	Y	N	N	414	N	N	Y
211	N	Y	Y	417	N	Y	N
212	N	Y	Y	427	Y	N	Y
213	N	Y	Y	430	N	N	Y
218	N	Y	Y	437	N	N	Y
219	N	Y	Y	438	N	Y	Y
220	N	Y	Y	439	Y	Y	Y
221	N	Y	Y	442	N	Y	Y
224	N	N	Y	443	Y	Y	Y
225	N	Y	Y	444	N	N	Y
226	N	Y	Y	446	N	Y	Y
230	N	Y	Y	449	N	N	Y
231	N	Y	Y	451	N	Y	Y
237	N	N	Y	452	N	N	Y
240	N	Y	N	453	N	N	Y
248	N	Y	N	456	N	Y	Y
252	N	Y	N	466	N	Y	Y
253	Y	N	N	471	Y	Y	Y
254	N	N	Y	472	Y	Y	Y
260	Y	N	N	474	N	Y	Y
276	N	Y	Y	476	N	Y	Y
281	Y	Y	N	477	N	Y	Y
284	N	Y	Y	482	N	Y	Y
401	N	Y	Y	484	N	Y	Y
403	N	Y	N	485	Y	Y	N

* Y/N stands for YES/NO

Table A1.2. Signals from UQVSD database for model evaluation. One pulse is extracted from each of the 32 records.

Record	*AF*	*PB*	*SR*	Record	*AF*	*PB*	*SR*
case01	N	N	Y	case17	N	Y	Y
case02	N	Y	Y	case18	N	Y	Y
case03	Y	Y	Y	case19	N	Y	Y
case04	N	Y	Y	case20	N	Y	Y
case05	N	Y	Y	case21	N	Y	Y
case06	N	Y	Y	case22	Y	N	N
case07	N	Y	Y	case23	N	N	Y
case08	N	N	Y	case24	N	N	Y
case09	N	N	Y	case25	N	Y	Y
case10	N	N	Y	case26	N	Y	Y
case11	N	Y	Y	case27	N	Y	Y
case12	N	Y	Y	case28	N	N	Y
case13	N	Y	Y	case29	N	Y	Y
case14	N	Y	Y	case30	N	N	Y
case15	N	N	Y	case31	N	N	Y
case16	N	N	Y	case32	N	Y	Y

* Y/N stands for YES/NO

Appendix A2 INITIAL PPG PULSE FITTING PARAMETERS

Table A2.1 provides the initial PPG pulse fitting parameters for various pulse modeling approaches.

Table A2.1. Initial sets of parameters used for PPG pulse modeling.

	Log-normal, Gaussian			*Gamma, Gaussian*			*Gaussian*			*Log-normal*		
	p	*lb*	*ub*	*p*	*lb*	*ub*	*p*	*lb*	*ub*	*p*	*lb*	*ub*
a_0	0.6	0.1	2.0	9.0	0.0	15.0	1.0	0.1	2.0	1.8	0.1	3.0
a_1	0.6	0.1	2.0	0.3	0.0	2.0	0.6	0.1	2.0	0.6	0.1	3.0
a_2	0.6	0.1	2.0	0.15	0.0	2.0	0.6	0.08	2.0	0.6	0.1	2.0
α	–	–	–	25.0	0.0	35.0	–	–	–	–	–	–
β	–	–	–	11.0	0.0	15.0	–	–	–	–	–	–
σ_0	0.2	0.1	1.0	–	–	–	–	–	–	0.3	0.1	0.5
σ_1	–	–	–	–	–	–	–	–	–	0.3	0.1	1.0
σ_2	–	–	–	–	–	–	–	–	–	0.3	0.1	1.0
b_0	1.0	0.1	1.0	–	–	–	0.4	0.1	2.0	1.0	0.1	1.0
b_1	0.6	0.1	2.0	0.8	0.0	2.0	0.5	0.1	2.0	1.0	0.1	1.0
b_2	0.9	0.1	2.0	0.9	0.0	2.0	0.2	0.2	2.0	1.3	0.1	2.0
τ_0	-4.0	-5.0	-3.5	-3.9	-5.0	-3.5	-1.0	-3.0	2.0	-4.4	-4.5	-3.0
τ_1	-1.4	-1.8	2.0	-0.5	-3.0	2.0	-0.4	-2.0	2.0	-3.4	-3.5	2.0
τ_2	0.3	-2.0	2.0	0.9	0.0	3.0	0.9	-1.5	2.0	-2.5	-2.0	0.5
h_0	0.0	-0.5	2.0	0.0	-2.0	1.0	0.0	-2.0	1.0	0.0	-2.0	1.0
h_1	0.0	-2.0	2.0	0.0	-2.0	1.0	0.0	-2.0	1.0	0.0	-2.0	1.0
h_2	0.0	-2.0	2.0	0.0	-2.0	1.0	0.0	-2.0	1.0	0.0	-2.0	1.0

Appendix A3 IMPLEMENTATIONS OF DEVELOPED ALGORITHMS IN SMART DEVICES

Figure A3.1 shows a screenshot of the application running on the smartphone. The PPG segment with the correctly detected PVCs during the episode of bigeminy is shown in a chart on the top of the application window. The bottom chart shows the normalized peak-to-peak intervals. The sliding panel on the right side provides important information about the number of detected PVCs and the PVC burden, determined by the percentage of PVC-related beats compared to a total number of beats.

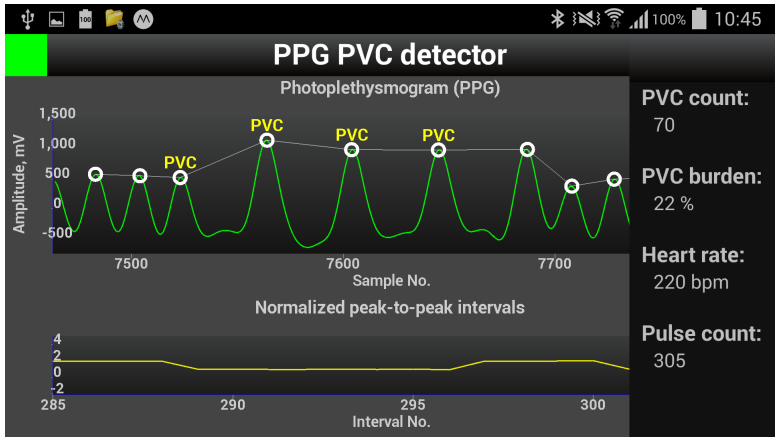

Fig. A3.1. Screenshot of the Android application with the implemented PVC detection algorithm. The application window shows the detected PVCs during a bigeminy episode, as well as other heart rhythm-related parameters. Note that this particular signal is characterized by a very high heart rhythm (220 bpm) outside the episode of multiple PVCs.

Figure A3.2 shows a screenshot of the application running on the smartphone. The PPG segment is shown in a chart on the top of the application window. The bottom chart shows the estimated SQI of the present segment. The sliding panel on the right side provides important information about the number of the detected AF beats and the AF burden determined by the percentage of AF-related beats compared to the total number of beats.

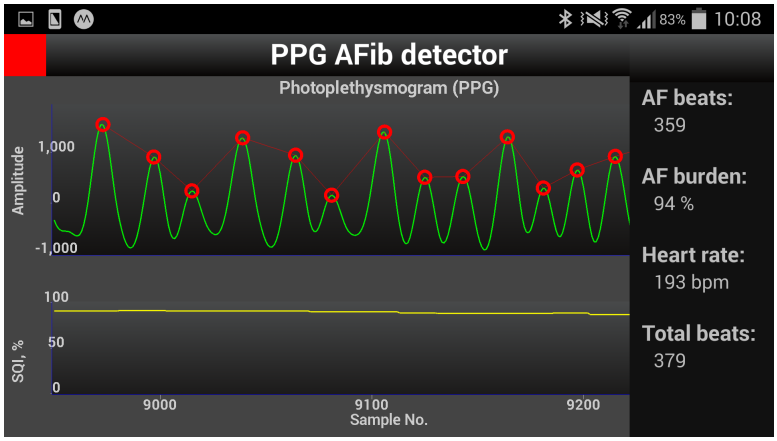

Fig. A3.2. Screenshot of the Android application with the implemented AF detection algorithm. The application window shows the PPG signal during AF, together with the estimated SQI and other heart rhythm-related parameters.